

6-23-2015

A Comprehensive Method For Coordinating Distributed Energy Resources In A Power Distribution System

Shahin Abdollahy

Follow this and additional works at: https://digitalrepository.unm.edu/ece_etds

Recommended Citation

Abdollahy, Shahin. "A Comprehensive Method For Coordinating Distributed Energy Resources In A Power Distribution System." (2015). https://digitalrepository.unm.edu/ece_etds/3

This Dissertation is brought to you for free and open access by the Engineering ETDs at UNM Digital Repository. It has been accepted for inclusion in Electrical and Computer Engineering ETDs by an authorized administrator of UNM Digital Repository. For more information, please contact disc@unm.edu.

Shahin Abdollahy

Candidate

Electrical & Computer Engineering

Department

This dissertation is approved, and it is acceptable in quality and form for publication:

Approved by the Dissertation Committee:

Dr. Olga Lavrova

, Chairperson

Dr. Chauki Abdallah

Dr. Andrea Mammoli

Dr. Satish Ranade

A Comprehensive Method For Coordinating Distributed Energy Resources In A Power Distribution System

by

Shahin Abdollahy

M.S., Electrical Engineering, Amirkabir University of Technology, 2000

B.S., Electrical Engineering, Esfahan University of Technology, 1994

DISSERTATION

Submitted in Partial Fulfillment of the
Requirements for the Degree of

Doctor of Philosophy
Engineering

The University of New Mexico

Albuquerque, New Mexico

May, 2015

©2015, Shahin Abdollahy

Dedication

*To my wife, Mehrnoosh, and my mother, Pari, for their support and encouragement and in
memory of my father, Mostafa.*

Acknowledgments

I would like to thank my advisers, Professor Olga Lavrova and Professor Andrea Alberto Mammoli, for their support and for helping me finish my work remotely.

I also thank my dissertation committee members, Professor Chauki Abdallah and Professor Satish Ranade for their valuable recommendations pertaining to this research and their assistance in my professional development.

Thankful for their invaluable help, I applaud my colleagues Feng (Lucy) Cheng and Yasser Yasaei.

I appreciate the opportunity to work with Dr. Abraham Ellis from Sandia National Laboratories, Steve Willard, Jonathan Hawkins and Brian Arellano from Public Service Company of New Mexico and Dr. John Simmins from Electric Power Research Institute.

Hereby, I would like to acknowledge Dr. Francesco Sorrentino, Dr. Majid Hayat and Nicholas Heine for their cooperation in parts of this research.

A Comprehensive Method For Coordinating Distributed Energy Resources In A Power Distribution System

by

Shahin Abdollahy

M.S., Electrical Engineering, Amirkabir University of Technology, 2000

B.S., Electrical Engineering, Esfahan University of Technology, 1994

Ph.D., Engineering, University of New Mexico, 2015

Abstract

Utilities, faced with increasingly limited resources, strive to maintain high levels of reliability in energy delivery by adopting improved methodologies in planning, operation, construction and maintenance. On the other hand, driven by steady research and development and increase in sales volume, the cost of deploying PV systems has been in constant decline since their first introduction to the market. The increased level of penetration of distributed energy resources in power distribution infrastructure presents various benefits such as loss reduction, resilience against cascading failures and access to more diversified resources.

However, serious challenges and risks must be addressed to ensure continuity and reliability of service. By integrating necessary communication and control infrastructure into the distribution system, to develop a practically coordinated system of distributed resources, controllable load/generation centers will be developed which provide substantial flexibility for the operation of the distribution system. On the other hand, such a complex distributed

system is prone to instability and black outs due to lack of a major “infinite” supply and other unpredicted variations in load and generation, which must be addressed.

To devise a comprehensive method for coordination between Distributed Energy Resources in order to achieve a collective goal, is the key point to provide a fully functional and reliable power distribution system incorporating distributed energy resources. A road map to develop such comprehensive coordination system is explained and supporting scenarios and their associated simulation results are then elaborated. The proposed road map describes necessary steps to build a comprehensive solution for coordination between multiple agents in a microgrid or distribution feeder.

Contents

List of Figures	xi
List of Tables	xx
Glossary	xxi
1 Introduction	1
1.1 Overview	1
1.2 Focus	9
1.3 The Road Map	13
2 Literature Review	16
2.1 Distributed Energy Resources	16
2.2 High Penetration Level of Distributed Resources	20
2.3 Distribution Grid and Load Modeling	23
2.4 A Complex Network Approach	25

Contents

2.4.1	Power Network Specific Topological Model	26
2.5	Control Concepts and Strategies for DER	29
3	Course of Study	38
3.1	Developing Fully Functional Models	38
3.1.1	Tools	39
3.1.2	Model Capabilities	43
3.1.3	Advanced Modeling Features	44
3.1.4	Comparing the Results for the Basic Analysis	47
3.1.5	Load Model	51
3.1.6	Adding Loads to the Model	54
3.1.7	Validating the Model	55
3.1.8	Generalizing	59
3.2	High Penetration Level of DER in Power Distribution	60
3.2.1	Voltage Profile	60
3.2.2	Do Capacitors Contribute to Voltage Smoothness?	65
3.2.3	Spatial effects of Highly Penetrated Distributed PV	66
3.2.4	Circuit Active Loss Profile	69
3.3	Network Model of the Distribution Feeders	70
3.3.1	Classic Network Model	70
3.3.2	Incorporating Electrical Laws in the Network Model	74

Contents

3.4	Coordinated Operation of the Agents	80
3.4.1	Coordinated Smoothing in Multi-Agent Systems	81
3.4.2	Coordinated Demand Management	92
3.4.3	Coordinated Load Shifting	107
3.4.4	Categorization	116
4	Conclusions	121
A	Classic Network Modeling Metrics	127
A.1	Degree Distribution	129
A.2	Clustering Coefficient	129
A.3	Average Shortest Path and Diameter	130
A.4	Assortativity	131
A.5	Betweenness	132
	References	133

List of Figures

1.1	Historical and projected electricity usage in the US over the 27-year period ending in 2035.	3
1.2	Load level on select feeders in Albuquerque in July 2012. Feeders H13 and S13 do not satisfy N1 contingency requirements (Data from PNM).	4
1.3	PV power at the Prosperity PV site during the first week of July 2012 (Data from PNM).	7
1.4	Studio14 distribution feeder in Albuquerque, NM, hosts a number of DER demonstration projects that could interact to maximize economic value and system performance.	10
3.1	PNM smart grid Demonstration Project schematic diagram. Points of common coupling to the feeders are marked up. The red triangle illustrates the connection point to end of feeder SP14 and the blue rectangle shows the point of coupling to feeder ST14 (Courtesy of PNM).	40
3.2	Top-view outline of SewerPlant14 and Studio14, generated in OpenDSS. Points of common coupling to the feeders are marked up. The red triangle illustrates the connection point to end of feeder SP14 and the blue rectangle shows the point of coupling to feeder ST14.	41

List of Figures

3.3	Top-view outline of Tramway11 feeder in 2012 by Google Earth. Installed rooftop PV systems are illustrated.	42
3.4	Run time versus analysis duration (Same feeder models/GridLAB-D and OpenDSS)	46
3.5	Run time versus analysis duration (Same feeder model/Different Operating Systems).	47
3.6	Simulated cumulative load at the substation in GridLAB-D (GL), OpenDSS (DSS) and percentage of the difference. The difference is negligible.	48
3.7	24-hour voltage profile of the closest node to the substation. Percentage of the difference between identical nodes are negligible.	49
3.8	24-hour voltage profile of a node moderately far from the substation transformer. Percentage of the difference between identical phases is increased.	50
3.9	24-hour voltage profile of the farthest node from the substation transformer. Percentage of difference between identical phases is increased but limited to less than 1%.	50
3.10	SewerPlant14 base load shape generated by normalizing the 15-minute demand data. Scaled and time-shifted variations of the original signal are also shown. Hashed area show the conceivable options.	52
3.11	Generated load shape for a random customer. To develop such a load profile, the substation load shape is selected as a base load profile, shifted randomly in time and then scaled stochastically.	54
3.12	Measured and simulated load at substation.	56
3.13	Calculated metrics after 100 random runs ($LRT = 1$ min). Average values are shown on the graph.	57

List of Figures

3.14	A random synthesized load shape and the base load (LRT = 30min).	58
3.15	Measured and synthesized load at the substation on September 2, 2010 (LRT = 30min).	58
3.16	Measured and synthesized load at the substation on June 4, 2010. (LRT = 30 min)	59
3.17	Measured and synthesized load at the substation on November 1, 2010 (LRT = 30 min).	60
3.18	Generated PV power for two different days at Prosperity.	61
3.19	PV effects on Bus1 phase voltages in a partly cloudy day.	62
3.20	PV effects on Bus2 phase voltages. In presence of PV, variations are more significant.	63
3.21	PV effects on Bus3 phase voltages. Farther nodes are less sensitive to PV induced intermittency.	63
3.22	Effects of PV intermittency on Bus1 phase voltages. PV induced fluctuations are negligible at a node located close to the substation.	64
3.23	Node voltages along the feeder. No significant change in voltage profile is observed after additional PV units are connected to the feeder. Node voltage vary based on the load and its location. Some nodes experience significantly higher voltage drops due to their longer distance from the substation. . . .	65
3.24	No significant effect is observed by removing capacitors.	66
3.25	Phase voltages at Bus2. Capacitors have no effect on smoothness.	66

List of Figures

3.26	Normalized absolute density of the spectral contents of the generated power for distributed PV units and the equivalent centralized PV unit. (Data from PNM)	68
3.27	Original losses and percentage of reduction in losses thanks to PV units. . .	69
3.28	Graphical representation of the feeder circuits (Data from PNM, circuit graph by OpenDSS).	70
3.29	Topological representation of ST14 (Data from PNM, Graph by NodeXL). .	71
3.30	Topological representation of the TR11 (Data from PNM, Graph by NodeXL). .	72
3.31	Frequency of Occurrence vs. Clustering Coefficients.	73
3.32	Probability Mass Function of the node degrees.	74
3.33	Topological representation of ST14 impedance graph. A few nodes exhibit high connectivity to the rest of the feeder. Those are “electrical hubs” which are highly effective buses in driving feeder behavior and are significantly effective if are used to position major coordinating agents. However, the electrical hubs may be vulnerable to disruptions (Data from PNM, Graph by NodeXL).	75
3.34	Topological representation of TR11 impedance graph. (Data from PNM, Graph by NodeXL) By eliminating the lower ranking nodes to make the graph more visually comprehensible, some useful information is lost. A single node in this case is highly connected to the rest of the feeder. Such a highly connected node could be regarded as an “electrical hub” and used for driving the feeder behavior or positioning major coordinating agents.	76

List of Figures

3.35	Clustering coefficients frequency of occurrence for the electrical network graphs. Electrical networks are heavily clustered as opposed to the corresponding connectivity graphs. It should be noted that the above graphs exhibit 2 different scales for clustering coefficient.	77
3.36	Probability Mass Function of the node degrees.	79
3.37	Feeder ST14 configuration diagram showing the connections to the PV and BES system, the NEDO microgrid, commercial and residential customers (Courtesy of PNM).	81
3.38	PV generation power in a partly cloudy day at Prosperity.	82
3.39	PV Ramping Rate in a partly cloudy day for a 500kW system.	83
3.40	Smoothing agent power reference controller block diagram implementing RRC method.	85
3.41	Control block diagram of the smoothing power reference calculation using SWMAC method.	86
3.42	NGPG and BES system contribution to RRC smoothing. NGPG follows the PV fluctuations, but due to limited dynamic response and power capabilities, is not able to follow the fast varying portion of the PV. On the other hand, BES system ramps up and down keeping up with PV variations.	87
3.43	PV power and the aggregated output. Despite smoothing, there are still signs of fluctuation in the aggregated output.	87
3.44	Frequency spectrum of the PV output and the smoothened aggregate power. Total energy concentration is shifted toward lower frequency ranges because of smoothing.	88

List of Figures

3.45	Energy exchange for smoothing between the BES system, the NGPG and the feeder.	89
3.46	NGPG and BES system contribution to SWMAC smoothing.	89
3.47	PV power and aggregated output. The aggregated output is smoother than the previous method at the expense of higher energy contribution by the battery.	90
3.49	Smoothing energy, exchanged between BES system, NGPG and the grid. Apparently, the storage system is under more stress than RRC method. Compared to the previous case, the aggregated output is smoother at the expense of more BES contribution.	90
3.48	Frequency spectrum of the PV output and the smoothed aggregate power. High energy concentration in the lower frequency range is prevalent.	91
3.50	Typical profile of a residential A/C load.	94
3.51	Typical residential water heater weekly load profile.	95
3.52	Typical daily load profile for plug loads.	95
3.53	Typical daily lighting load profile.	96
3.54	Typical refrigerator daily load profile.	96
3.55	Typical house daily load profile on weekdays is shown. Significant and frequent load surges are related to the A/C on cycles. Because the A/C load constitutes the major portion of the total load, it is expected to be an ideal candidate for coordinated controlled operation for load management.	97
3.56	Typical weekly load profile of a community of 7 houses.	98
3.57	Typical EV charging profile over a weekend.	98

List of Figures

3.58	Weekly load profile of a community of 7 houses. 4 residents drive PHEVs) and plug their vehicles at their convenience and without any coordination with other PHEV users or with the grid operator. Frequent peaks exceeding 25kW and increase in demand is observed.	99
3.59	Weekly load profile of a community of 7 houses in presence of 4 PHEVs. The smart chargers consider peak load as a constraint and do not initiate a charging cycle if total community demand exceeds 25kW.	101
3.60	Weekly load profile of a community of 7 houses in presence of 4 PHEVs. Smart charge threshold is 20kW.	102
3.61	Typical cumulative rooftop PV generation profile for a 7-house community in a cloudy day.	103
3.62	Weekly load profile of the community of 7 houses in presence of 4 PHEVs. Some houses have rooftop PVs. Negative demand and frequent peaking load are the potentially destructive outcomes of high penetration of PHEVs and PV generation in a microgrid.	104
3.63	Weekly load profile of the community of 7 houses in presence of 4 PHEVs. Smart charge threshold is 25kW. Some houses have rooftop PVs. Coordinated operation of the EV chargers mitigates or minimizes the peak demand problem but negative demand is still inevitable.	104

List of Figures

3.64	Weekly load profile of the community of 7 houses in presence of 4 PHEVs. Smart charge threshold is 20kW. Some houses have rooftop PVs. Coordinated operation of the EV chargers mitigates or minimizes the peak demand problem but negative demand is still inevitable. In a grid-tied system, occasional negative demand does not cause serious issues other than the need for readjusting some protective devices to allow reverse flow of energy. In an islanded system, that problem must be addressed by other means such as storage systems.	105
3.65	Expected demand of 10 commercial buildings estimated based on sample demand data from the Mechanical Engineering building.	107
3.66	Expected cooling demand of the commercial complex estimated based on sample demand data from the Mechanical Engineering building.	108
3.67	Sample 24-hour cooling demand for the commercial complex.	109
3.68	Simulated total load for the commercial complex.	110
3.69	Total cooling load at the feeder after ice-storage system was added to each building. Shorter but significantly higher demand bursts are detected which are not desirable and must be avoided.	111
3.70	Total feeder load after ice-storage systems been added to each building. Shorter but higher peaks in feeder demand are not desirable.	112
3.71	Total cooling load at the feeder after ice-storage systems been added to each building and coordination is implemented.	113
3.72	Total load at the feeder after ice-storage systems been added to each building and coordination is implemented. Total demand is well within the specified limits (4-8MW).	114

List of Figures

3.73	Total cooling load at the feeder in presence of ice-storage systems and different sets of limits (6-8MW).	115
3.74	Total load at the feeder in presence of ice-storage systems and different sets of limits (6-8MW).	115
3.75	PV power spectral contents in a partly cloudy day. The spectrum is divided into frequency ranges based on the amount of energy contents (Data from PNM).	117
3.76	Topological representation of ST14 impedance graph. The electrical hubs carry a considerably large portion of the energy exchange by being central nodes. (Data from PNM, Graph generated in NodeXL)	119

List of Tables

3.1	Graph metrics for the feeders	73
3.2	Graph metrics before and after “electrification”	78

Glossary

<i>ADN</i>	Active Distribution Network
<i>AMI</i>	Advanced Metering Infrastructure
<i>BES</i>	Battery Energy Storage
<i>CARC</i>	Center for Advanced Research Computing
<i>DER</i>	Distributed Energy Resource
<i>EV</i>	Electric Vehicles
<i>FO</i>	Feeder Operator
<i>HPC</i>	High Performance Computing
<i>HEV</i>	Hybrid Electric Vehicles
<i>HVAC</i>	Heating, Ventilation and Air Conditioning
<i>LRT</i>	Load Response Time
<i>MPC</i>	Model Predictive Control
<i>MAS</i>	Multi-Agent System
<i>NGPG</i>	Natural Gas Powered Generator

Glossary

<i>OLTC</i>	On Load Tap Changer
<i>PSO</i>	Particle Swarm Optimization
<i>PHEV</i>	Plug-in Hybrid Electric Vehicles
<i>PCC</i>	Point of Common Coupling
<i>PET</i>	Power Electronic Transformer
<i>PMF</i>	Probability Mass Function
<i>RR</i>	Ramping Rate : $\delta P_{out}/\delta t$
<i>RRC</i>	Ramp Rate Compensation
<i>RTP</i>	Real-Time Pricing
<i>RMS</i>	Root Mean Square
<i>SoC</i>	State of Charge
<i>SVR</i>	Step Voltage Regulators
<i>SWMAC</i>	Sliding Window Moving Average Compensation
<i>ToU</i>	Time-of-Use
<i>VPP</i>	Virtual Power Plants
<i>WLS</i>	Weighted Least Squares

Chapter 1

Introduction

1.1 Overview

Utilities, faced with increasingly limited resources, strive to maintain high levels of reliability in energy delivery by adopting improved methodologies in planning, operation, construction, and maintenance [1]. From an economic stand point, deciding to implement any reliability criterion, and the corresponding system design, to satisfy such reliability requirements, should be based on comparison between the cost of providing extra reliability and the benefits accruing to the customers from the additional reliability [2]. As the electric utility industry enters an increasingly competitive environment in unregulated markets, utility companies must concern themselves with the market value of the services they provide and the cost of providing those services. At the same time, they are still burdened with the obligation to serve their customers with adequate reliability. Utilities must undertake new investments in demand-side resources such as but not limited to Demand-Response, active load management, distributed energy resources at secondary circuit level to meet those obligations [3]. The planning of electric power distribution systems is related to the analysis of the investments required to expand the distribution network because of the increase in energy

Chapter 1. Introduction

consumption and the need to serve customers with adequate quality and reliability [4].

Demand for electricity in the US is expected to grow by 22 percent, from 3,877 billion kWh in 2010 to 4,716 billion kWh in 2035 [5]. Residential demand is also expected to grow by 18 percent over the same period, to 1,718 billion kWh in 2035, spurred by population growth, rising disposable income, and continued population shifts to warmer regions with greater cooling requirements [5]. Commercial sector electricity demand is expected to increase by 28 percent, to 1,699 billion kWh in 2035, led by demand in the service industries. In the industrial sector, electricity demand has been generally declining since 2000, and it is estimated to grow by only 2 percent from 2010 to 2035, slowed by increased competition from overseas manufacturers and a shift of U.S. manufacturing toward higher efficiency practices [5]. Electricity demand in the transportation sector is small, but it is expected to more than triple from 7 billion kWh in 2010 to 22 billion kWh in 2035 as sales of electric plug-in vehicles increase [6]. The annual energy outlook released by the U.S. Energy Information Administration shows a steady increase in electricity usage in the United States [7]. The incremental usage of electric power is illustrated in Figure 1.1. Excluding large customers in industrial and transportation sectors, major portion of the total consumed electricity is delivered to the customers via power distribution systems, which consequently will face an increase in peak and average demand. Normal operation (also known as system intact or N0 contingency), is the condition under which all electric infrastructure equipment is fully functional. First contingency operation (also known as N1 contingency) is the condition under which a single element (feeder circuit or distribution substation transformer) is out of service. A feeder circuit should be loaded up to no more than 75% of its capacity under N0 conditions. For example, a 12MVA feeder circuit is designed to be loaded to 9MVA during normal operating conditions. This loading level provides reserve capacity that can be used to carry the load of adjacent feeders during first contingency N1 conditions [8].

Distribution systems load is estimated, measured and forecast with the goal of serving all customers during system intact and first contingency conditions. In the event of an outage

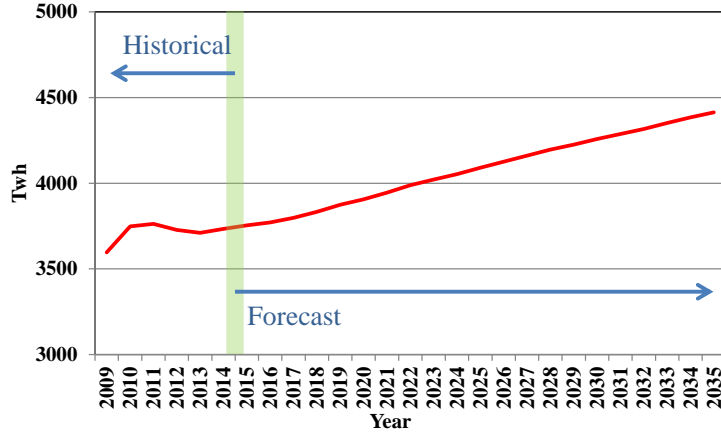


Figure 1.1: Historical and projected electricity usage in the US over the 27-year period ending in 2035.

of any single element in an electric power delivery system with adequate N1 capacity, all the services can be quickly restored through distribution system reconfiguration by means of electrical switching. Of the critical design and operations objectives, the followings are the most critical [8]:

- Adequate N1 substation transformer capacity
- No overload in normal (N0) conditions
- Adequate field tie capability for feeder first contingency (N1) restoration

Figure 1.2 illustrates daily load on a number of distribution feeders in Albuquerque for a 9 day period in July. Feeders H13 and S13 do not satisfy N1 contingency requirements for several hours during peak load hours.

Spatial and thermal limitations restrict the number of feeders between a distribution substation and the loads. Consequently, the substation size and capacity is bound by practical limitations. When new feeder circuits are added to a mature distribution system, minimum

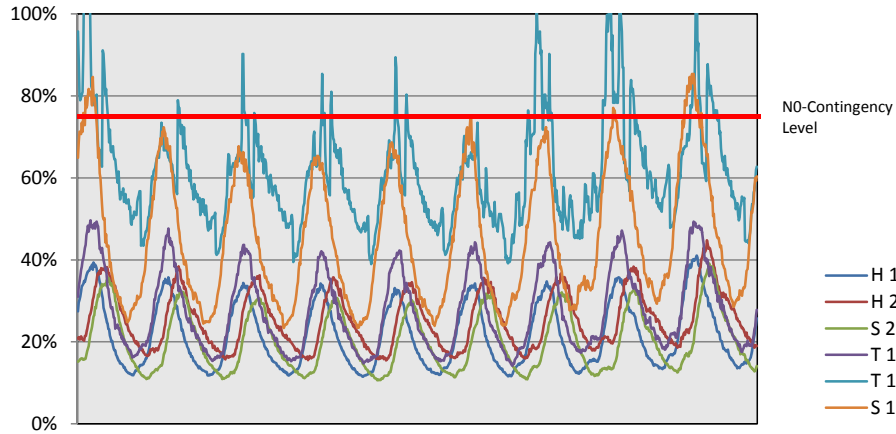


Figure 1.2: Load level on select feeders in Albuquerque in July 2012. Feeders H13 and S13 do not satisfy N1 contingency requirements (Data from PNM).

allowable spacing between feeder circuit main line cables sometimes cannot be achieved because of right-of way limitations or a high concentration of feeder cables. Adding express feeders (feeders dedicated to serve high-load concentrations at distant locations) requires cable installation across distribution service areas where they do not serve any customer load. Cable spacing limitations and/or feeder cable concentrations frequently occur where many feeder cables must be installed in the same corridor near distribution substations or when crossing natural or man made barriers [8].

A distribution feeder usually supplies energy to a variety of loads. A study shows that by mid 21st century, energy consumed in commercial and residential buildings and the peak load seen by the utilities will increase in the Southwest region of the US [9]. Moreover, the peak load months will spread out to spring and fall. The Pacific Northwest will be hotter in the summer. Longer and hotter summers will force the penetration and the usage of A/C systems in the Pacific Northwest to increase significantly over upcoming years [10]. Consequently, load pattern in many areas will change from a low summer cooling load and high winter heating load to summer peaking because of climate change. Overall, the Western US grid may see more simultaneous peaks across the North and the South in the summer months.

Chapter 1. Introduction

That puts more stress on the feeders already loaded close to their capacity and reduces the system's tolerance against possible disturbances [11]. Increased penetration level of the renewable energy resources such as PV may change this pattern however those resources in general reach their peak capacity at non-peak hours. Usually, PV generation peaks at noon and wind generation peaks at late night hours which in neither case peak generation coincides with normal peak load hours and therefore have limited effect on the expected load pattern.

Driven by steady research and development and increase in sales volume, the cost of deploying PV systems has been in constant decline since their first introduction to the market [12]. PV deployment has recently exploded into a number of industrial markets, where it is quite simply the lowest-cost source of power available. These include highway warning signs, rural irrigation applications and remote electrical and communications devices. Similarly, for any application more than about half a mile away from the electrical grid, a solar system will likely prove less expensive than will power line construction [13].

The most rapidly-growing segment of the solar industry is for “grid connected” systems, i.e. rooftop solar panels on homes or businesses that remain connected to the conventional electrical grid. In some cases, as where electricity is more expensive during the middle of the day, or when solar is used to support power-critical applications which require highly reliable source of power (e.g. banking, microchip manufacturing), the economics are very compelling without further incentives. In other places, comparatively modest state or federal incentives can make solar a great investment for home or business owners that improve every year [14].

Distributed PV generation has become a concern for many utility companies. Although the overall PV penetration level in the United States is not significant yet, increasing penetration of PV systems at the distribution level has raised concerns about future of distributed generation. The gradual increase in incorporating PV systems into power distribution networks has broadened potential areas for study. The potential impact that the high penetration of PV could impose on distribution system performance, and ultimately a feeder's

Chapter 1. Introduction

hosting capacity for PV, depends upon many factors, including such items as the distribution feeder characteristics, location of the PV along the feeder, feeder operating criteria and control mechanisms, and electrical proximity of PV on the circuit to other PV systems [15]. Some distribution circuits can accommodate considerably higher levels of PV penetration before their “health indicators” show signs of deterioration. A large PV system connected close to the feeder substation has a much different impact than when connected farther away from the substation. Distribution feeders that are short in length (cover a smaller area) and designed for higher demands, are capable of accommodating much higher levels of PV power and still operate in healthy conditions. Conversely, those that have wider geographic footprint may show signs of unhealthiness at far lower PV penetration levels. Geographic dispersity and load capacity are among the factors that must be taken into account when evaluating the impact of PV on distribution system performance. Those factors determine how much PV capacity could be accommodated respectively before the system is pushed beyond its design limits [16].

Similar to other distributed energy resources, increased PV power production can result in over-voltage problems in the distribution system. In addition, the variability of the PV due to partial cloud coverage can result in voltage flicker. Figure 1.3, illustrates the output power of an existing 500kW PV system during a seven-day period. On the second day, a typical sunny day, a small amount of cloud coverage in the afternoon causes relative reduction in PV power. Major concern in such a day would be the potential risk of over-voltage. In Figure 1.3, days 1,3,4 and 5 are typical cloudy days with white cumulus clouds passing through the area. During a partially cloudy day, output power of PV systems can fluctuate sharply. Ramping Rates (RR) close to 50% of nominal power per second are not unusual. RR in this context refers to rate of change in output power. Such sharp fluctuations may potentially impact voltage regulation and power quality and could result in excessive operation of On Load Tap Changers (OLTC) and switched capacitors which are designed to compensate or correct such irregularities [16].

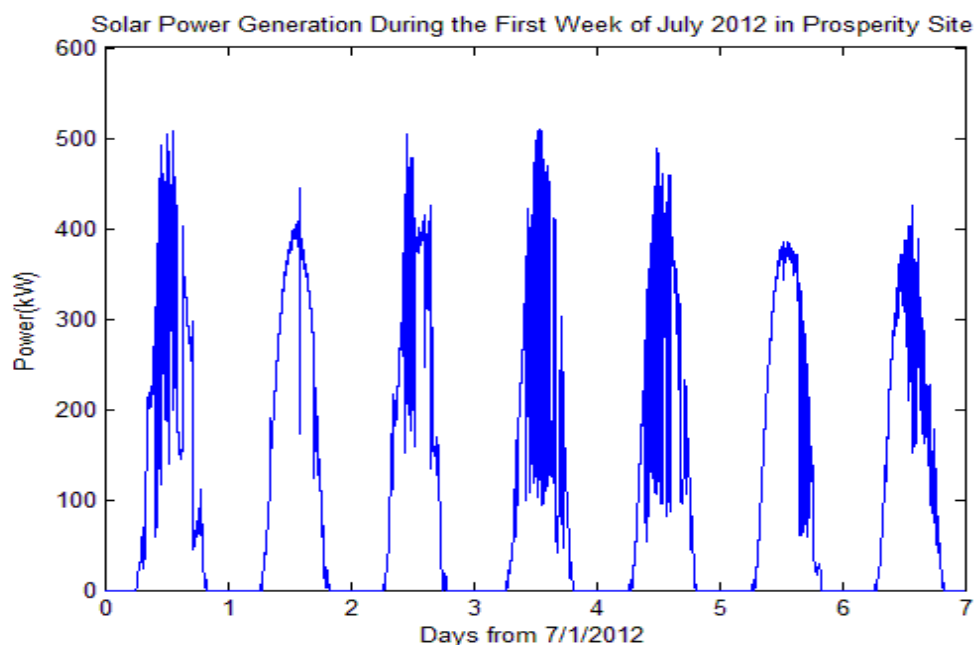


Figure 1.3: PV power at the Prosperity PV site during the first week of July 2012 (Data from PNM).

The topology of a feeder is traditionally a tree of conductors, transformers, switches and other equipment, utilized for protection and isolation, delivers electricity from the substation, the connection point of the distribution system to the transmission system, to the customers. Feeders are normally designed to accommodate unidirectional energy transfer. In such circuits, energy is delivered from a source (substation) to customers.

The increased level of penetration of DER systems in power distribution infrastructure presents various benefits such as resilience against cascading failures, access to more diversified resources and potentially reduction of the power loss in transmission and distribution. However, serious challenges and risks must be addressed to ensure continuity and reliability of service. By integrating necessary communication and control infrastructure into the distribution system, distributed generation units and loads will be transformed to controllable assets (energy resources) which provide substantial flexibility for the management and op-

eration of the distribution system. On the other hand, if operated in islanded mode, such complex distributed system is prone to instability and black outs due to lack of a major “infinite” supply and other unprecedented variations in load and generation.

The main task of a power system is to produce electricity and to deliver it to customers who consume it in a variety of ways. In traditional power systems, power plants are the sole responsible entities in charge of power generation. They participate in frequency and voltage control to guarantee a stable operation for the whole system. Grid stability could be threatened by the installation, at a high penetration level, of distributed generation units which don’t participate in frequency and voltage control and may have inherent intermittency. Such circumstances must be investigated on a case by case basis [17] because there is no unique configuration for power distribution systems design. DERs like PV generators, combined heat and power (CHP), community energy storage systems and micro grids which are gaining increasing interest, do not always provide frequency and voltage control. Their ever increasing deployment into the power grid and especially into low voltage distribution systems has raised questions about how they could affect the grid stability.

The concept of “smart grid” promises changes to the worldwide production, delivery and usage of electricity, in ways that are sometimes yet to be understood. Smart grids have several features including distribution automation, DER integration and management, demand-side management and advanced metering infrastructure (AMI). A broader definition of smart grids may include dynamic pricing criteria such as Real-Time Pricing (RTP) and Time-of-Use (ToU) rates as well. While which concepts do not explicitly define a smart grid, they may be necessary in some cases for distributed control practices which could be implemented in smart grids.

1.2 Focus

The Electric Power Research Institute (EPRI) is participating in a smart grid demonstration project funded by the Department of Energy (DOE) and in collaboration with the Public Service Company of New Mexico (PNM). At the time this research was commenced, PNM were interested in assessing impacts of the growing number of installed small generators (primarily roof-top PV) and Plug-in Hybrid Electric Vehicles (PHEV) on their distribution feeders. The University of New Mexico (UNM) is participating in the project by developing comprehensive models for several distribution feeders to analyze potential benefits of current trends toward DER deployment, while providing awareness of potential threats. Based on these models, several use cases have been developed and studied [18].

Of the distribution feeders studied as benchmarks for the future smart grid, Studio14 (ST14) which is located in Mesa del Sol, Albuquerque was more interesting. A 500kW PV farm and a 1MWh utility scale storage system which consists of a 500kW ultra fast smoothing battery and a 250kW shifting battery are connected to the feeder at a location relatively close to the substation. At a nearby location, a micro grid demonstration (NEDO) which incorporates a 240kW natural gas-powered generator (NGPG), a 80kW fuel cell, a 50kW PV generator, a lead-acid battery storage system, and hot and cold thermal storage is also installed and connected to the feeder through a 1000kVA transformer [19]. The utility scale battery storage system at Mesa del Sol has been under several tests to demonstrate its capabilities for smoothing the PV output in cloudy days, to shift the off-peak generated power of the PV system to peak consumption times and to firm the total PV/BES system as a dispatchable resource for the utility. One objective in this research is to devise and simulate some techniques which enable the system operator to take advantage of other available DER connected to the feeder and reduce the storage battery cycling. If financially and operationally plausible, implementation of such methods could substantially increase the expected life time of the Battery Energy Storage (BES) System and the associated power converters.

Chapter 1. Introduction

One type of DER that is gaining increasing interest is the microgrid, in light of increased needs for both energy efficiency and high reliability. A microgrid is a collection of DERs that, from the viewpoint of the utility, is controllable, acts as a single load, and is able to function in both grid-tied and islanded mode [20]. An islanded microgrid must have enough storage to compensate for any mismatch between load and generation while islanded.

A second type of DER that is receiving renewed attention is thermal storage [21]. In the commercial and residential building sector, cooling loads account for much of the peak demand (approximately 40%) [22]. Cold storage devices allow the cooling load to be shifted to periods of lower demand. While individual cold storage devices are too small to affect the overall system demand when acting, their aggregated action could be significant [23].

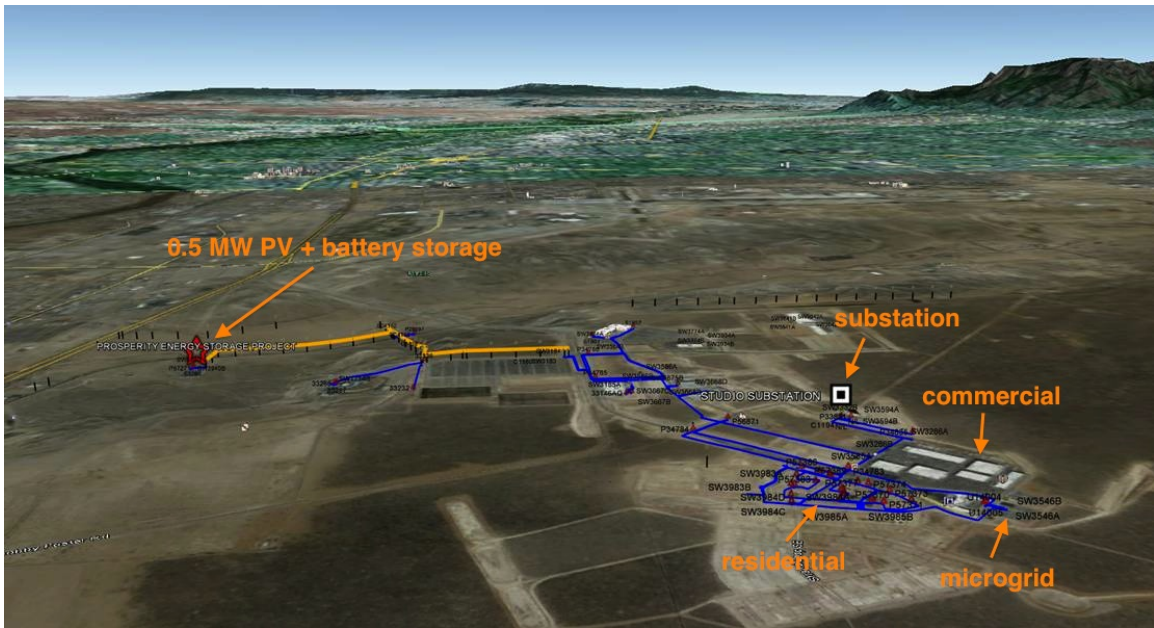


Figure 1.4: Studio14 distribution feeder in Albuquerque, NM, hosts a number of DER demonstration projects that could interact to maximize economic value and system performance.

Hybrid Electric Vehicles (HEVs), Plug-in Hybrid Electric Vehicles (PHEVs), and all-Electric Vehicles (EVs) – also called electric drive vehicles collectively – use electricity either as their primary fuel or to improve the efficiency of conventional vehicle designs. HEVs are

powered by an internal combustion engine or other propulsion source that runs on conventional or alternative fuel and an electric motor that uses energy stored in a battery. The battery is charged through regenerative braking and by the internal combustion engine and is not plugged in to charge. PHEVs are powered by an internal combustion engine that can run on conventional or alternative fuel and an electric motor that uses energy stored in a battery. The vehicle can be plugged into an electric power source to charge the battery. Some PHEVs are also called Extended Range Electric Vehicles (EREVs). EVs use a battery to store the electric energy that powers the motor. EV batteries are charged by plugging the vehicle into an electric power source. EVs are sometimes referred to as Battery Electric Vehicles (BEVs) [24]. PHEVs and EVs are gaining interest among consumers. Although their popularity is yet to increase significantly, advances in battery technologies, financial incentives and increase in fossil fuel prices will help those become a major game changer in the area of personal transportation while showing remarkable advantages in commercial fleet and public transportation [25]. If not managed properly, overloading of the distribution feeders due to EV charging, could be very disruptive. Deploying large numbers of EVs and PHEVs without enough attention to their collective charging effects will not only increase the total demand on the distribution feeders but also can reduce the life time of the transformers and other distribution system assets.

Due to potential benefits hidden in the energy stored in their batteries and also adverse effects on power grids during the charge cycle, PHEVs and EVs have received attention from researchers in the power distribution industry. Lopes *et al.* [26] presented a conceptual framework to successfully integrate electric vehicles into electric power systems. Their proposed framework covers two different domains: the grid technical operation and the electricity markets environment. Their study continues with several simulations illustrating the potential impacts and benefits of the EV to grid integration, both steady-state and dynamic. Effects of uncoordinated charging, multi tariff and smart charging of a population of EVs are then compared. Galus and Andersson [27] introduced an agent based energy hub system for PHEV integration. In such a system, nonlinear pricing is adapted to model and manage

Chapter 1. Introduction

recharging behavior of a large number of autonomous PHEV agents connected to an energy hub. The proposed scheme incorporates price dependability. An aggregating entity, with no private information about its customers, manages the PHEV agents whose individual parameters are set based on their technical constraints and local objectives.

Dyke *et al.* [28] simulated a futuristic electrical network, in which a symbiotic relationship between electric vehicles is incorporated to effectively and economically dispatch the electricity and to eliminate a necessity for installing large fast-responding generation units. That scheme would allow the unused capacity of the batteries installed in the electric vehicles to form a dispatchable resource. Such a resource could be utilized to compensate the peak consumption and fluctuations of the fast acting loads. Results also show that, to promote EVs to become the preferred road transportation vehicle in the future, a significant investment in electrical infrastructure would be urgently necessary.

Introduction of distributed energy resources into the power distribution systems on the one hand provides opportunities for grid operators and customers and on the other hand challenges the utility companies to change their traditional planning and operating methods. It is imperative for the researchers, planners and operators to identify potential challenges, threats and opportunities due to the large scale implementation of DERs. To develop a broad understanding about costs and benefits of such “smart grid” teams of researchers from all around the world have made significant efforts and result are presented in numerous journals and conferences.

A different approach is pursued in this research. It is first started from developing detailed models of the existing distribution feeders which share many characteristics with the near future smart grid. Potential challenges are then reviewed and the applicable ones are selected for further investigation. A topology based approach modified to fit the physical characteristics of the power distribution systems is then elaborated to detect electric hubs (driver nodes) which have the potential to drive the behavior of the distribution grid. It is then shown that without proper coordination between various DERs it is almost impossible

to fulfill necessary power quality measures. A few scenarios based on the available resources are later defined and studied. Results are used to define a comprehensive method which could be tailored based on each particular case. Necessities and benefits of such system of coordinating resources are ultimately established.

1.3 The Road Map

By January 2010 the PNM smart grid demonstration project was under development and teams in ECE and ME departments at UNM were partnering with PNM and DOE to lead the research aspects of the smart grid demonstration. It was planned to build an extensive model of the available system and use it for further investigations.

Early phases of the study were mostly focused on data gathering and model development. At PNM, the main resource for distribution system data, the corresponding teams did an extensive work to extract and provide the required data from their Geographic Information System (GIS), not originally designed to perform time series analysis down to the load level. There were also broken links between the GIS data and the customers because the most granular information on the system was the secondary transformer.

Since there was no standard tool available to translate the GIS information to GridLAB-D or Open-DSS scripts, the required tools were developed. Translation included extracting all power delivery equipment data from the source (the substation transformer) to the loads and putting those equipment as components in the model. Since the behavior of the protective and switching devices such as fuses and breakers was not important for this research and essentially it was assumed that during the course simulation the configuration of the grid would remain unchanged, it was realistic to replace all those equipment with very low impedance conductors in the model.

A time consuming part of the job was debugging the model. There was no standard

Chapter 1. Introduction

debugging tool for either of the software packages and due to high number of nodes in well developed distribution feeders it was not practical to debug the models manually. Therefore, necessary software tools were developed which were later used to debug the feeder models and detect and remove broken points.

Next step for the research was to meet the needs for an extensive computation load. The required memory and processing power to run the simulations grow rapidly when the number of nodes increases, which is the case for most distribution feeders. The UNM center for high performance computing (HPC) provided the foundation for building and running the models on their parallel processing machines. GridLAB-D models of the targeted distribution feeders were successfully built on the HPC machine. There was no compatible version of Open-DSS available, therefore Open-DSS models were only run on a Windows machine. Larger models with more resource intensive simulations were executed on a HPC machine.

After building fully functional models, the study continued along the following paths:

- To simulate the prospective high PV penetration scenarios for PNM on some of their distribution feeders,
- To detect the nodes in the studied distribution feeders which could have potential voltage or load problems,
- To build a topology model of the feeders to designate the high connectivity and central nodes,
- To build different case studies to investigate potential benefits and limitation on the use of DER systems,
- To draw a road map to develop case based solutions based on available resources and targets.

The first chapter in this dissertation provided an introduction and a big picture of the materials covered by the research. The second chapter includes a review of the related works

Chapter 1. Introduction

of other researchers active in this field. Chapter 3 demonstrates solutions and results of different simulations based on the defined scenarios. In chapter 4 a summary of the different paths and a conclusion on how the methods introduced in chapter 3 could be aggregated into a comprehensive solution is provided.

Chapter 2

Literature Review

2.1 Distributed Energy Resources

Recent advances in small scale power generation, increasing concerns about CO₂ emissions, uncertainties about foreign oil supplies, high start-up costs coupled with growing public opposition over safety in nuclear reactor construction [29] and electricity business restructuring are the main factors responsible for the growing interest in the use of DER. It is argued that the connection of small generation units to low voltage networks has the potential to increase the reliability of the delivered power to final consumers. On the other hand, it can bring additional benefits for global system operation and planning [30]. The concept of integration of DER into the power grid includes small generators, energy storage, load control and – for certain classes of systems – advanced power electronic interfaces between the generators and the bulk power provider [31]. Incorporating a large number of small scale local energy resources into distribution systems has urged researchers, planners and designers in this field to investigate potential draw-backs while trying to take the most advantage from possible benefits and opportunities.

From the utility perspective, a smart microgrid can be regarded as a controlled entity

within the power system that can be operated as a single aggregated load [31]. Existing studies have investigated many microgrid architecture designs and control strategies. Piagi and Lasseter have proposed methods for autonomous control of each micro-source contributing to keeping the feeder health factors in the required range while maintaining feeder operation even during islanded periods [32]. Lu *et al.* have considered a DR method along with other DER to achieve the required control over the microgrid to maintain its operation in islanded situations [33].

Grid tied power systems currently have storage in the form of generator's inertia, which maintains the system's frequency during sudden changes in the total system load or supply. According to [31], a microgrid can not usually rely only on its own generator's inertia and must provide some form of storage to ensure continuity of power balance. Adequate total storage capacity in the system is a necessary prerequisite for decoupling voltage and frequency characteristics of the system from load variations.

On the other hand the induced fluctuations due to the intermittent nature of the renewable energy resources like solar and wind, implies incorporating some type of storage system to decouple voltage and frequency characteristics of the system from sudden changes in the supply, when the penetration level of the renewable sources becomes large. The most promising energy storage systems which have been appearing quickly are flywheel and battery energy storage technologies. They are also installed in smart grid demonstration projects [34, 35]. There are some hydraulic storage systems (Pumped-Hydro) in use, but those require a specific geography that permits the deployment of those systems [36]. Necessity of such "specific geography" limits the penetration of Pumped-Hydro systems [37].

For years, researchers have dedicated great efforts studying various effects of high PV penetration levels and suggested solutions to the problem. Thomson and Infield conducted detailed simulations of a very high penetration of PV within a typical UK urban distribution network [38]. Their study performed unbalanced three-phase load-flow analysis on an entire feeder within a time-domain simulation framework using load and generation data at

1-minute intervals. Their study results indicate that even at very high penetrations of PV, network voltage rises are small and unlikely to cause problems [39]. A team in the Electric Power Research Institute (EPRI) introduced some methods for modeling distributed PV systems and incorporating the developed models into a framework for analyzing the power distribution systems [40]. To perform high-penetration PV analysis, their study concentrates on developing models for PV systems while focusing on variability and its potential impacts on voltage regulation, short-circuit capacity, reactive power control and harmonic analysis. Authors have also investigated specific impacts, analysis methods and a summary of available software tools used to support such simulations. Feng and Wei [41], studied a typical structure of distribution network, analyzed the power flow and set up the simulation model. Their simulations on different cases show that in mid-voltage or low-voltage distribution networks, reverse energy flow from distributed generation (DG) systems is the primary reason for voltage quality problems. Moreover, variations in active power balance in presence of a relatively high line impedance ratio (X/R), which is common in distribution systems, deteriorates the power quality. Voltage quality could be improved by injecting (and sinking) reactive power to regulate the bus voltage by means of inverter-based DERs. Kato *et al.* [42] proposed a method to estimate the standard deviation of the bus voltages in presence of high penetration levels of distributed PV systems dispersed in a large area. According to their report, the risk of losing load frequency control in presence of high PV penetration in the area is imminent.

In a survey [43], Joseph A. Carr *et al.* investigated ways to mitigate the unreliability of many renewable DERs due to the intermittent nature of their supplies, by using energy storage (ES) systems. It is claimed that by incorporating ES systems, additional benefits including load leveling, frequency control, and power quality compensation could be attained. However, to adopt these technologies, some barriers such as the need for interfaces between the different voltage levels and waveforms produced by the various systems must be overcome.

Wei Wu *et al.* [44] have discussed new opportunities and challenges to intelligent mar-

keting by large-scale application of DERs. They have proposed a developmental outlook of DERs, in which information management of three-level control, principle of power-consumed, virtual marketing, and demand-side guidance with distributed generation (DG) units are introduced.

Pudjiant *et al.* [45] described the “Active Future” DER in which DERs and demand side management are fully integrated into network operations. In such a future grid, demand side management along with adequate distributed generation and storage will be responsible for :

- Delivery of system support services,
- Taking over the role of central generation.

To accomplish that mission, a shift from the traditional central control to a new control paradigm of coordinated centralized and distributed control of distribution networks will be necessary. According to the proposed road map, a future active, smart distribution network can provide:

- Frequency and voltage control,
- Back up and reserve,
- Black start,
- Network management,
- Other functions such as demand shaping, automation in system operation and monitoring.

Zhu and Tomsovic [46] investigated the benefits of DERs as providers of ancillary services such as load following and contingency reserve in distribution systems. In their report, slow

dynamic models for microturbines and fuel cells were presented to explore the benefits of providing energy and ancillary services from DERs. They derived an adaptive power flow algorithm, appropriate for the simulation of slow dynamics in the distribution systems. An optimal distribution power flow strategy for coordinated dispatch and operation of DERs is also developed which decomposes the overall system problem into two sub-components:

- Economic dispatch for energy and ancillary services
- Power loss minimization

The authors believe that there are several reasons enough for local procurement of the ancillary services as opposed to acquiring them from a competitive ancillary service market. Among those reasons, the following were deemed more important:

- Use of remote sources might be prevented due to congestions in transmission level,
- Local services such as voltage control are generally more effective and more efficient than remote services,
- It might be more reliable to provide ancillary services from several local small resources than a few large and most likely remote central resources.

2.2 High Penetration Level of Distributed Resources

The increasing penetration rate of distributed generation, in form of renewable resources such as wind and PV, is likely to change the behavior of the power grid. An active contribution of the available distributed resources which includes coordinated operation of the controllable ones with respect to the balance will be required to cope with the potentially negative impacts of a high penetration level of uncontrollable resources [47].

On the other hand, an increase in penetration level and share of uncontrollable energy resources, usually the renewables, necessitate the incorporation of a new ancillary service to ensure the reliability of the power distribution system. According to Rahimi [48], this new service may be characterized by either “Slow Regulation” or “Net Load Following” and is based on the need to have adequate 5-minute (slow) dispatchable capacity to counteract the combined fluctuations in load and variable generation. which otherwise necessitate utilizing the relatively expensive 4-second (fast) regulating products to follow such fluctuations.

Zong *et al.* argued that the task of controlling the system becomes increasingly demanding by the time integration of 50% wind energy into electricity system by 2025 in Denmark is accomplished. By achieving that milestone, strong demands on flexibility in the system will be unavoidable. The research team exploited a research facility for exploring the technical potentials of active load management in a distributed power system. That power system is characterized by a high penetration of renewable energy resources. The research has been concentrated on how to implement a thermal model predictive controller for power consumption prediction [49].

Due to limited availability of the ancillary services, without establishing adequate ancillary services, the technical constraints of the conventional generators in small autonomous islanded systems result in limited ability to incorporate renewable energy sources (RES) in vast scales. Vrettos and Papathanassiou think that to overcome such limitations, energy storage would be a necessary element. In very small islanded systems battery energy storage (BES) systems constitute viable solutions with considerable potentials. In their study, the sizing of the hybrid system components is then investigated by conducting a parametric analysis and then optimized by applying genetic algorithms [50].

Farag *et al.* [51] proposed a control structure consisting of a multilayer distributed multi-agent framework to tackle technical challenges caused by high penetration of DGs. They have divided the multi-agent control structure into three main layers of intelligent agents, regional coordination agents and distribution management system (DMS).

Smith *et al.* [52] considered certain characteristics in the system impact and planning processes to effectively evaluate the outcomes of deploying renewable resources at high-penetration levels in power distribution system. Of those, the time-varying nature of the renewable resource and location-based impacts are proven to be the most important.

Zhao *et al.* [53] focused on high penetration of PV systems paired with micro-inverters operating under burst mode. They found out that although under light load conditions, this combination tends to improve efficiency figure, it creates power quality impacts to the grid. After small scale burst mode operation has been studied, the results are applied to a large-scale power system for high-penetration PV studies. Their study indicates potential voltage flicker in cases with high penetration levels. In those micro grids in which PV was the main energy source, the flicker issue could be intensified.

Lin *et al.* [54] investigated the stochastic nature of electric loads connected to the distribution networks. They realized that because of the intermittent nature of the solar irradiance, high penetration PV will intensify the randomness of power tracking in the distribution network. These stochastic processes can cause a great difference between the actual power flow and the associated predictions. That in return will make power generation planning difficult. They have also researched the effectiveness of energy storage systems in solving the fluctuation issues in power generation in cases with high penetration of uncontrollable resources. According to them, optimization of power and capacity in energy storage devices is critical to successfully implement this concept in practice.

A coordinated control method for distributed energy storage systems is proposed by Liu *et al.* [55]. Traditional voltage regulators including transformers with On Load Tap Changer (OLTC) and Step Voltage Regulators (SVR) are suggested to solve the voltage rise problem caused by the high PV penetration in the low-voltage distribution system. The main objective of the proposed method is to relieve the OLTC operation stress, to shave the peak load and to decrease the power losses while taking advantage of high PV penetration. In the proposed control method, the energy storage depth of discharge is limited to extend

the life expectancy of the batteries as much as possible.

Estanqueiro *et al.* [56] focused on barriers and solutions for high wind penetration in power systems. They understood that the use of “frequency flexible” power electronics would provide a relevant contribution to power system robustness. According to them, that could be accomplished by avoiding the disconnection of grid electronic interfaced wind generators from the grid when the resource induced disturbances take place.

2.3 Distribution Grid and Load Modeling

Incorporating a proper modeling tool in design, deployment and operations is critical in modern electric power systems. This is especially true of the emerging generation of technologies such as voltage optimization, demand response, electric vehicle charge and discharge, distributed intermittent energy resources and energy storage [57]. There are many efforts to build partial or comprehensive models of the new elements of a smart or revolutionized distribution system. Acha *et al.* [58] proposed a power flow tool that performs a simultaneous assessment on some technical impacts that a high penetration of heat-driven co-generation units may have on power networks. Mihalache *et al.* [59] modeled a distribution system with different levels and types of renewable energy resources and analyzed dynamic behavior in Matlab/Simulink using the IEEE 34 bus system as a candidate testbed. Eajal *et al.* [60] modeled the distribution system by developing detailed models for system components in order to conduct harmonic power flow analysis and optimum capacitor placement and sizing. There are also many commercial packages designed to simulate distribution systems able to model unbalanced multi-phase systems for radial, looped or meshed networks [61].

Wen *et al.* [62] investigated a methodology to construct power system load models using intelligent learning techniques based on system measurements. They have proposed a load model to represent the loads in a limited area. In their approach, a genetic algorithm (GA) based on population diversity is developed to obtain the structure and parameters of the

load model.

Wan and Miu [63] focused on Weighted Least Squares (WLS) approaches to the problem of load estimation (LE) in unbalanced power distribution systems. A WLS load parameter method and a DSE solver method are introduced for load estimation.

To develop the next generation of online energy management methods, Palensky *et al.* [64] studied a simulation environment for demand response (DR) algorithms with large-scale grid simulations. It includes an accurate but computationally inexpensive dynamic model for domestic housing and small business loads and simulates the state changes of thermostatically controlled processes, yet with minimal complexity. In this approach, building operations provide services to contribute to grid optimization and reliability. The essential electric loads providing such services are heating, ventilation and air conditioning (HVAC), lighting and pumps. The available thermal inertia in the buildings is simulated as a virtual energy storage system. In their research, the authors have also considered a third degree of flexibility provided by PHEVs, which if well utilized, can store and supply energy when necessary.

Qian *et al.* [65] presented a methodology for modeling and analyzing the load demand in a distribution system in presence of connected electric vehicles. The suggested stochastic method accounts for the stochastic charge time and the initial battery state-of-charge. Different scenarios are investigated based on uncontrolled charge, uncontrolled off-peak charge, coordinated charge and uncontrolled community charge. Their approach also included developing a numerical model for EV battery charging load which allows a statistical distribution of the states of charge of the batteries at the beginning of the charge cycle, and a stochastic distribution of the start to charge signals.

2.4 A Complex Network Approach

Topological analyses of a wide variety of networks has yielded detailed theoretical insights into the behavior and evolution of the systems they support. Many classifications of network structures are studied and some comprehensive reviews are reported in the field of complex systems, statistical mechanics, and social networking [67, 68]. The random network of Erdős and Renyi [69] and the “small world” [70, 71] are the two most influential models. In a random network model, nodes and edges are connected randomly. The small-world network is defined largely by relatively short average path lengths between node pairs, even for very large networks. An important class of small world networks is the “scale-free” [71, 72], which is characterized by a more heterogeneous connectivity. In a scale-free network, most nodes are connected to only a few others, but a few nodes (known as hubs) are highly connected to the rest of the network. An important property of a scale-free network is a power-law distribution of node connectivity or degree.

Power grids as networks of transmission lines (edges) and substations/interconnections (nodes) are studied since the emergence of the complex systems researches. Hines *et al.* [73] showed that power grids differ substantially from abstract models in degree distribution, clustering and diameter. They concluded that those abstract models do not provide adequate information for understanding the behavior of power grids. Watts and Strogatz measured the characteristic path length and clustering in power grids, and found similarities to “small world” network models [71]. Some studies measure the degree distribution of various power grids. Amaral *et al.* [74] concluded that the data from electric power grid of Southern California reject the hypothesis of power law distribution for the connectivity. Albert *et al.* [75] classify the western power grid as a single-scale network. Crucitti *et al.* [76] demonstrated that the structure of an electric power grid is able to tell important information on the vulnerability of the system under cascading failures. They reported power-law/scale-free degree distributions for the GRTN Italian grid, which is very homogeneous in the node degree, but shows a high heterogeneity in the node load. Most nodes handle a small load, but there are a

few nodes that have to carry an extremely high load. Chassin and Posse [77] used scale-free network models to better quantify grid resilience.

Study of the behavior of the electric power grid as a whole would be helpful to have an idea in real time of what happens following a given external perturbation [76]. Traditional models are developed to perform the structural vulnerability analyses and are employed in real-world networks [78]. Historical data shows that the frequency of occurrence of major black-outs and the number of affected customers are not reduced over the course of electrification history [79]. That is a major reason for researchers to find network-based solutions for avoiding black-outs and brown-outs. In Appendix A some metrics used in classical analysis of the networks are reviewed.

2.4.1 Power Network Specific Topological Model

The topology-based methods mentioned previously ignore the electrical characteristics of power grids. A significant shortcoming of those methods is that they measure the network structure of electrical grids without incorporating the physical laws governing the flow of electricity within those networks. Current flowing through the network is governed by Kirchhoff's laws and not by the network's structural topology. To perform more accurate analyses, complex network theory must be combined with electrical characteristics [80]. To address incorporation of physical laws into the network structural studies, Hines and Blumsack [81] introduced an electrical connectivity metric named "electrical centrality" which utilizes the information contained in the system impedance matrix. Brandes and Fleischer [82] proposed two centrality measures based on Kirchhoff's Law and current flow. Chen *et al.* [78] calculated electrical efficiency based on the admittance matrix but still assumed that power was transmitted through the most effective paths. Bompard *et al.* [83] defined an electrical betweenness metric based on the power transmission line flow limits, and proposed a new

index called net-ability to evaluate the vulnerability of power grids.

To study specific power grids topological model, some simplifications are deemed necessary. In the undirected graphs each node represents a bus. It is important to note that in the physical grid, buses can have different electrical properties, however in this chapter, nodes are assumed to be homogeneous. Therefore, generators, loads or other shunt connected equipments connecting to the bus are all treated the same as nodes. In the same way, all transmission lines and transformers are modeled as edges with equal weights. Physical length and electrical impedance are ignored in the undirected graph representation. However, electrical impedance of the lines is later used to demonstrate a novel concept of “effectiveness”.

A reasonably complete characterization of the network structure of the power grid would need to incorporate the following properties of electrical systems [81]:

- Flow in a power network is governed by Kirchoff’s Laws and not by decisions made by individual actors at individual nodes [81].
- Power networks are best described by undirected graphs. However, due to the highly non-linear and generally non-convex nature of the equations that govern power flow in AC electrical systems, it is possible that small changes in the state of the network can reverse the direction of power flow along a particular path [81].
- Because flows are governed by Kirchoff’s laws, there is no a priori way to tell whether the hubs represent generators, load centers, substations or other physical structures.

Hines and Blumsack [81] examined the differences between power networks and other generic network models. First, they used the information contained in the network impedance matrix to calculate equivalent electrical distances between pairs of nodes and examined the properties of the graph based on this distance metric. Second, they constructed the

“electrical” networks and the electrical properties of these networks were compared with those of an actual network of a similar size.

Mathematically, the power network equations can be formed in the bus form in which the performance is described by n linear independent equations for $n+1$ nodes. The characteristic equation can be described by Kirchoff’s Laws as:

$$\bar{I}_B = \bar{Y}_B \cdot \bar{V}_B, \quad (2.1)$$

where \bar{I}_B is the vector of injection bus currents. The usual convention for the flow of current is that it is positive when flowing toward the bus and negative when flowing away the bus. \bar{V}_B is the vector of bus or nodal voltages measured from the slack bus and $\bar{Y}_B = (Y_{kl}^{bus})_{n \times n}$ is the bus admittance matrix [84], where

$$Y_{kl}^{bus} = \begin{cases} G_{kl} + jB_{kl} & k \neq l \\ -\sum_{k \neq l} (G_{kl} + jB_{kl}) & k = l \end{cases} \quad (2.2)$$

The definition of the Y_{bus} matrix used here captures both the real and reactive portions of the line admittances. In this analysis the inverse of the Y_{bus} matrix is used which is traditionally denoted the Z_{bus} (or impedance) matrix. Inverting the sparse Y_{bus} matrix for a fully connected electrical power network, yields a non-sparse (dense) matrix, denoted Z_{bus} . The equivalent electrical distance between nodes k and l is thus given by the magnitude of the relevant entry of the Z_{bus} matrix. Smaller $|Z_{kl}^{bus}|$ corresponds to shorter electrical distances. In other words, if a scale-free or random network has properties similar to Kirchoff’s Laws, it will be very difficult to contain the propagation of information to a small area. The power network has substantially more information propagation than that shown by the second neighbor lattice structure, but much less than the random and scale free test cases [81].

2.5 Control Concepts and Strategies for DER

Dang [85] defined an Energy Web as a power ecosystem in which information and communication technology can revolutionize power market and power on demand. Some technical barriers and challenges have to be overcome before such energy web becomes fully functional. Among them real-time metering, real-time pricing, standard control and communication for DERs, price-smart power network nodes and “DER ready” power distribution network are the most important. In such a system, the real-time price signal is generated and sent to the participants using real-time data from the power markets and the energy flow is monitored in real-time by the system operators.

Robinett and Wilson [86] developed the swing equations for renewable generators connected to the grid. Those equations for the renewable generators are formulated as a natural Hamiltonian system with externally applied non-conservative forces. A two-step process is used to analyze and design feedback controllers for the renewable generators system. Their proposed formulation justifies the decomposition of the system into conservative and non-conservative systems to enable a two-step, serial analysis and design procedure. This formulation demonstrates the effectiveness of proportional feedback control to expand the stability region. The Second Law of Thermodynamics is then applied to the power flow equations to determine the stability boundaries (limit cycles) of the renewable generators system. Necessary and sufficient conditions for stability of renewable generators systems are then determined based on the concepts of Hamiltonian systems, power flow, exergy (the maximum work that can be extracted from an energy flow) rate and entropy rate.

A. Vaccaro *et al.* [87] studied optimal voltage regulation in a smart grid. They proposed the concept of a decentralized non-hierarchical voltage regulation architecture based on intelligent and cooperative smart entities to overcome the shortcomings of the traditional hierarchical control paradigms where the constant growth of grid complexity and the need for high penetration of DERs require more scalable and more flexible control and regulation

schemes. They suggested the adoption of a series of distributed controllers, each regulating the voltage magnitude of a specific smart grid bus by utilization of a set of sensors acquiring local bus variables and of a dynamical system (oscillator) initialized by sensor computations. In such a system, the oscillators could quickly synchronize to the weighted average of the variables sensed by all the controllers in the smart grid. Each voltage controller then can assess the important operational parameters of the smart grid in a decentralized way.

Over the course of their studies, Pu *et al.* concentrated on a smart grid demonstration project in the Pacific Northwest involving 60,000 customers from 12 utilities, covering from generation to consumption, built around an infrastructure of deployed smart meters. They defined a transactive control method which can be used to manage distributed generation and demand response. In such hierarchical but decentralized control system, each node of the power grid uses local signals of demand and price to match supply with demand at varying frequencies. All responsive demand assets bid into and controlled by a single, shared, price-like value signal, which may be influenced by local and regional operational objectives of the power distribution grid [88].

Shah *et al.* [89] proposed a power management scheme for a smart microgrid, utilizing a power electronic transformer (PET) at the point of common coupling (PCC). This decentralized control strategy utilizes the change in local grid frequency to control the active power generation and consumption within the microgrid. The PET allows restricted active power flow to the microgrid, at the PCC, at a desired value. In the grid connected mode of a microgrid, the DGs are controlled to supply a pre-set value of active power. In the event of a sudden load change in the microgrid, the active power flow at the PCC can vary significantly which may be undesirable during the peak load demand from the power system grid. In their proposed topology, the PET substitutes the conventional distribution transformer. In this scheme the PET ensures that only a predetermined value of active power is made available to the microgrid which results in a decrease in grid frequency within the microgrid. It could be sensed locally by the DGs and the controllable loads. To operate in sync with the grid, load

demand is dynamically controlled. Thanks to the PET, the two AC systems at either side of the PET can operate at different frequencies. Therefore, smooth transition from islanded mode to grid connected mode can be achieved without grid-frequency synchronization. This also provides with an extra degree of freedom for the microgrid in a possible deregulation and market strategy within the microgrid.

Zhenhua Jiang [90] presented an agent-based control framework for DER microgrids. In this study, it is indicated that the agent-based control framework is effective to coordinate the various DERs and manage the power and voltage profiles. Agents, in a DER system, can make decisions with limited information received from a central system coordinator. To achieve this autonomy, the agents are driven by a set of driving rules such as: “Charge the batteries when the cost of purchasing electricity and SoC are simultaneously low.” In addition, availability of the resources regulated by the agent affect the level of autonomy of every agent. Such agents should be able to perceive the changes in their environment and respond to those changes whenever necessary. They also have proactive abilities to maintain and achieve their own targets and not just react to external motives and to do such, they initiate necessary actions. Social capability is another important aspect of the agents characteristics. Self-organization is a prerequisite for the agents to operate independently in the system. By being self-organized, the agents contribute to scalability and robustness of the microgrid. They can join or leave the microgrid at their own discretion.

Pedrasa *et al.* [91] developed a methodology for making robust day-ahead schedules for controllable residential DERs to provide the most benefits to the consumers from energy services and not necessarily from electric energy. It maximizes consumer net benefit by scheduling the operation of DER. That schedule is derived using a stochastic programming approach. Consumer net benefit is characterized by an objective function to be maximized over a set of conditions covering a range of uncertainties. The proposed scheduling results in a lower expected cost however at a higher computation cost. To reduce such costs, the consumer can prepare some predefined DER schedules and simply choose the one to

implement. The stochastic optimization problem may then be solved by converting it to a substitute deterministic optimization problems.

The market oriented smart grid concerns the energy market and not the network operations, and it aims to increase the level of interaction between electricity suppliers and retail consumers. According to Slootweg *et al.* in such scheme, consumers receive more advanced pricing schemes based on power exchange prices driven by unbalance markets which reflect the availability of energy from various sources. Consequently, prices reflect the cost structure of electricity production and the availability of energy. The grid oriented smart grid concept, defined in the research, only concerns the grid operator, to reduce investments in grid reinforcement, supporting outage restoration as well as semi-automated restoration of the network after outages. This concept focuses on two major goals of optimizing utilization of network capacity and minimizing the number and duration of supply interruptions. A system oriented smart grid aims at optimizing the system, to maintain the energy balance grid service continuity. The system oriented smart grid concept includes the grid operator and at the same time enables the grid oriented smart grid concept by establishing the required data collection and communication equipment. This concept is essentially a combination of the previous two. Both energy market and local capacity are controlled by dedicated price information. Consequently, the communication infrastructure plays an even more important role to make this possible. The market oriented smart grid concept intended to enable retail consumers to participate in the electricity market which implies the need for price information. The grid operator although not an essential player in this concept, can facilitate data exchange and communication [92].

A distributed model predictive control (MPC) framework, suitable for controlling large-scale networked systems such as power systems is presented in studies done by Venkat *et al.* [93]. In their research, the overall system is decomposed into subsystems, each with its own MPC controller, each works iteratively and cooperatively. The suggested model-based control strategy uses a prediction of system response to establish an appropriate control

response. The distributed MPC controllers must account for the interactions between the subsystems. Each MPC determines the optimal current response and generates a prediction of future subsystem state. According to their study, distributed MPC offers controller coordination and performance improvements and reduces the burden associated with centralized control. This concept relies on decomposing the overall system model into subsystem models. A system comprised of Formula interconnected subsystems will be used to establish these concepts. In this decentralized modeling framework, it is assumed that the interaction between the subsystems is negligible and the effects of the external subsystems on the local subsystem are negligible and ignored.

Franco *et al.* [94] addressed the problem of cooperative control of a team of distributed agents with decoupled nonlinear discrete-time dynamics. In this study, agents are assumed to evolve in discrete-time, based on local control laws and by coordinating with a subset of neighboring agents. The cooperative control problem is formulated in a receding-horizon framework, where the control laws depend on the local state variables and on delayed information gathered from cooperating neighboring agents.

Delghavi and Yazdani [95] proposed a voltage/frequency control strategy for the islanded operation of a set of dispatchable DERs based on a discrete-time mathematical model. Their proposed control strategy utilizes a combination of deadbeat and repetitive control to enhance the performance of the control system under unbalanced and/or distorted load currents while maintaining the effectiveness of the repetitive control under variable frequency operational scenarios. In their suggested solution, the control strategy employs feedforward compensation techniques to mitigate the impact of load dynamics on the regulation process. Under the proposed control strategy, the DR units offer black-start capability, are robust to load switching incidents, and can be employed for decentralized frequency and voltage regulation.

Nian and Zeng [96] studied a control strategy for a DG system in stand-alone (islanded) mode. In such a system, voltage and frequency are controlled by the load-side inverter

under unbalanced and non-linear load conditions. A dual-loop control method based on a stationary reference coordinate is suggested for the load-side inverter. The outer-loop voltage controller consists of a proportional controller and a resonant regulator tuned at low-order harmonic frequency which compensates for the low-order harmonic components of the output voltage. A predictive current control scheme based on space vector modulation is adopted in the inner-loop current controller to improve the transient performance under the sudden load disturbances.

Zong *et al.* [97] introduced an experimental platform to demonstrate control and power system communications in distributed power systems. A thermal MPC to predict the heaters power consumption is defined which can realize load shifting to better matching of demand and supply.

Piagi and Lasseter [98] investigated the technical difficulties related to control of a significant number of DERs keeping in mind that a failure of a control component or a software error will bring the whole or major parts of the system down. They claimed that the issue of optimal placement of the resources could be tackled by keeping in mind that DGs don't all have to be placed together but can be located where the loads are needed. A sub optimal placement of those resources could be foreseen. According to this study, the small size of distributed generation technologies permits generators to be placed optimally in relation to heat or cooling loads. Those resources have the potential to increase system reliability and power quality due to the decentralization of supply. The system under study offers the autonomous reconnection of the microgrid after islanding. On the other hand, in such a system, when there is a problem with the utility supply, the microgrid can isolate from the grid while providing a seamless power to the sensitive loads. An autonomous control in a peer-to-peer and plug-and-play operation model is suggested by the researchers for each component of the microgrid. The former eliminates the need for a central controller and the latter implies that a unit can be placed at any point on the electrical system without re-engineering the controls .

Chapter 2. Literature Review

Lu *et al.* [99] investigated the control strategies for DERs to achieve high penetration of wind energy in a rural microgrid. Energy storage and DR are suggested to contain the frequency deviations.

Wang [100] proposed a secondary voltage control based on multi-agent system theory. Task sharing in the proposed multi-agent system can be achieved by either communication or local estimation, for a common objective of maintaining the regional voltage profile. In such system, the communication between different agents is also unnecessary since the voltage controllers have little or no influence on each other as far as the voltage control is concerned.

Pedrasa *et al.* [101] developed a decision-support tool that optimizes interactions with energy service providers using particle swarm optimization (PSO). Such a tool enables the end users to assign values to desired energy services, and then to schedule the DER to maximize net benefits or minimize net cost. By determining improved DER schedules, potential consumers can gain value added benefits using such coordinated DER scheduling. By comparing the end-user costs using the enhanced algorithm against the costs when each DER schedule is solved separately, the added value is calculated. This comparison provides a base line for the end users to determine whether they need to solve a more complex coordinated scheduling problem, or to decompose the problem into multiple simpler optimizations .

An application of multi-agent systems (MAS) for DER management in a microgrid is presented in the research performed by Logenthiran *et al.* [102]. In such a system, agents have certain behaviors and are planned to satisfy certain objectives using their available resources. Consequently, the behavior of the agents represents the objectives they are planned to achieve .

Nguyen *et al.* [103] proposed a multi-agent system to manage autonomous control actions and to coordinate between the agents in an active distribution network (ADN). In such a network, a smart power router can integrate network areas and manage power flows. They showed that the ADN can operate efficiently and optimally with the support of the power

router interface. The power router manages power inside and across the boundaries to avoid congestions while keeping voltages within a suitable range.

Hommelberg *et al.* [104] utilized the “Power Matcher” as a control concept for coordination of supply and demand in electricity networks with a high share of distributed generation. In that concept, each device is represented by an agent, which tries to operate the process associated with the device in an optimal way. The electricity consumed or produced by the device is bought or sold by the device agent on an electronic exchange market. As a market agent providing coordination services for the suppliers and consumers of electricity, the PowerMatcher has associated market protocol definitions which define the characteristics of the markets. When an execution event occurs, the PowerMatcher sends a request to all agents asking for bids. Bids are then aggregated and passed on upwards. The market price would then be determined and communicated back to the intermediate market agents and the device agents. The market price and the bidding strategy programmed into each agent, the device agent can determine the allocated power to purchase or deliver.

Dominguez-Garcia and Hadjicostis [105] proposed distributed resource allocation algorithms for control and coordination of loads and DERs with focus on linear iterative algorithms to maintain a set of values used by each node to determine contribution to load curtailment or to resource request. In that control strategy, an aggregator initially sends requests to the available resources in its control territory. Each resource can exchange information with a number of neighboring resources and make a control decision based on locally available information.

Vandoorn *et al.* [106] investigated the feasibility of the microgrid secondary control for applications in virtual power plants (VPP). They presented a hierarchical primary and secondary control structure in which, smart microgrids deal with local issues and primary and secondary control. The microgrids are then aggregated in VPPs. In that system, a tertiary control, forming the link with the electricity markets and dealing with issues on a larger scale would then be necessary. According to this study, the microgrid primary control is

responsible for a robust and reliable operation of the network with limited access to communication and is different in grid-connected mode from the islanded mode and consequently needs a fast control strategy. However, the secondary control operates on a slower time frame and deals with supervisory aspects of the system, such as the power exchange between utility network and microgrid, resource allocation, voltage profile optimization and frequency restoration. Communication would then be a necessity for such control system.

Dominguez-Garcia *et al.* [107] studied distributed algorithms resilient against potential packet drops in the communication links between system components in a coordinated DER system to provide ancillary services in electrical networks. In such a system, each DER maintains and updates a set of variables through information exchange with neighboring DERs. It is then shown that as long as the underlying graph of the information exchange between components is strongly connected, and the total amount of active and/or reactive power does not violate the capacity constraints, DERs can calculate their fair contribution. That team has focused on developing a method to robustify the algorithm so that it can tolerate failures in communication links and allow each node to converge to the correct value.

Mokhtari *et al.* [108] proposed a new coordination approach based on distributed control algorithm. Accordingly, the network is divided into hierarchical communities where each community is controlled by an agent. In their approach, customers are controlled by their smart-metering system. At the same time, as a part of a community of their neighbors, they are controlled by a master controller called community agent. At a higher level, phase agents have the responsibility to manage and coordinate the community agents. The neighboring communities are responsible for the coordination of their operation for the under-voltage and over-voltage problems. Normal state is when all customers within the community experience an in-range voltage. In such condition, the target could be to maximize the injection of the locally generated power to the grid. In an alert state, the voltage of at least one customer violates the desirable level. The alert state could be managed by utilizing storage capacities by entering charge or discharge mode respectively .

Chapter 3

Course of Study

3.1 Developing Fully Functional Models

Developing a computer-based simulation tool that can take into account the interaction of multiple energy resources within a smart grid or a smart microgrid would be essential to understand their dynamic behavior and performance, and would help in the design and planning of scenario-based optimal operations.

To perform the required analyses, either it is possible to use the standard IEEE test feeders developed for the selected software tools (GridLAB-D and OpenDSS) or develop specific feeder models. The former option is useful in cases with no geographical or topology preferences, while the latter provides base case platform for further case-specific analysis with options of comparing to real data.

PNM, the local utility company, is able to export GIS information to CSV files. Each file contains identifiers, node names and other relevant data for a unique feature. Data are extracted from PNM GIS system, which is not originally designed to provide standard output to be fed directly into the modeling software. Therefore, feeder data should be transformed

to a software-readable script. The very first step was to develop intermediary applications. Fully functional applications are developed to transform the GIS data to software readable scripts and used to build the basic model of each feeder to be studied.

SewerPlant14 (SP14), Studio14 (ST14) and Tramway11 (TR11) are the local distribution feeders selected for further studies thanks to their unique characteristics such as:

- ST14 and SP14 feeders are selectively connected to the PNM Prosperity site,
- A collection of different DERs including a PV farm, a Gas powered generator, a fuel cell unit, an ultra battery for smoothing, a battery energy storage system for energy services and cold storage systems is available,
- TR11 is hosting the highest number of rooftop PV systems and PHEVs in the area. Their number is expected to grow even more.

3.1.1 Tools

OpenDSS by EPRI and GridLAB-DTM by Pacific Northwest National Laboratories (PNNL) are two open-source software tools, designed to simulate distribution systems in the time domain, taking into account all possible variations in the system's topology, load composition, distribution level generation while having ability to demonstrate capabilities of modern power grids.

OpenDSS is a comprehensive electrical system simulation tool for electric utility distribution systems. It basically supports all Root Mean Square (RMS), steady-state (frequency domain) analysis commonly performed on electric power distribution systems, such as power flow, harmonic analysis and fault current calculations [109].

GridLAB-DTM incorporates advanced load modeling techniques with high-performance solution algorithms to deliver end-use load modeling coupled with power system models,

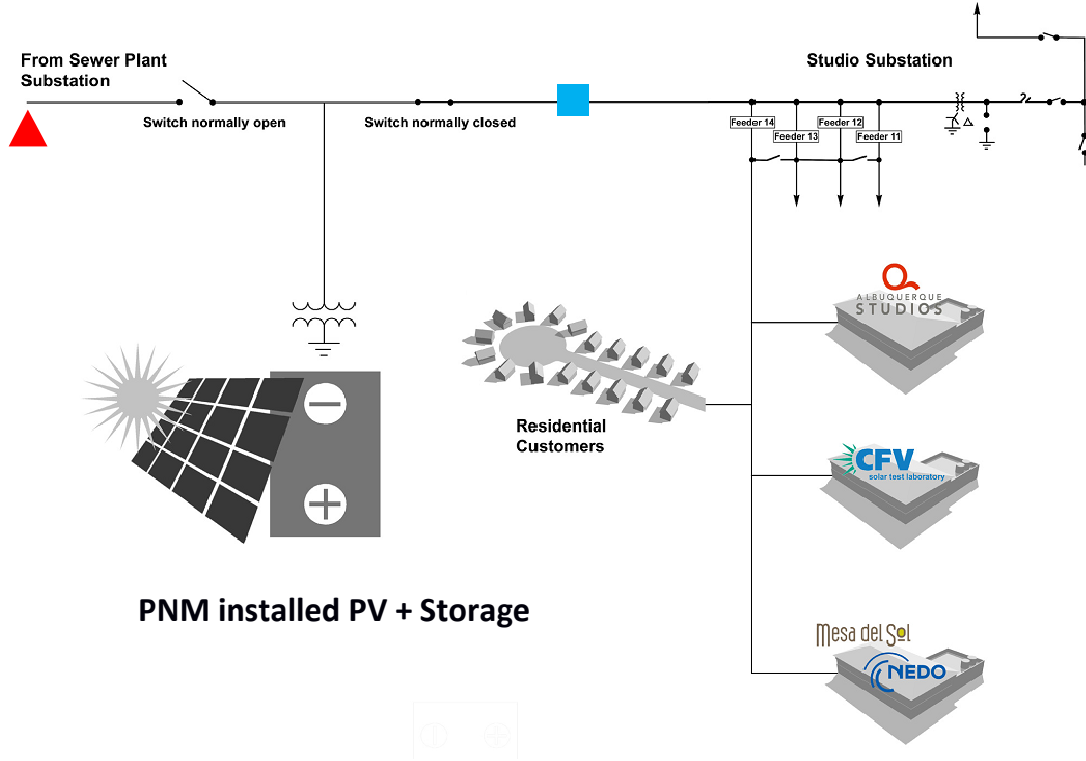


Figure 3.1: PNM smart grid Demonstration Project schematic diagram. Points of common coupling to the feeders are marked up. The red triangle illustrates the connection point to end of feeder SP14 and the blue rectangle shows the point of coupling to feeder ST14 (Courtesy of PNM).

market models, distribution automation models, and software integration tools for users of many power system analysis tools [110].

To build a feeder model, all available feeder features like transformers, underground or overhead lines, fuses, switches and so on must be added as an object. All traditional features which could be found in a typical distribution feeder are available as developed object models in both software. Even both software provide object models for more advances features like storage systems and PV generators.

Both modeling tools have a complete selection of fully developed object models to be

used to build the feeder script. For the purpose of this research, fuses, switches, reclosers, capacitor controllers and regulators were not included in the model and replaced with fixed objects or simple conductors. The tap changer state at the substation transformer was fixed over the course of the simulations, however changing the tap position does not violate the validity of the results. The aerial outline of the feeders are shown in Figure 3.2.

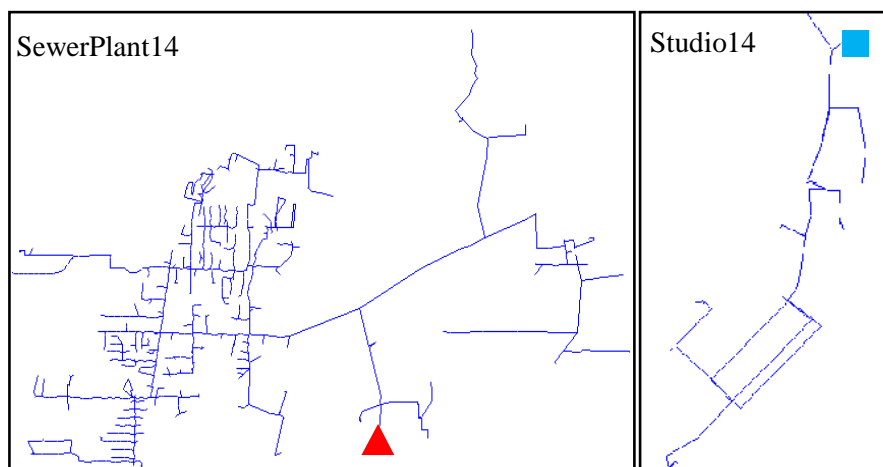


Figure 3.2: Top-view outline of SewerPlant14 and Studio14, generated in OpenDSS. Points of common coupling to the feeders are marked up. The red triangle illustrates the connection point to end of feeder SP14 and the blue rectangle shows the point of coupling to feeder ST14.

Syntax Errors and Debugging Capabilities

After each compile command, OpenDSS generates one syntax error message for the first error found. The process may be aborted or the error may be ignored to allow the interpreter to check the rest of the model. Unfortunately, the generated error message does not contain any reference to error location in the file. GridLAB-D stops working after detection of the very first syntax error which could not be ignored and should be resolved before it could proceed. However, a significant advantage of GridLAB-D in syntax error detection is that it generates a reference to the location of the error in the corresponding file.

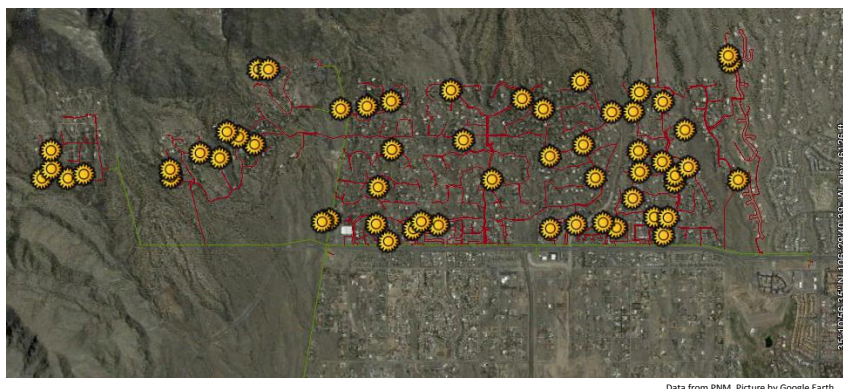


Figure 3.3: Top-view outline of Tramway11 feeder in 2012 by Google Earth. Installed rooftop PV systems are illustrated.

Topology Validation

After fixing syntax errors, topology validation is the next step toward developing a fully functional model. As the models get larger, this process could take significantly longer to complete.

An essential tool for such software tools is the ability to debug the topology of the circuit under study. A topology related error can be a missing part of the feeder, a single phase device connecting two multi-phase parts of the feeder, an isolated device or any other topological errors which could be initiated by errors in GIS data and unfortunately is likely to happen.

To detect and fix the topological errors in the model, it has to be compiled by the software. OpenDSS is able to converge even in presence of islanded subsystems or phase mismatches in the model. Converge in this context is to generate a set of output files indicating electrical parameters and some topological details such as islanded subsystems, mismatched phases and out-of-range voltages. That capability facilitates the model debugging process. After each convergence, OpenDSS can generate a list of isolated objects, loops and buses. List of

isolated objects shows all separate islands with any object connected to that island. The list could be used to find the disconnect point. Loop list and bus list are other resources for a model developer to find any discrepancy in the model topology or configuration.

On the other hand, GridLAB-D does not converge when the model contains isolated nodes. All objects must be connected in order to have a model converged. This makes topology debugging hard, especially when dealing with moderate and large feeders with thousands of nodes.

The solution for non-converging of GridLAB-D in presence of disconnects or phase mismatch in the model is to build the model in OpenDSS, to use the available tools in OpenDSS to debug the model completely. The detected issues and discrepancies are then used to debug the model in GridLAB-D. This method helped to resolve numerous issues in developing models for different feeders in Albuquerque.

3.1.2 Model Capabilities

To be effective analysis tools, other than being just simple power flow solvers, both OpenDSS and GridLAB-D are capable of performing time-series analysis. Both tools have the option of simulating the system behavior over a period of time as opposed to being snap-shot solvers. In time-series analysis variations in load, generation and other properties over the course of study are examined to identify problems such as over/under voltage incidents, over loads, excessive OLTC operations and capacitor controllers operations.

For the simplest type of time-series analysis, some properties have to change in specific times. In OpenDSS, it is possible to define and use load shapes (profiles) as multiplier or reference for both load or generation power. Load shapes can have either fixed time steps or variable time steps with indicating time stamps for every change in their value. Load shapes in OpenDSS could be either embedded in the model as scripts or loaded from text/CSV files. In case of a limited length load shape, it can be easily embedded in the scripts, but

for large load shapes which could be used in yearly/monthly analysis and/or in second-scale simulations, storing the data in a separate file and calling them in the script seems more practical. In GridLAB-D, players and shapers are used to form a time-series reference for an object's property, and they can either be defined in the model's body or invoked from a text file. An essential difference between GridLAB-D and OpenDSS is that in GridLAB-D, shapers and players could be used to control not only the power but also other time varying properties of any object, while in OpenDSS, a load shape, could only be used to control load or generation power. Another important difference is that in OpenDSS, for running a simulation in variable mode, all variable parameters should have the same time step while in GridLAB-D, different time steps for different properties could be defined. This is an advantage compared to OpenDSS when multiple properties with different granularities are simulated.

Recorders in GridLAB-D and monitors in OpenDSS, are both designed to log the required properties and generate the necessary data log files. In GridLAB-D there is more flexibility to modify and generate the desired report format while more properties must be set to do so. On the other hand, in OpenDSS, the monitors could be defined easier and fewer properties should be defined to generate the same result. However, there is less flexibility in modifying the generated output format.

3.1.3 Advanced Modeling Features

GridLAB-D is an object-oriented software, which gives its users the capability of modifying the object or class properties and also defining run-time classes and user-defined modules to satisfy modeling requirement, while in OpenDSS, the user is bound to a set of predefined properties. Such options in GridLAB-D give its users the capability to simulate complicated or highly customized cases when dealing with new concepts of a modern grid such as demand-response, market based analysis, optimized EV charge/discharge and distributed storage

simulation.

In one case run-time classes were defined to control load objects, by using a base load profile -invoked from a CSV file- and performing advanced calculations consisting of multiple stochastic parameters. That option provides options to perform complicated analysis without need to use third party calculation engines such as MATLAB. On the other hand, OpenDSS has a COM library, which is designed as an in-process server to be driven from an existing software platforms for highly customized types of distribution system analysis. For some cases OpenDSS was linked with MATLAB to run the customized analysis on multiple feeder models. It is a strong package consisting of numerous computation capabilities of MATLAB together with specialized distribution modeling potentials of OpenDSS. In one case, clouds passing over the feeder area were modeled while PV generators were injecting intermittent power to the feeder and other feeder control equipment such as VAR regulators were able to maintain the feeder voltage level and load within their allowable limits.

Server mode is another interesting feature of GridLAB-D. In this mode, the user is able to communicate with a real-time working model in GridLAB-D to send and receive control commands and data. One potential usage for this property is to use a web based monitoring/control application as an interface between users and the simulation engine.

Platforms

OpenDSS is designed to operate on Windows, without any parallel processing capabilities. On multi-core systems, it can just utilize one CPU. While today's most high performance computing (HPC) machines run on Linux [111], OpenDSS has no capability to run on Linux, i.e. on most HPC machines, which leads to limited use of OpenDSS for simulating very large models especially when fast response is required. On the other hand, GridLAB-D is equipped with multi-threading capabilities to run on parallel computing platforms, while it also comes with a Linux version which – in spite of difficulties during the build process – could run

on a Linux based HPC machine. A Linux version of GridLAB-D is built on one HPC machine, Pequena, in the UNM Center for Advanced Research Computing (CARC) [112] and is used for running large simulations and for comparison and verification of results from other machines/platforms.

Performance

To compare performance of the two software tools, a model of the same feeder was built for both. The selected feeder is Studio14 which currently supplies power to a small number of commercial buildings and has around 140 nodes. Different periods of analysis, from 1 to 30 days are studied. For each case, simulation is performed 5 times and the run time is averaged. Both simulations are done on the same Windows 7 platform. Results show that on average, OpenDSS is more than 10 times faster than GridLAB-D. Run time results are shown in Figure 3.4.

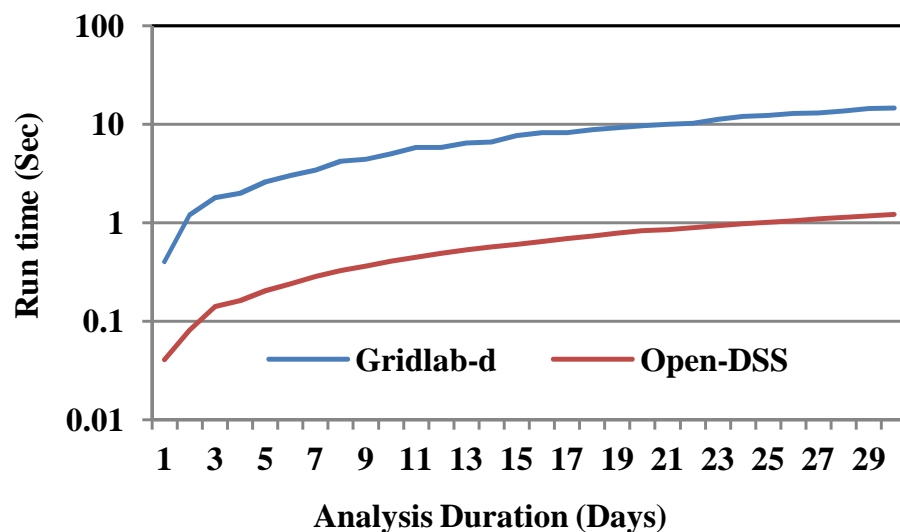


Figure 3.4: Run time versus analysis duration (Same feeder models/GridLAB-D and OpenDSS)

Similar comparison is performed for the same GridLAB-D model on the same machine but different operating systems. A single model is simulated on the same hardware platform but with different operating systems, Windows 7 and Ubuntu 10.4. Results show that the Windows version is twice as fast as the Linux one.

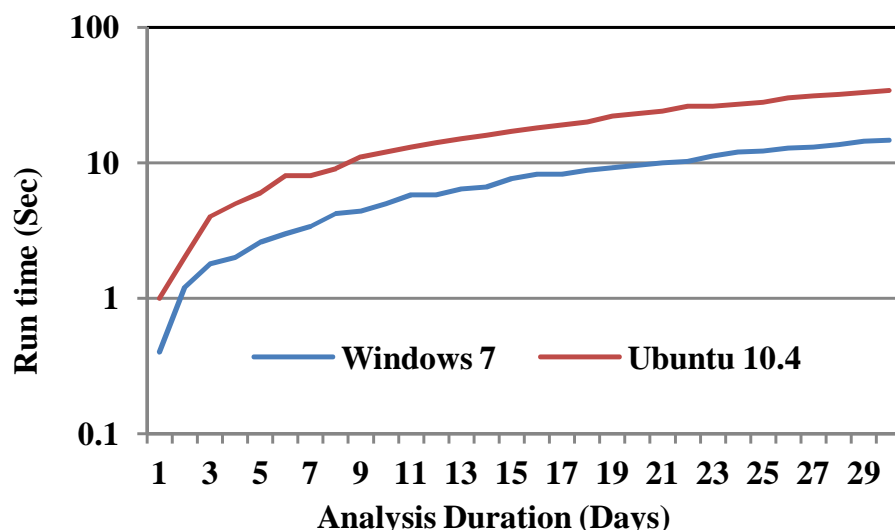


Figure 3.5: Run time versus analysis duration (Same feeder model/Different Operating Systems).

3.1.4 Comparing the Results for the Basic Analysis

One of the very first research objectives was to compare both software's results. Several time series analysis on many feeder models were performed. Results of the study are presented in the following sections.

Cumulative load test

In this test, all loads are set to follow the same load shape for a 24-hour period. They have the same power factor and matching nominal powers based on the substation capacity.

Cumulative load seen at the substation for both cases and percentage of the difference between the two are shown in Figure 3.6.

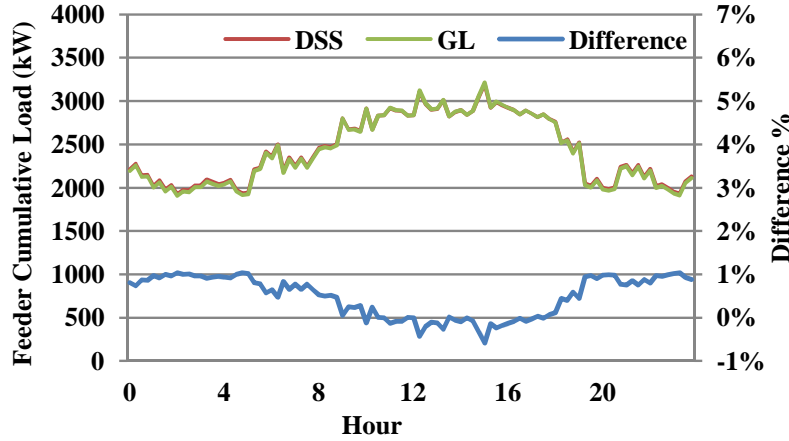


Figure 3.6: Simulated cumulative load at the substation in GridLAB-D (GL), OpenDSS (DSS) and percentage of the difference. The difference is negligible.

Voltage Profile

To compare the voltage calculation results, 3 random nodes with relatively short, moderate and long distance from the substation are selected. The tap position of the OLTC at the substation and the primary voltage are assumed constant. The simulation is performed with the same load as previous case for a 24-hour period. Figure 3.7 illustrates the voltage profile of the very first node downstream of the substation transformer during the same period. The results were expected to show minimal deviation due to relatively short distance from the source, which limited the expected error. Maximum deviation is less than 0.1%.

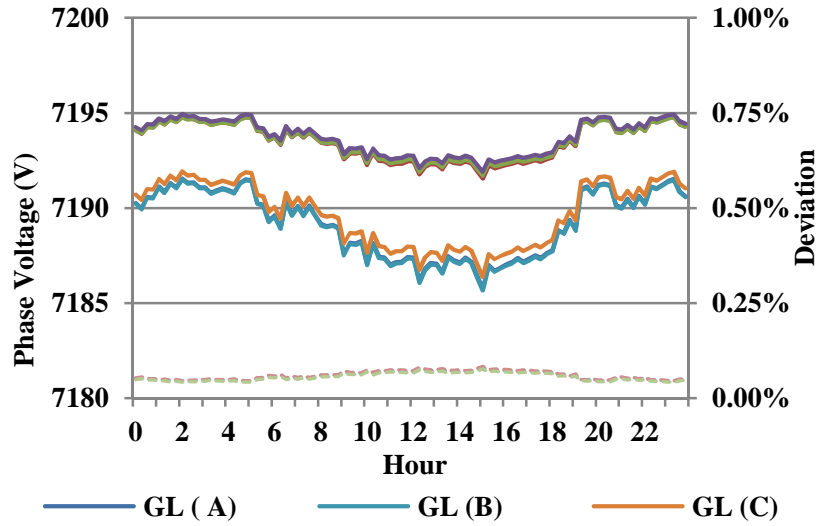


Figure 3.7: 24-hour voltage profile of the closest node to the substation. Percentage of the difference between identical nodes are negligible.

In a traditional single source distribution system model, more mismatch between analysis results is expected for the nodes located further down from the source, because errors and mismatches tend to accumulate. In Figure 3.8, the voltage profile of a node, located moderately far from the substation, is shown. It is important to note that OpenDSS results show voltage reduction, while GridLAB-D results show no significant change compared to the previous case.

Analysis results for the farthest node from the substation transformer show increased mismatch between the corresponding results and are shown in Figure 3.9. As expected, mismatch is increased, yet still limited to less than 1%. Interestingly, no significant voltage reduction was observed in GridLAB-D results, while the same analysis in OpenDSS demonstrated further reductions in nodal voltage which was expected.

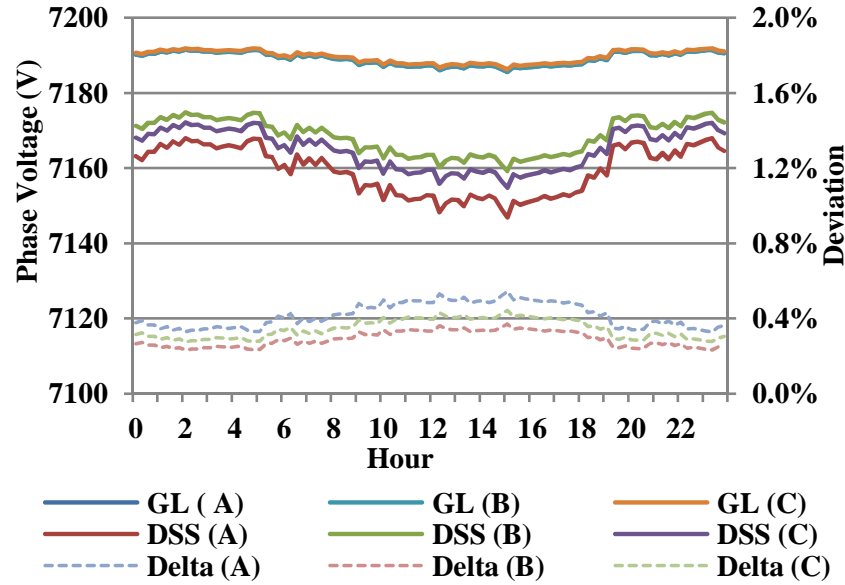


Figure 3.8: 24-hour voltage profile of a node moderately far from the substation transformer. Percentage of the difference between identical phases is increased.

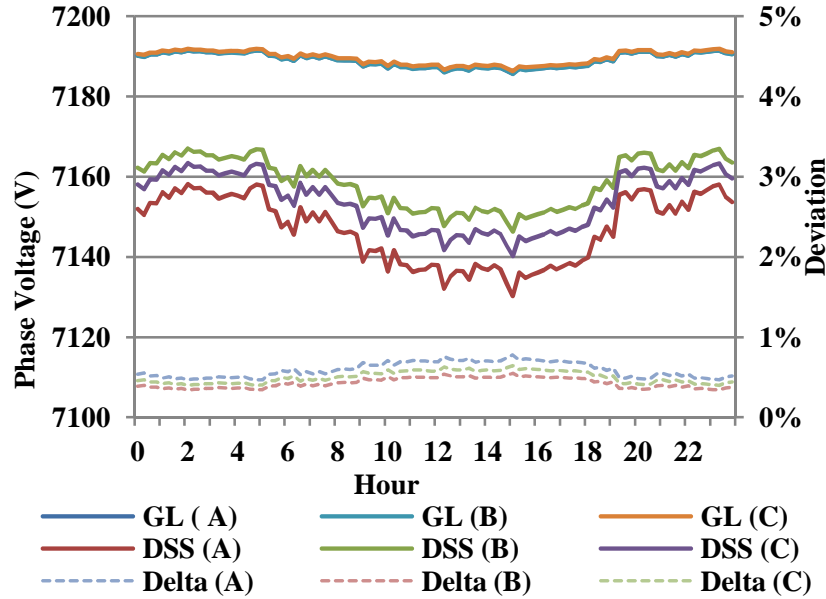


Figure 3.9: 24-hour voltage profile of the farthest node from the substation transformer. Percentage of difference between identical phases is increased but limited to less than 1%.

It was beyond the scope of this research to investigate the roots of the observed differences and to study the technical reasons differentiated the results of two software tools. For this research purposes, it was imperative to find an upper limit for the expected errors and mismatches; the findings showed that both software tools could provide solutions with acceptable accuracy.

3.1.5 Load Model

For detailed load analysis, the ideal load representation would be the load measured at each distribution transformer or even the load measured at each service drop. Absent real time load data for every customer, that will only become available through AMI, it was necessary to construct accurate estimated of the highly distributed loads connected to the distribution feeders. Extensive efforts have been conducted by many researchers to build load models. Some have proposed to develop load profiles for each type of customers. Some have used limited data from distribution SCADA to augment the estimated customer load profiles [113]. Advances in AMI development have helped utilities to obtain more accurate and time stamped load information, while also enabling demand side management capabilities [114].

Until time stamped load information becomes readily available through large scale deployment of AMI, a large percentage of the required data for load estimation is obtained from historical data. More specifically, the estimates could be obtained from the given load curves, weather and time-of-day data, and the customer billing information [115]. This research was not focused on developing algorithms for load estimation; therefore a relatively simple but efficient method to allocate loads connected to the feeders under study was used.

In general, during week days, peak load for residential customers occurs twice a day, early morning, when most people leave their homes and go to work, and late evening, when people return home. Weekend load profiles differ from weekday profiles, since most people have

different life patterns for their “off days”. Moreover, load profile varies by season, ambient temperature, day of the week and geographical location. For commercial customers, load increases dramatically during business hours and declines after closing. For the industrial sector, very flat load patterns have been found relating to continuous manufacturing processes and implementation of various demand management programs [115].

A mixed number of residential and commercial customers constitutes the typical load connected to SP14 feeder. As a consequence of the limited information about each individual customer’s consumption behavior, an exact load model could not be determined. While power flow and corresponding power quality throughout the feeder is the primary concern of this research, the load recorded at the substation is the only available benchmark to validate the estimated customers’ load profiles. Therefore the load seen at the substation transformer was used as a basis for building load shapes that could be expected at each customer’s service drop. The feeder load shape was generated by normalizing 15-minutes demand data based on the feeder nominal rating as shown in Figure 3.10.

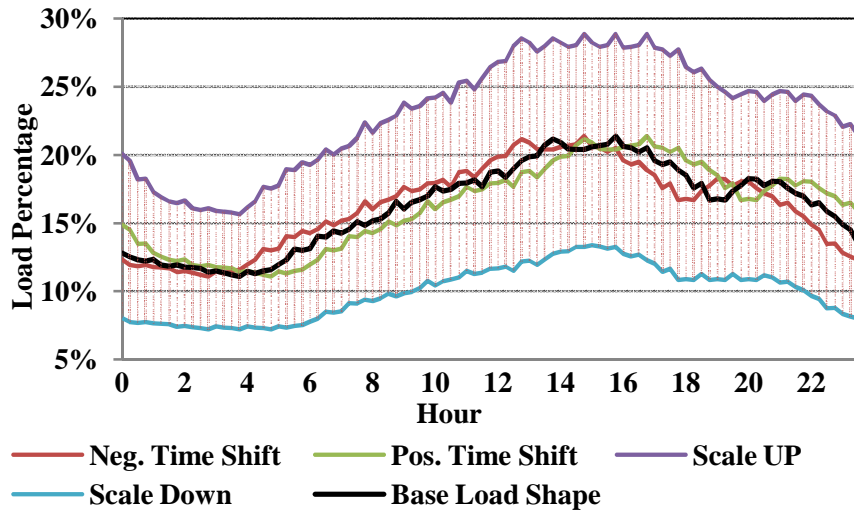


Figure 3.10: SewerPlant14 base load shape generated by normalizing the 15-minute demand data. Scaled and time-shifted variations of the original signal are also shown. Hashed area show the conceivable options.

Chapter 3. Course of Study

A heuristic idea for generating custom load profiles was to time shift the base load shape and to scale the load shape. Assuming the base load percentage at any given time t is $l_b(t)$, the load percentage for customer i at the same time would be defined as below:

$$l_i(t) = l_b(t + \alpha_i(t)) \cdot \beta_i(t), \quad (3.1)$$

$$\alpha_i(t) = G_1(\Delta)_i, \quad (3.2)$$

$$\beta_i(t) = G_2(\delta, t)_i, \quad (3.3)$$

where Δ and δ are the selected distribution function's parameters. An initial value was chosen as an approximation of the optimum values. G_1 and G_2 are Gaussian (Normal) distributions of the shifting time and the scaling values. The value of G_1 remains constant for each customer during the simulation period because it is a measure of how much the load profile of the customer is leading or lagging the feeder's load profile. On the other hand, the value of G_2 has temporal variations for every customer.

Visual representation of Equation 3.1 and the resulted margins are shown in Figure 3.10. Upper and lower bounds show the limits for each load.

To analyze the feeder behavior with the minimum required granularity, the load shapes must have equal or higher resolution than the desired values. The substation metering system, stores the data every 15 minutes. However, at least 1-minute resolution was desired for this research. Additional data points were extrapolated assuming a smooth transition of the load between any two consecutive logs. Different scaling factors and shifting time are studied to find the best match. In Figure 3.11 an estimated load shape for an arbitrary customer is presented.

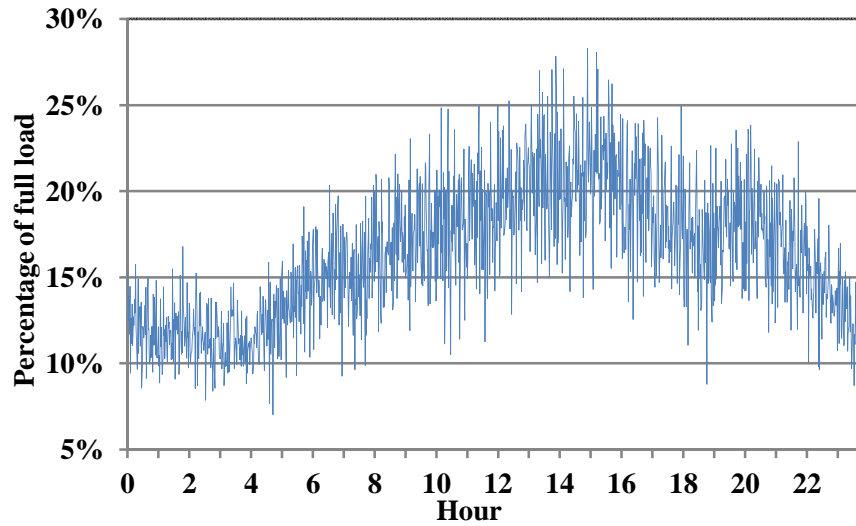


Figure 3.11: Generated load shape for a random customer. To develop such a load profile, the substation load shape is selected as a base load profile, shifted randomly in time and then scaled stochastically.

3.1.6 Adding Loads to the Model

Having developed a method to synthesize a load shape for every customer, the next step was to add the loads to the feeder model. A list of connected service drops was used to define all load objects. Each premise (customer) was identified by a combination of a unique ID number plus the transformer ID.

Load allocation was not a trivial task to do. Although service capacity was known for all customers, it could give a sense about the available service to each customer and not the real-time value. It was not realistic to use the service capacity as a measure of the actual load. An algorithm was developed to allocate each load a percentage of the available capacity based on the feeding transformer's nominal rating and the number of loads served by that

transformer (Equation 3.4).

$$C_n = \sum_{i=1}^n m_i \cdot T_i + L, \quad (3.4)$$

where C_n is the nominal feeder capacity, L is the full load loss, m_i is the load multiplier for customer i and T_i is the nominal rating of the transformer feeding customer i .

Figure 3.11 depicts the load as a fast changing variable, which is not a realistic assumption for the type of loads normally seen at the distribution level. In general, neither residential nor commercial loads exhibit such rapidly changing behavior. To address that, a new metric was incorporated in load estimation formula: average time between consecutive changes in load. It was called Load Response Time (LRT).

3.1.7 Validating the Model

Once the loads were added to the model, the results had to be validated. The difference between the observed demand and the calculated demand at the substation was selected as a measure of accuracy of the model. However, it should be noted that the purpose of this research was not individual load modeling. As shown in Figure 3.12, cumulative load at the substation with 1-minute LRT has sharper variations than the observed demand data while it follows the feeder demand pattern. It was then necessary to calibrate the load shapes to get the best cumulative load at the feeder level.

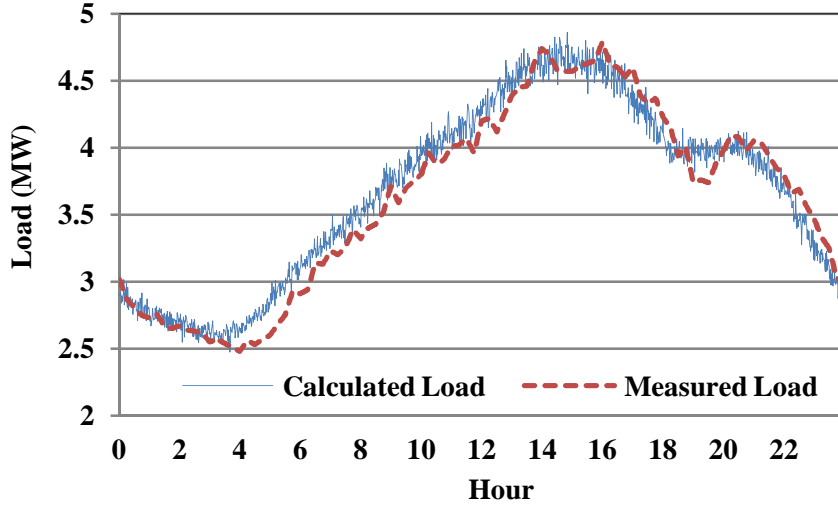


Figure 3.12: Measured and simulated load at substation.

Some metrics were developed to compare the mismatches between actual and calculated load at the substation. Those metrics could be optimized, where necessary, to find the best load model matching the feeder's total loads. $\Delta\alpha$, $\Delta\epsilon$ and ΔP were defined as:

$$\Delta\alpha = \frac{\sum_{t=1}^T \frac{|CalculatedLoad_t - RecordedLoad_t|}{RecordedLoad_t}}{T} \quad (3.5)$$

$$\Delta\epsilon = \frac{\sqrt{\sum_{t=1}^T \left(\frac{CalculatedLoad_t - RecordedLoad_t}{RecordedLoad_t} \right)^2}}{T} \quad (3.6)$$

$$\Delta P = \max_t \left(\frac{|CalculatedLoad_t - RecordedLoad_t|}{RecordedLoad_t} \right) \quad (3.7)$$

$\Delta\epsilon$ is the stored energy of the difference between the two signals. $\Delta\alpha$ is a measure for dissimilarity and ΔP is the maximum difference between the two. To find the expected value of the introduced metrics for each case, simulations were repeated 100 times ($T = 100$). Figure 3.13 shows the metrics assuming $LRT = 1$ min.

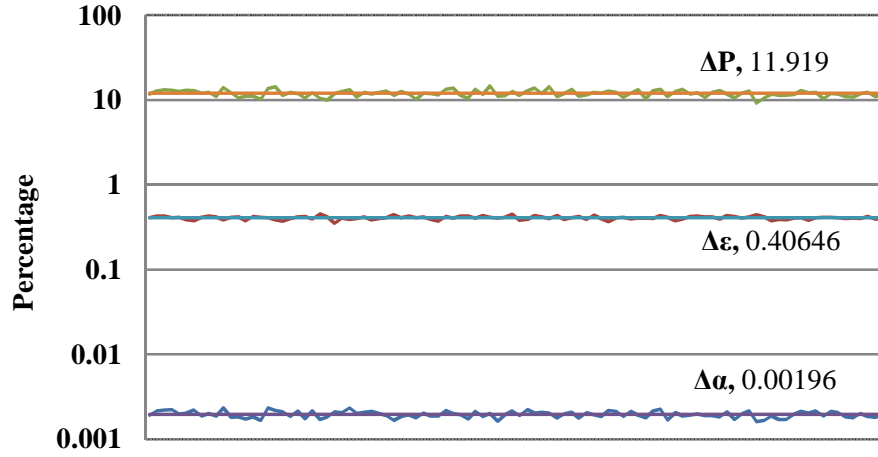


Figure 3.13: Calculated metrics after 100 random runs ($LRT = 1$ min). Average values are shown on the graph.

Commercial and residential loads are expected to have high LRT values since, in general, at this level almost no rapidly changing loads are used. Typical loads change in the orders of tens of seconds to hours. To include the LRT concept, Equation 3.4 is modified to 3.8. The idea is to wait for $\gamma(t, i)$ seconds following a change, before the next variation in load_{*i*} is allowed.

$$l_i(t + \delta t) = \begin{cases} l_b(t + \alpha_i(t)) \cdot \beta_i(t) & \delta t < \gamma_{t,i} \\ l_b(t + \delta t + \alpha_i(t + \delta t)) \cdot \beta_i(t + \delta t) & \text{otherwise} \end{cases} \quad (3.8)$$

$$\gamma_{(t,i)} = P(LRT, i, t) \quad (3.9)$$

In this research, γ was assumed to have a Poisson distribution between zero and LRT. Other functions could also be a choice but never investigated. In Figure 3.14, the base load shape and a randomly selected customer load shape are shown.

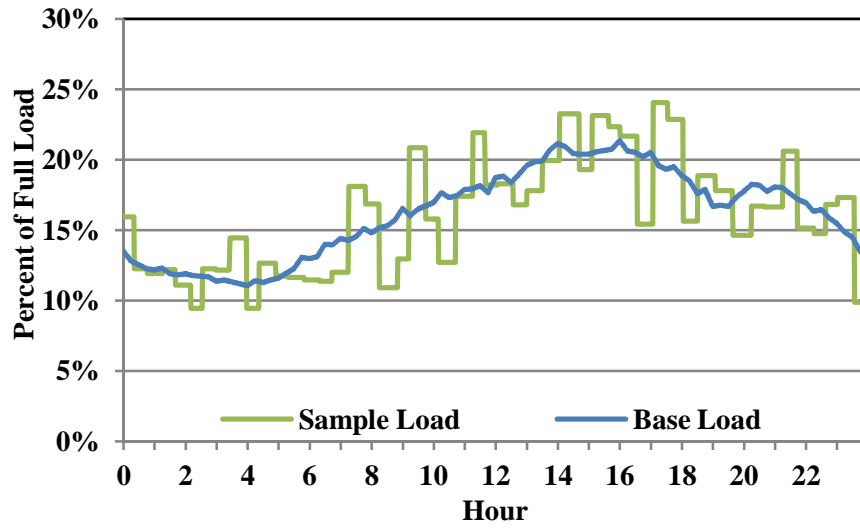


Figure 3.14: A random synthesized load shape and the base load (LRT = 30min).

In Figure 3.15, the observed load and the synthesized load at the substation are shown. Corresponding $\Delta\epsilon$ and $\Delta\alpha$ values have shown a close approximation of the observed load.

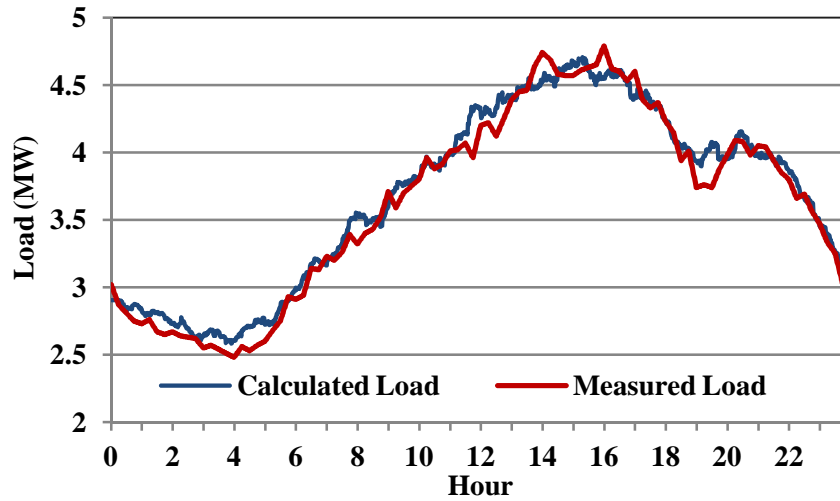


Figure 3.15: Measured and synthesized load at the substation on September 2, 2010 (LRT = 30min).

3.1.8 Generalizing

To show whether the proposed method is sensitive to the changes in the feeder's load level, simulation period, seasonal load composition and topology, several cases were studied. Different seasons and demand levels were randomly selected and studied. However, the feeder topology over the course of simulation was considered constant. That means the status of all protective devices, breakers and switches remained unchanged over the course of study. Expected error and performance metrics were consistent for all cases. Figure 3.16 and 3.17 illustrate similar load patterns synthesized for different cases. The observed error levels had minimal variations and complied with the results for different load allocations.

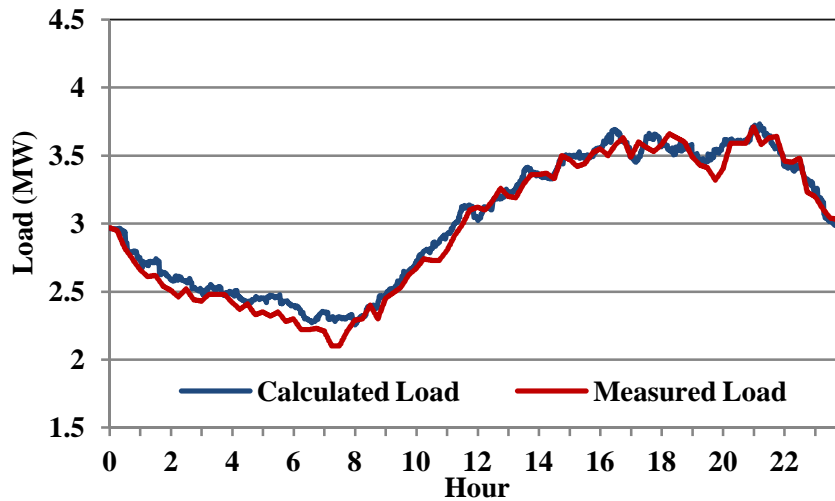


Figure 3.16: Measured and synthesized load at the substation on June 4, 2010. (LRT = 30 min)

Although the described method is not designed to model the exact profile of each individual load, it provides a close match to the whole feeder load and the results provide sufficient accuracy for the purposes of this research. The synthesized load profiles were used in the next phases of the research such as studying the effects of high penetration level of DER, distributed storage systems and deploying PHEVs in large scale.

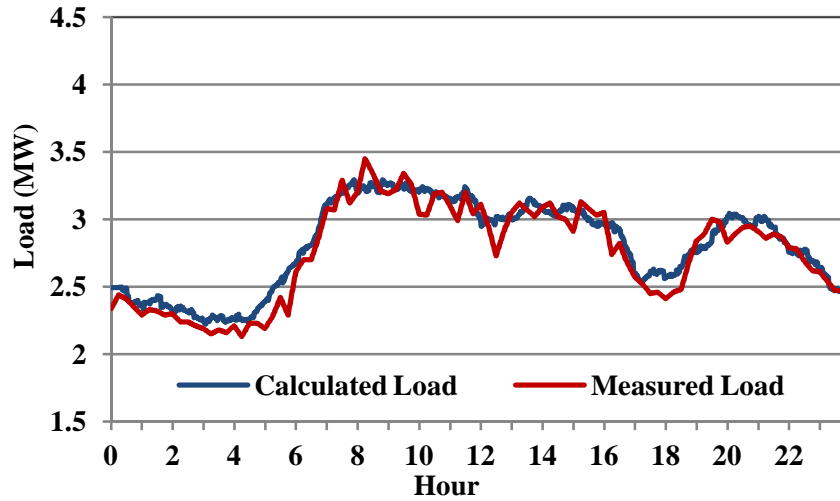


Figure 3.17: Measured and synthesized load at the substation on November 1, 2010 (LRT = 30 min).

3.2 High Penetration Level of DER in Power Distribution

The validated model provides a practical test bed for further studies. Analysis of deploying DERs especially PV systems and their effects on the feeder's voltage profile, circuit loss, effects of distance from substation on the voltage levels are separately analyzed and the associated results are described in the following sections.

3.2.1 Voltage Profile

Voltage profile is an important factor that is a measure of the health of the system. SP14 was selected as a benchmark for a fully developed large feeder with around 6000 nodes. To investigate the potential effects of connecting PV generators in high numbers, some important nodes were selected and further studies were focused on those. The select nodes

are:

- Substation (Bus1)
- Point of common coupling of Mesa del Sol PV system (Bus2)
- The farthest node from the substation (Bus3)

A centralized 500kW PV system (equal in capacity to the Prosperity PV system at Mesa del Sol) was connected to the feeder model. The Mesa del Sol PV system went online in summer 2011 and was originally connected to ST14 at a node close to the substation. It was designed to switch to SP14 with connections to the end of the feeder, if necessary.

Two different solar irradiation patterns were selected for further studies; one during a clear sunny day and one in a partly cloudy day. The PV output power during the selected days is shown in Figure 3.18. The PV system was set to feed only active power and not to contribute to Volt/Var control.

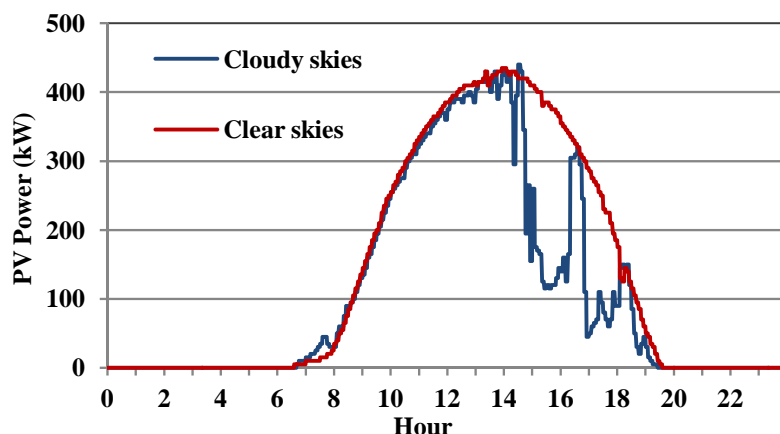


Figure 3.18: Generated PV power for two different days at Prosperity.

As depicted in Figure 3.18 for cloudy skies, almost no clouds were spotted until around 2 PM. Right after that, clouds passed through the area and caused sharp and high frequency

fluctuations in PV output. The peak PV power was around 440 kW and at the same time total feeder load was 4.58 MW, which translates to almost 10% penetration level. At this level no major side effects due to PV intermittency are expected. The following results confirm the speculations.

Simulations were repeated with two different setups to investigate potential effects of injecting intermittent PV power into the grid when the penetration level of PV is high. First, the PV was disconnected from the feeder and then, in a partly cloudy day, PV was connected. Voltage profiles for the three selected buses are shown in Figures 3.19, 3.20 and 3.21 for both cases. Effects of intermittency on voltage profile as a function of distance from the source.

Compared to “no-PV” case, an increase in voltage levels was seen at all the buses. The farther from the substation and the closer to the PV point of common coupling (PCC), the more significant PV side effects would get. That is a concerning issue which is induced by the power being injected into the system. A large PV system, not acting in Volt/Var control mode, and connected far from the substation, is expected to induce severe voltage fluctuations at nearby nodes.

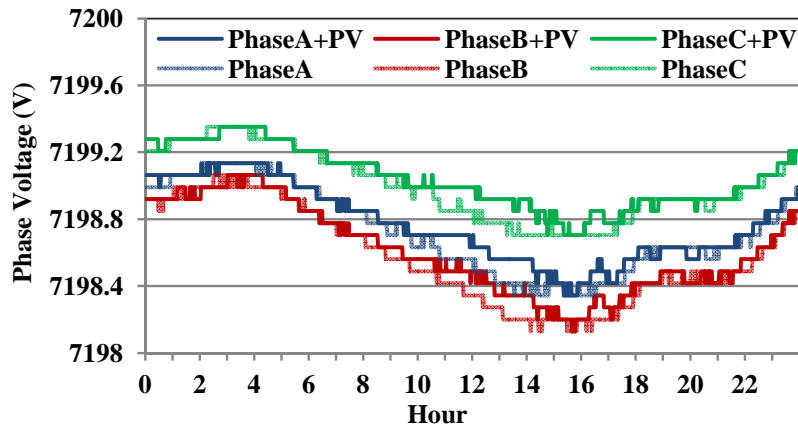


Figure 3.19: PV effects on Bus1 phase voltages in a partly cloudy day.

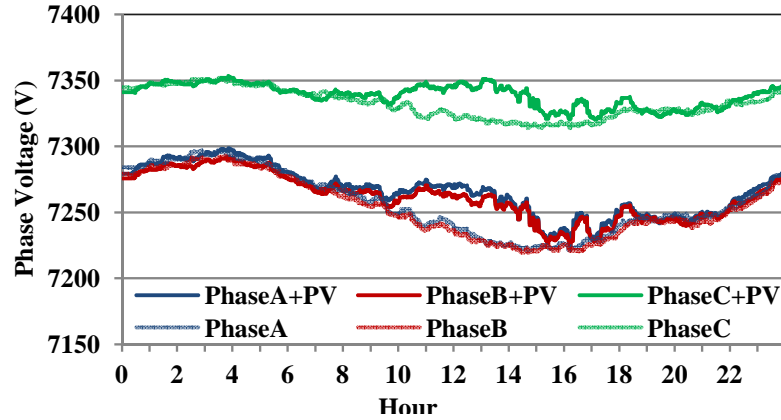


Figure 3.20: PV effects on Bus2 phase voltages. In presence of PV, variations are more significant.

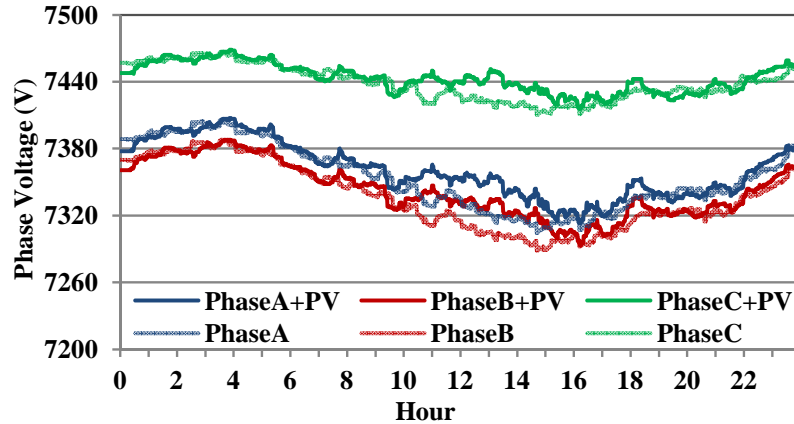


Figure 3.21: PV effects on Bus3 phase voltages. Farther nodes are less sensitive to PV induced intermittency.

The same study was performed with the exception of the smooth PV pattern. Figure 3.22 shows voltage profile at the substation with smooth and intermittent PV outputs. No significant change is observed at the substation due to PV fluctuations. It could then be inferred that by shortening the distance between the DER and the feeder body, the undesired effects of the intermittent PV output could be eliminated or reduced.

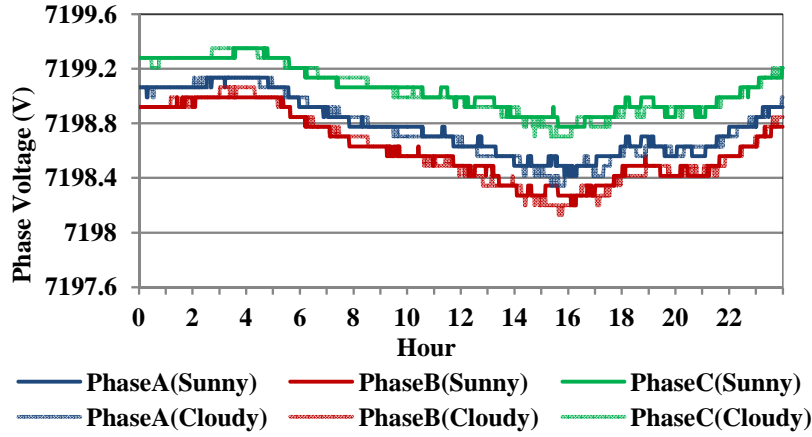


Figure 3.22: Effects of PV intermittency on Bus1 phase voltages. PV induced fluctuations are negligible at a node located close to the substation.

Power distribution systems will soon be facing increased number of PV installations in the form of roof top small scale PV systems. To modify the developed model of the distribution feeder (ST14) and study high PV penetration, number of PV systems and subsequently peak generation power was then assumed to increase 5 fold. Prospective PV systems were randomly distributed over the feeder area and connected to random nodes, resembling a 2025 scenario.

Figure 3.23 illustrates a typical 24-hour voltage profile of all feeder nodes in presence of the additional PV systems. No significant change in voltage profile is observed for most nodes except the nodes connected to the end of weak laterals. Even highly fluctuating PV generation didn't make noticeable difference in feeder voltage profile. Results conform with the study on high PV penetration [116] showing that distributed PV systems installed close to the main body of the feeder do not cause significant voltage fluctuation. However remote nodes connected to long and weak feeder laterals may suffer from voltage flicker, sag and swell due to variations in PV generation.

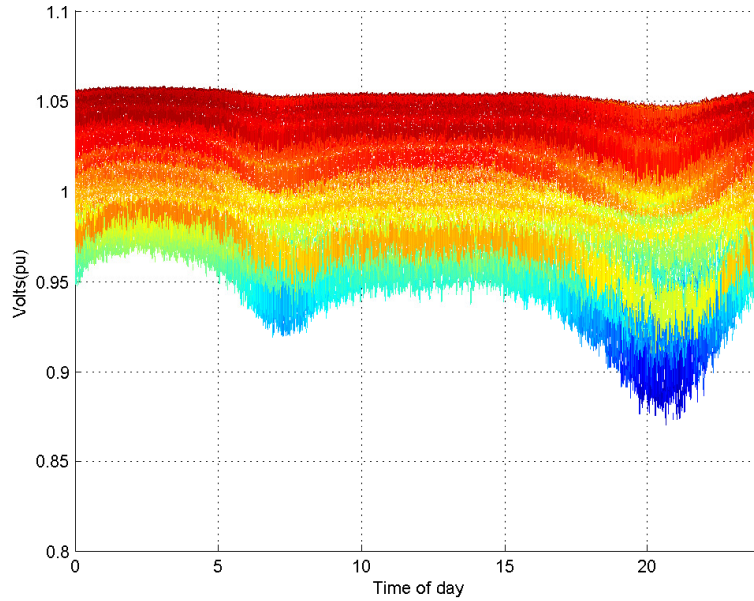


Figure 3.23: Node voltages along the feeder. No significant change in voltage profile is observed after additional PV units are connected to the feeder. Node voltage vary based on the load and its location. Some nodes experience significantly higher voltage drops due to their longer distance from the substation.

3.2.2 Do Capacitors Contribute to Voltage Smoothness?

It is imperative to ask if PV output intermittency should be smoothened and whether the VAR compensating capacitors could contribute to such a service. To find out, simulations were repeated while all capacitors were disconnected and intermittent PV power was injected into the feeder. Figure 3.24 shows the phase voltages at Bus1 for both cases. No significant change in signal smoothness is observed after connecting the capacitors. Figure 3.25 shows the phase voltages at Bus2 for both cases. Again, no significant change in signal smoothness is observed after connecting the capacitors. However, the lower voltage level in the “no-Capacitor” case is due to lower reactive power injection after disconnecting the capacitors.

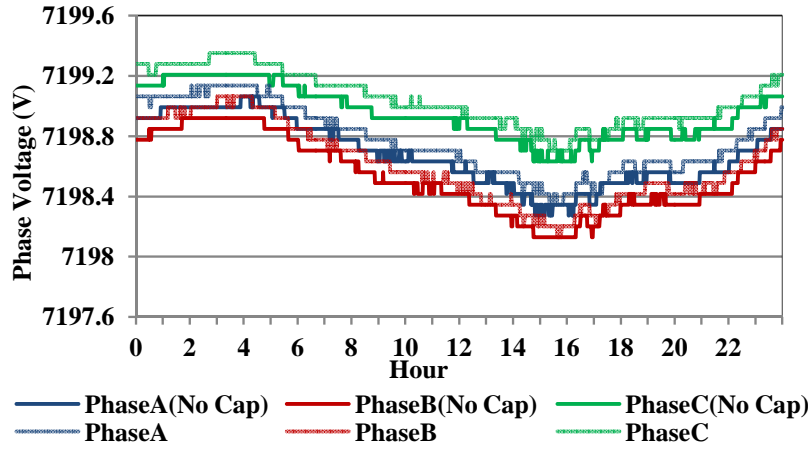


Figure 3.24: No significant effect is observed by removing capacitors.

3.2.3 Spatial effects of Highly Penetrated Distributed PV

Traditionally, distribution systems have been designed based on unilateral flow of energy from the substation into points where electricity is consumed. On the other hand, mechanisms put in place to maintain the power quality could not efficiently operate in existence of excessive variations in voltage and load and also bidirectional flow of energy. Voltage regulating

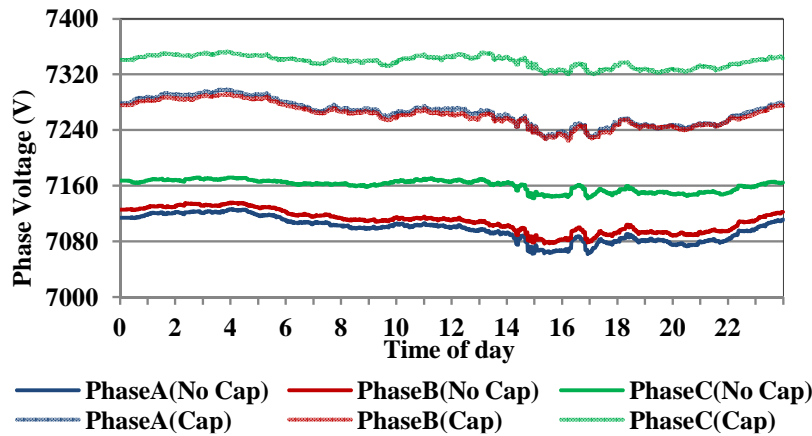


Figure 3.25: Phase voltages at Bus2. Capacitors have no effect on smoothness.

devices such as tap changers and VAR compensating equipment are set not to respond to high frequency changes. Therefore, by incorporating large capacities of renewable energy resources into the power distribution system, utilities face critical challenges to maintain power quality and continuity of service in presence of fluctuating power generation; uncontrolled behavior of the resources with natural origin, such as PV and wind turbines, is an inherent characteristic of such resources [117].

It was planned as a part of this research to claim that spatial diversity is an inherent consequence of semi-uniform integration of large numbers of RE resources in distribution feeders. Higher frequency components of the total generated power would be eliminated as a result of such spatial diversity. That is studied by adding PV to a number of random nodes to achieve a desired PV penetration level, assuming that high-altitude (cloud-level) wind is blowing at maximum 60 mph from north to south and moves clouds in that direction, which respectively causes sharp fluctuations in PV power. Low speed wind is not important, because of minor contribution to high ramp rate PV power fluctuations. At the assumed wind speed, it takes at least 6 minute for the same cloud pattern to move from the northernmost node to the southernmost node in the feeder. For simplicity, cloud coverage is modeled by a uniformly distributed time delay between zero and maximum. Solar irradiance level is assumed constant during the period a cloud pattern affects the northernmost nodes and the southernmost nodes.

To understand the differences in spectral concentration of the PV energy between a distributed PV system and an equally sized centralized PV plant, a large PV generator is modeled. The large aggregated PV system (APVS), has a generation capacity equal to the total cumulative power of the distributed PVs connected to the same feeder. The APVS is considered spatially centralized which means all PV cells are subjected to the same solar irradiance at any point in time. Spectral analysis of the output power in a 24 hour period reveals that spatial distribution of the PV systems over the feeder area reduces the high frequency contents of the power spectrum significantly. In Figure 3.26, the

spectral density function which is defined as the Cumulative Density Function (CDF) of the Fast Fourier Transform (FFT) of the output power is shown for two cases: Distributed PV and APVS. The smoothing effect thanks to the spatial diversity of the PV system could be understood by comparing the frequencies below which 95% of the total energy of the associated signal is concentrated. The 95% point in distributed PV case is almost a tenth of the corresponding value for APVS. That means the higher frequency contents of the PV power due to partial cloud coverage are filtered out as a result of distributing PV generators. Also a large portion of the delivered energy is concentrated in the lower frequency range. Therefore, by distributing the energy resources (in this case PV systems) over the service area, necessity of any BES system to mitigate the PV output fluctuations would be reduced substantially. In contrary, is the PNM demonstration project which is comprised of a PV farm and a 500kW smoothing battery designed to mitigate the high frequency PV power variations.

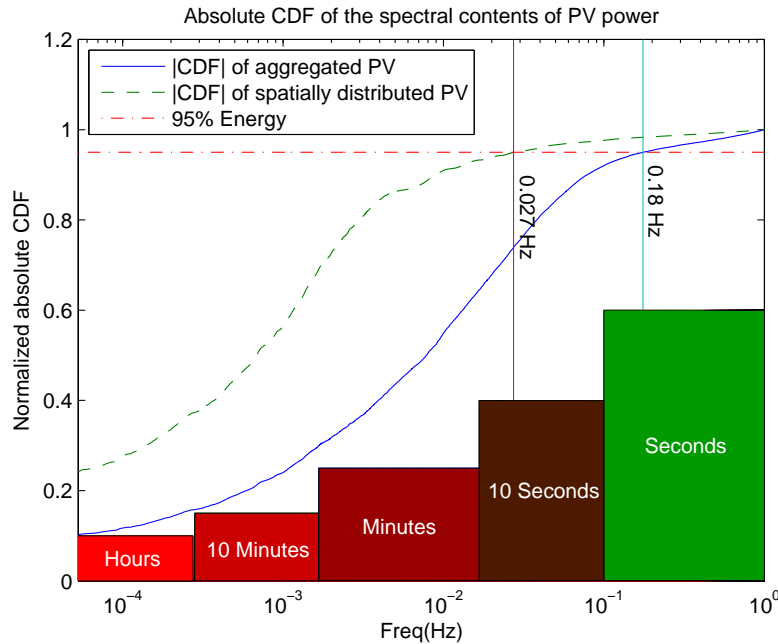


Figure 3.26: Normalized absolute density of the spectral contents of the generated power for distributed PV units and the equivalent centralized PV unit. (Data from PNM)

By incorporating exact coordinates, availability of the resources and nominal rating of each PV unit, more detailed analysis could be carried out, if desired. However, steady and uniform growth in installation of new PV systems eliminates the need for such detailed simulation. A uniform distribution of the PV systems is an unintended, yet desired consequence of the ever increasing use of rooftop PV systems.

3.2.4 Circuit Active Loss Profile

A potential effect of installing DER systems is loss reduction. Figure 3.27 shows losses in the primary circuit for three different cases: No PV, centralized PV and distributed PV units. PV generation power is identical in both centralized and distributed cases. Percentages of the loss reduction due to addition of PV generators are also shown. $\Delta 1\%$ is the reduction in losses due in the centralized case and $\Delta 2\%$ is the reduction in losses in the distributed case. Simulations show that distributing PV units across the area could potentially double the amount of reduction in losses.

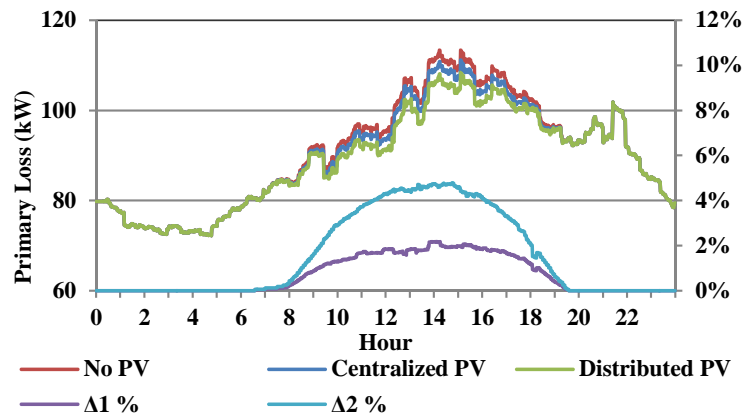


Figure 3.27: Original losses and percentage of reduction in losses thanks to PV units.

3.3 Network Model of the Distribution Feeders

3.3.1 Classic Network Model

The models developed for the select distribution feeders (TR11 and ST14) were used to build the corresponding network models. The metrics introduced in section 2.4.1 are calculated for those feeders and their structural behavior is defined. For the purposes of this research, loads, regulators, fuses and other protection and control devices are not considered as a part of the topology. The feeder is modeled as a network of connected conductor pieces (links) and buses (nodes or vertices). Pictorial representations of the feeders are shown in Figure 3.28.

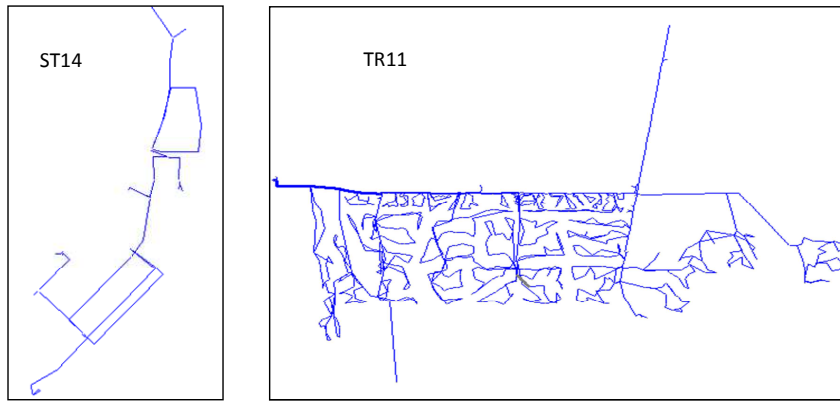


Figure 3.28: Graphical representation of the feeder circuits (Data from PNM, circuit graph by OpenDSS).

The admittance matrix and other information is extracted from the developed OpenDSS models (Section 3.1). The admittance matrix is used for building the adjacency matrix by simply replacing all admittances by constant unit admittance. This is followed by building the vertex and link list. NodeXL [118] is used for generating graphical representation of the selected networks topology.

In Figures 3.29 and 3.30, topological representation of both feeders are shown. Unlike a

power transmission network, in a power distribution feeder, individual phases are modeled separately because a distribution feeder is not necessarily a balanced three phase system. Therefore, instead of one node representing all three phases in a bus, three, two or one node might be available at each bus respectively. On the other hand, because of the existence of mutual admittance between phases, nodes are shown with cross connections in non-single phase buses.

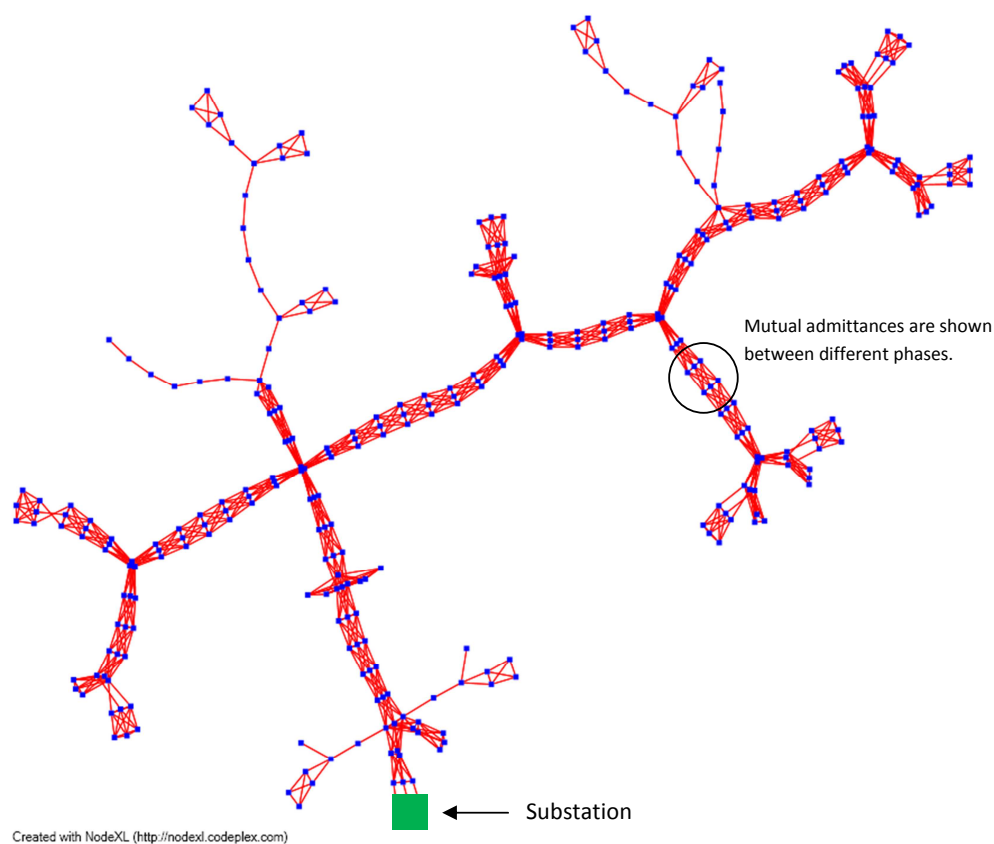


Figure 3.29: Topological representation of ST14 (Data from PNM, Graph by NodeXL).

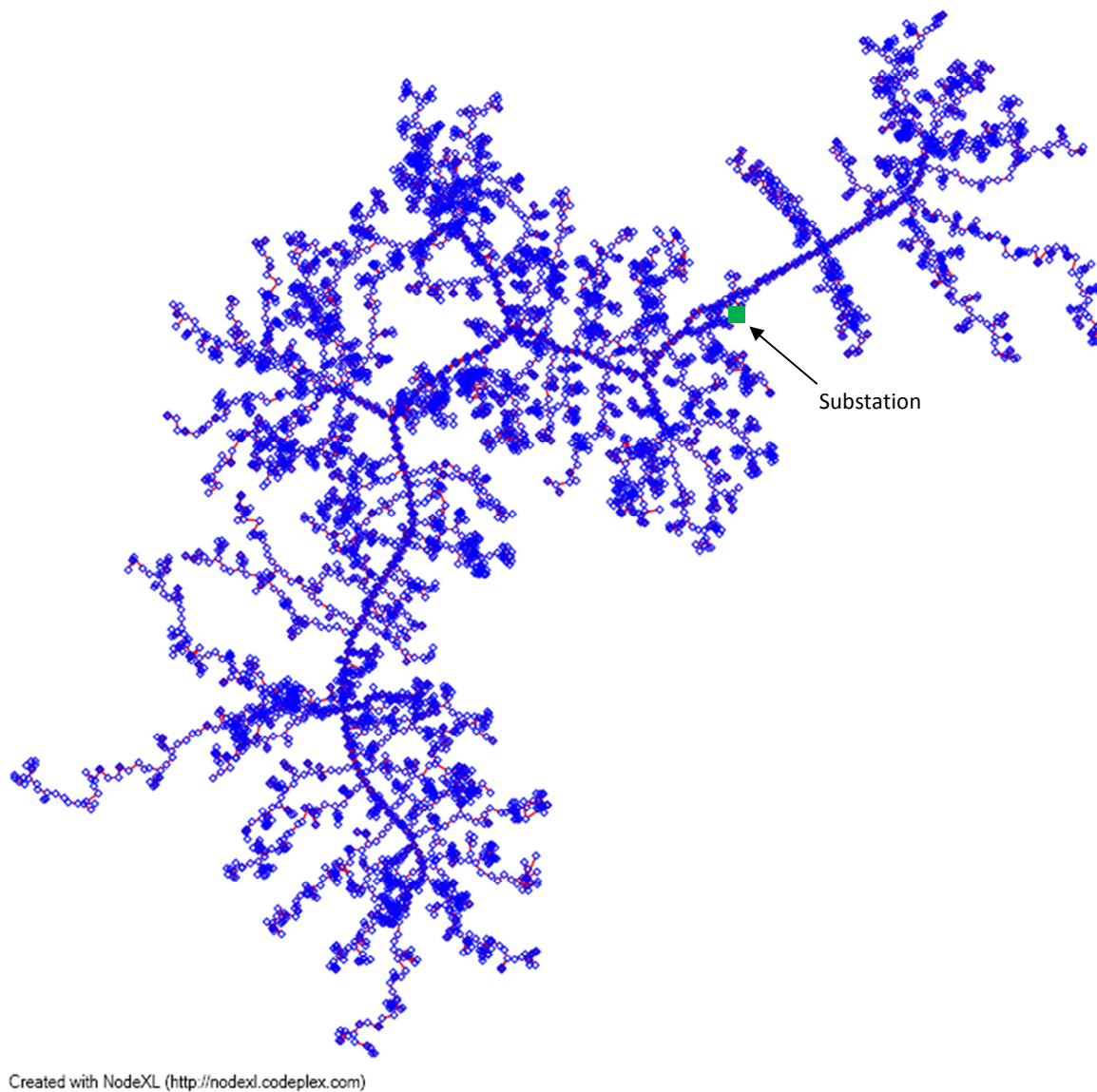


Figure 3.30: Topological representation of the TR11 (Data from PNM, Graph by NodeXL).

The network representations for the feeders, shown in Figures 3.29 and 3.30, do not immediately reveal any highly-connected hubs that would suggest a scale-free network structure.

Chapter 3. Course of Study

Similarly, the degree distributions of the two feeders (Figure 3.31), do not fit well with a power law statistic. In Table 3.1, some network measures are provided. The geodesic paths between random node pairs are longer than would be suggested by a Watts-Strogatz [71] small world structure. The topological structure of the feeder networks shown above would lead us to agree that without incorporating the laws of physics, governing the electrical circuits, power distribution systems are not generally characterized by scale-free structures.

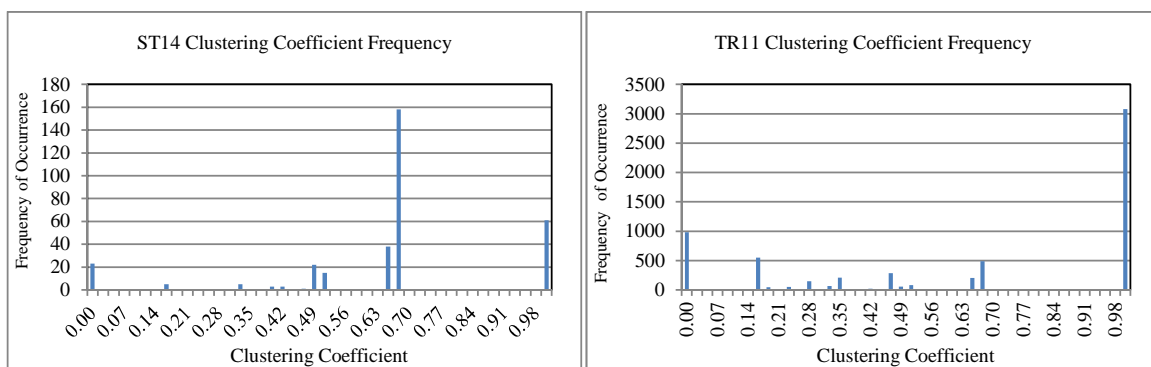


Figure 3.31: Frequency of Occurrence vs. Clustering Coefficients.

In figure 3.32, the probability mass function (PMF) of the degree distribution for all feeder nodes is shown. Apparently, power-law pattern is not readily observed.

Table 3.1: Graph metrics for the feeders

Graph Name	TR11	ST14
Vertices	6318	334
Total Edges	26646	2278
Connected Components	1	1
Maximum Geodesic Distance (Diameter)	181	41
Average Geodesic Distance	64.754422	18.407096
Graph Density	0.000667639	0.020481559

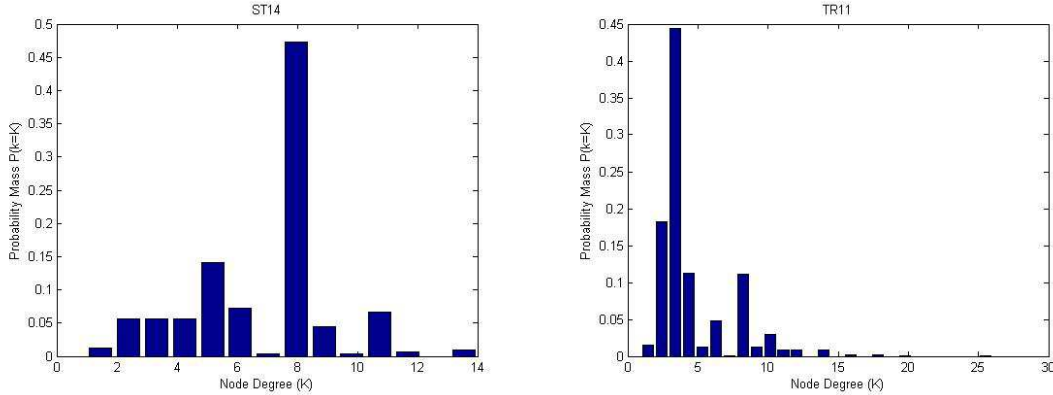


Figure 3.32: Probability Mass Function of the node degrees.

3.3.2 Incorporating Electrical Laws in the Network Model

To demonstrate the differences between the topological and the electrical representations of the feeders, the $|Z_{kl}^{bus}|$ matrix is used to build the electrical graph as discussed in Section 2.4.1. In Figures 3.33 and 3.34, the graphical representations of the feeders are shown. For better clarity of the ST14 network image, all links with $|Z| < 0.3$ and the associated nodes are removed. Hubs or high connectivity nodes are distinguished. There are 55444 distinct node-to-node connections in the Z_{bus} matrix in ST14 case; the links shown in Figure 3.33 represent the first 3782 node pairs with the highest electrical connections. For TR11 feeder, some nodes and links with relatively low $|Z|$ are removed to help improve the visibility of the network.

The network graph becomes too complicated by the time the $|Z_{kl}^{bus}|$ exceeds a moderate size and that's the case for almost all distribution feeders. In this research, some lower degree nodes were eliminated to provide a visually comprehensible picture. However, this strategy is not the best option if not the worse. Better strategy includes using a high power computing machine and a high resolution large screen to fit as many nodes (as much information) as possible.

From a topological point of view, the feeder networks look neither like a random network nor like a scale-free network. However, from an electrical perspective, which captures the behavior of the network (not simply the physical structure), both networks look to have distinct groups of nodes that are “electrical hubs”. Electrical hubs are the buses with the highest electrical connectivities to the rest of the network. Governed by Kirchoff’s Law, power, flowing through the electrical network, most likely pass through one or more of those hubs. In the language of social networks, those would correspond to nodes with a high betweenness or information centrality.

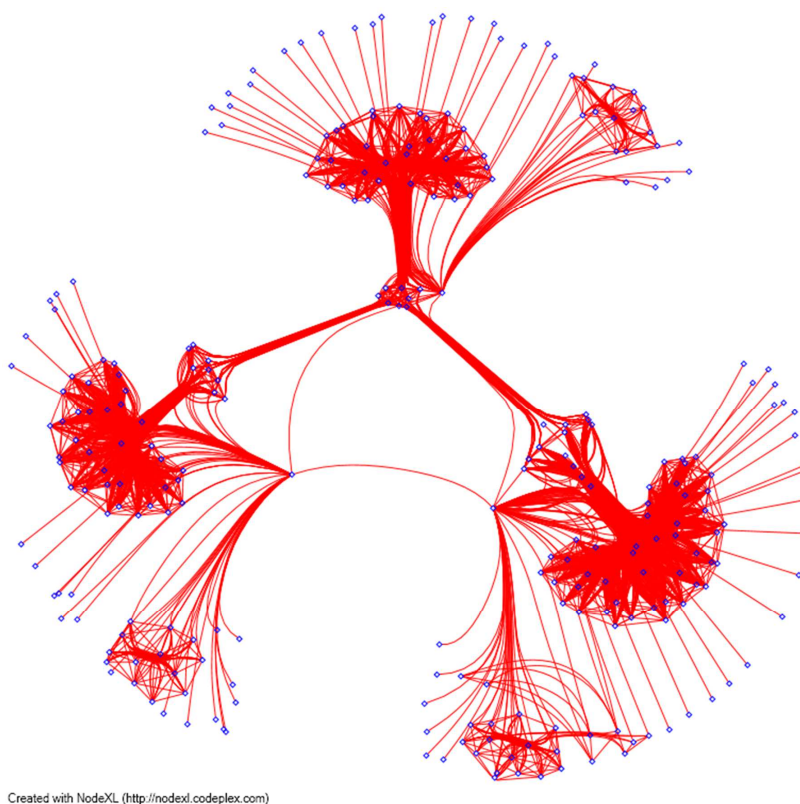


Figure 3.33: Topological representation of ST14 impedance graph. A few nodes exhibit high connectivity to the rest of the feeder. Those are “electrical hubs” which are highly effective buses in driving feeder behavior and are significantly effective if are used to position major coordinating agents. However, the electrical hubs may be vulnerable to disruptions (Data from PNM, Graph by NodeXL).

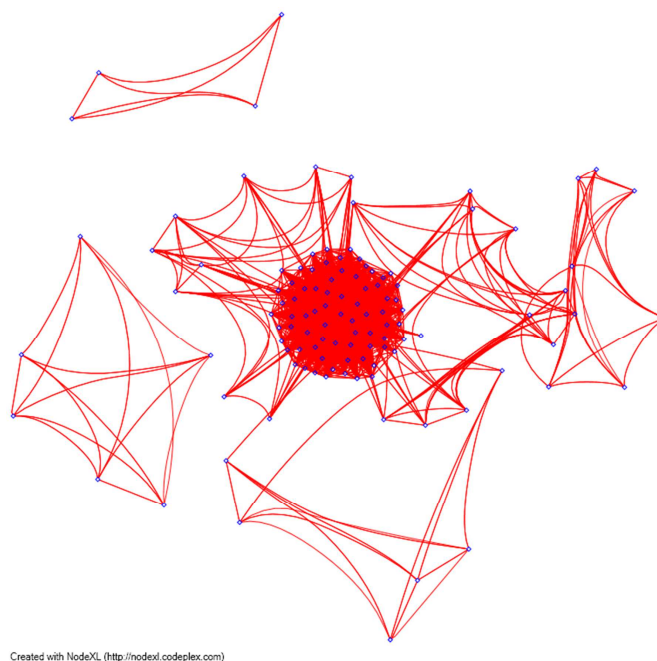


Figure 3.34: Topological representation of TR11 impedance graph. (Data from PNM, Graph by NodeXL) By eliminating the lower ranking nodes to make the graph more visually comprehensible, some useful information is lost. A single node in this case is highly connected to the rest of the feeder. Such a highly connected node could be regarded as an “electrical hub” and used for driving the feeder behavior or positioning major coordinating agents.

The clustering coefficient distribution of the electrical network is shown in Figure 3.35 for both feeders. Some highly clustered nodes are recognizable, which represent the nodes through which a large portion of the power pass. Other nodes have minor impacts on the behavior of the power system from the connectivity stand point. The clustering coefficient distribution also reminds us that even if highly clustered node are rarely seen in the feeder network graph, if the electrical laws governing the flow of power in the feeder are taken into account, the electrical network graph would divide into highly clustered portions.

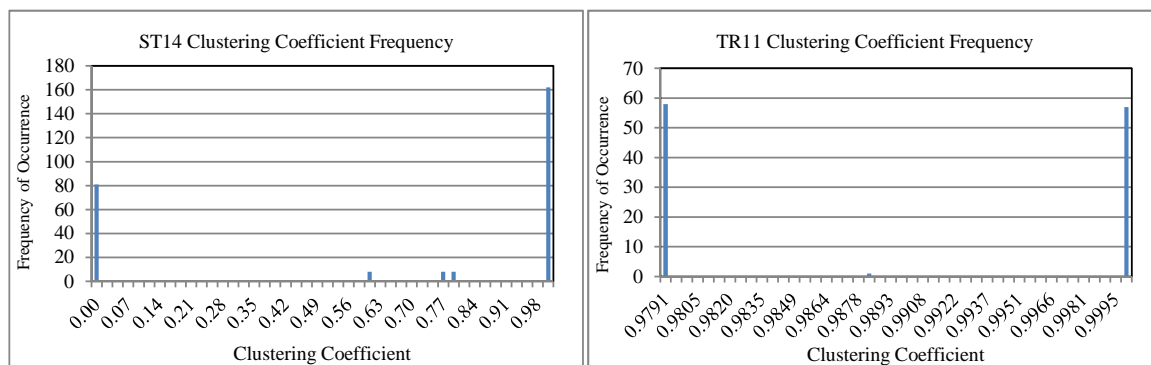


Figure 3.35: Clustering coefficients frequency of occurrence for the electrical network graphs. Electrical networks are heavily clustered as opposed to the corresponding connectivity graphs. It should be noted that the above graphs exhibit 2 different scales for clustering coefficient.

Table 3.2 demonstrates fundamental differences between the topological representation of the feeders and the associated “electrified” version of the topology. Maximum geodesic distance is remarkably reduced and resembles a scale-free network.

Table 3.2: Graph metrics before and after “electrification”

Graph Name	TR11	TR11 (Impedance)	ST14	ST14 (Impedance)
Vertices	6318	116 (Insignificant Nodes Removed)	334	270 (Insignificant Nodes Removed)
Total Edges	26646	5257	2278	3782
Connected Components	1	7	1	1
Maximum Geodesic Distance (Diameter)	181	2	41	3
Average Geodesic Distance	64.754	0.998	18.407	2.497
Graph Density	0.00067	0.39895	0.02048	0.10414

In figure 3.36, the probability mass functions of the degree distribution of all nodes in both feeder, after modeled by incorporating electrical laws, are shown.

If proper parameters are selected, power networks resemble scale-free networks. Electric hubs are not easily detected through simple network topology analysis though. By incor-

Chapter 3. Course of Study

porating electrical laws in the network structure, it was shown that the distribution feeders share many properties with other scale-free networks. Hubs, in power distribution systems, if highly connected with other hubs, may indicate a “central” and probably vulnerable “core” or connection center.

On the other hand, disturbances in one part of an electrical network affect neighboring areas substantially more than the far nodes or regions. Therefore, in power distribution systems, disturbances are expected to propagate less widely compared to some other network structures. This is a valid claim unless the stability of the whole network is compromised due to other collective faults or contingencies.

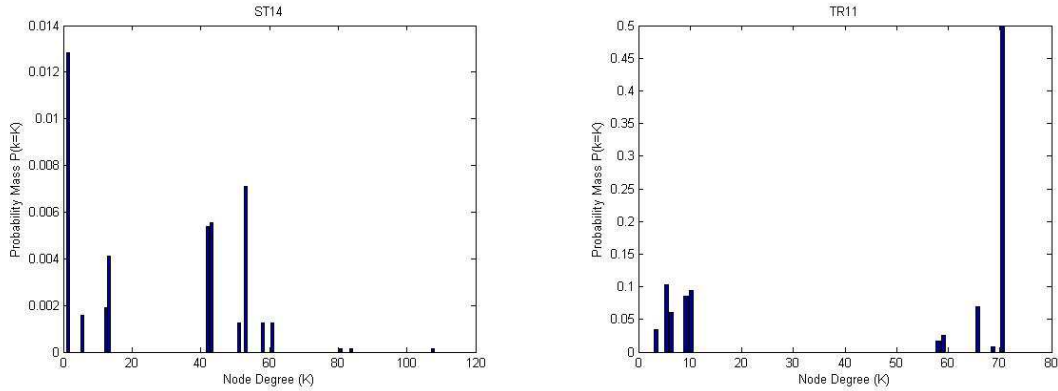


Figure 3.36: Probability Mass Function of the node degrees.

3.4 Coordinated Operation of the Agents

A power distribution feeder which is traditionally a tree of conductors, transformers, switches and other distribution level equipments, delivers electricity from the substation, the connection point of the distribution system to the transmission system, to the customers. Feeders are normally designed to operate in a one-way energy transfer direction. Energy is delivered from the source (substation) to the customers which are distributed spatially along the feeder.

Increasing the penetration level of DER into the distribution feeders is considered an opportunity and a challenge. By integrating necessary communication and control infrastructure into the distribution feeders, controllable load/generation centers will be developed which provide substantial flexibility for the business and operation of the distribution system. On the other hand, such a complex distributed system is prone to instability and black outs due to lack of a major “infinite” supply and other unpredicted variations in load and generation if isolated from the grid.

The feeder ST14 is located in Mesa del Sol, Albuquerque. A 500kW PV farm and a 1MWh utility scale storage system which consists of a 500kW ultra fast smoothing battery and a 250kW shifting battery are connected close to the feeder source. At a nearby location, a micro grid demonstration (NEDO) which incorporates a 240kW natural gas-powered generator (NGPG), a 80kW fuel cell, a 50kW PV generator, a lead-acid battery storage system, and hot and cold thermal storage is also installed and connected to the feeder through a 1000kVA transformer. The storage system has been under several test cases to demonstrate its capabilities for smoothing the PV output in cloudy days, to shift the off-peak generated power of the PV system to peak consumption times and to firm the total PV+BES system as a dispatchable resource for the utility.

3.4.1 Coordinated Smoothing in Multi-Agent Systems

The system configuration is shown in Figure 3.37. Feeder ST14 is the major power supplier to a number of commercial customers, the NEDO microgrid and to the developing residential community of Mesa del Sol. However, there are a few DERs such as a fuel-cell and a natural gas-powered generator connected to this feeder which can supply power back to the grid or to their designated load centers. The PV farm and the BES system are located 2 miles away from the NEDO microgrid. In the current configuration all those subsystems are operating independently. The customers get their required energy from the feeder. The BES system is smoothing the PV output based on the adjustments done by the utility and each individual resource in the microgrid generates power according to the operator's adjusted settings.

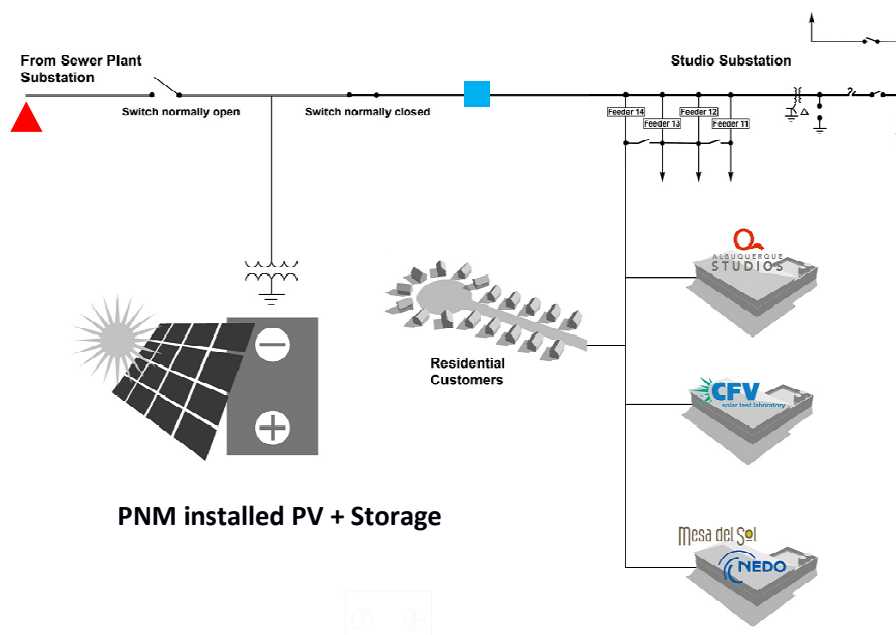


Figure 3.37: Feeder ST14 configuration diagram showing the connections to the PV and BES system, the NEDO microgrid, commercial and residential customers (Courtesy of PNM).

The energy resources that are studied here are assumed not to contribute to Volt/Var or frequency control. Net real power is exchanged with the grid and also the energy exchange

efficiency is assumed to be 100%. In a partially cloudy day – based on the amount of smoothing required by the utility – the BES system could be under severe stress to compensate the intermittency of the solar generation. A 24-hour PV generation in a partially cloudy day is shown in Figure 3.38. Drastic variations in the order of 20%/Sec is recorded (Figure 3.39).

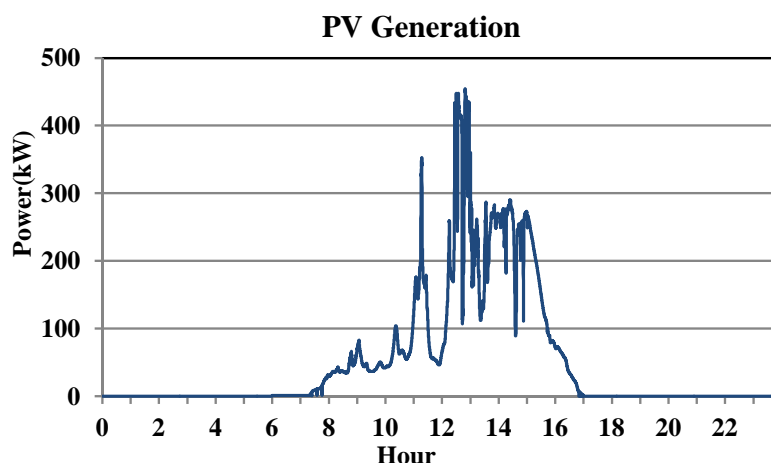


Figure 3.38: PV generation power in a partly cloudy day at Prosperity.

The idea is first to demonstrate how the BES system can contribute to smoothing out the fluctuating output power of the PV system. Then, to show how a natural gas powered generator (NGPG) could be controlled in order to contribute to the smoothing process based on its capacity and dynamic capabilities. As a matter of fact the BES system can operate in charge mode and in discharge mode. It means the BES system can sink energy from the grid when the batteries have to be charged and can inject energy to the grid and discharge. During BES system operation, the SoC of the batteries has to be maintained within allowable range. On the other hand, depending on how the baseline for power reference is set up, the NGPG can just operate in generation mode and can not sink energy from the grid.

The smoothing resource, must be capable of bidirectional energy exchange because the instantaneous rate of change in the PV generation (Ramp Rate) can be either positive or negative. To adapt the NGPG to operate in both positive and negative rate regions, its

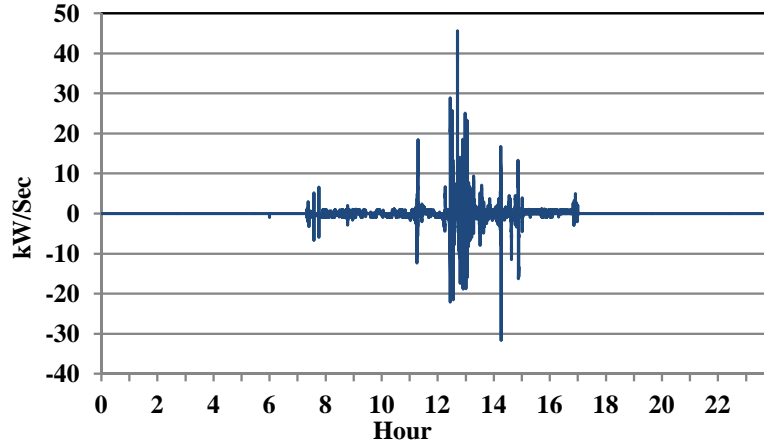


Figure 3.39: PV Ramping Rate in a partly cloudy day for a 500kW system.

normal operation power is set at 180kW and the control system is allowed to ramp it up to ± 60 kW at 0.12%/Sec rate . Therefore, the NGPG behaves like a storage system ramping up and down, while its net generated energy is positive.

The internal controller characteristics of the BES system and the NGPG were not studied in this research. They are assumed to be able to follow the power reference signal within their practical limits. The reference signal is sent by the virtual controller which is introduced in the next section.

The ultimate goal is to design a decentralized control method for each agent (DER) to be able to contribute to an optimum smoothing scenario. Those optimum scenarios won't be necessarily unique and will vary based on the associated cost functions.

Two different approaches are introduced for smoothing. One is based on compensating the ramp rate (RR) and the other is based on compensating the deficit or abundance in PV generation. In this research, it is assumed that the instantaneous generation power data for every DER is available to all agents with no delays. Future work will cover the effects of delay or error and transparency of data for every agent.

Ramp Rate Compensation (RRC)

In this method, each DER receives the aggregate RR of the higher ranked contributing resources as input signal and tries to change its power proportional to RR and in the opposite direction with regard to its maximum RR and capacity characteristics. Output power control signal is equal to the integral of the RR signal plus the initial operating value. Two internal loops try to maintain the smoothing energy and the output power close to their preset values.

Every DER is ranked based on the total operational costs and/or other priorities. For this research, the NGPG is given a rank of 1 (highest priority) and the BES system is given a rank of 2 (lower priority) establishing a higher priority for NGPG than the BES system.

Internal control loops oppose the compensation procedure because the compensation RR tries to keep the output RR as close to the reference RR as possible which pushes the DER to sink/source more energy, while the average smoothing power and energy is desired to be as low as possible. Accordingly, there is a trade-off between smoothness and average exchanged energy and power.

Conceptually, producing smoother output requires instantaneous RR calculation. Hence, 1-Sec RRC, which produces smoother aggregate output compared to 20-Sec RRC necessitates faster response devices to be installed and used. Nevertheless, delay in measurement and transmission may cause significant error which may not only generate a lesser smooth output but also may act in reverse direction and add even more fluctuation to the aggregate output. Investigating the possibility of such delays and finding appropriate solutions are beyond the scope of this research.

A simplified block diagram of the controller implementing RRC method for adjusting the smoothing DER power set point is illustrated in Figure 3.40. As it was mentioned previously, the BES system has a lower rank than NGPG. Therefore it has to compensate the aggregated RR of the PV and the NGPG.

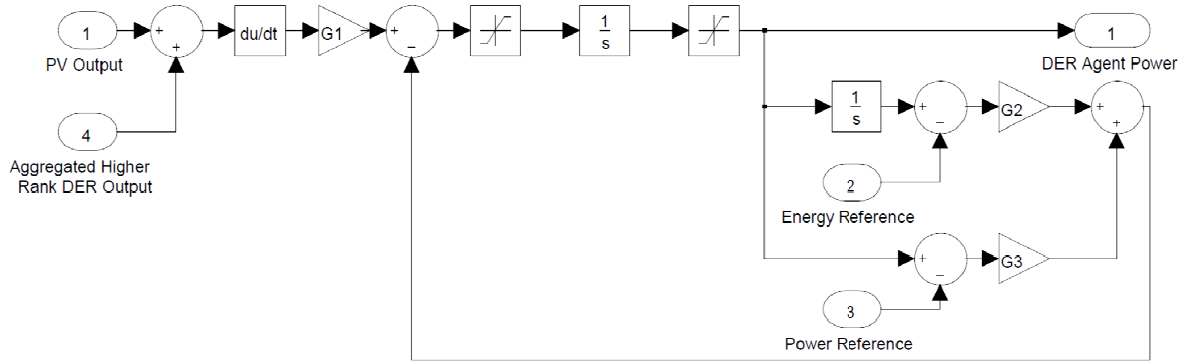


Figure 3.40: Smoothing agent power reference controller block diagram implementing RRC method.

Sliding Window Moving Average Compensation (SWMAC)

In this method, each DER receives the difference between the aggregate power and its sliding window moving average of the higher ranked contributing resources and tries to compensate the measured deficit or abundance in power proportional to its available capacity and permissible ramping rate.

Smoother output is equivalent to wider sliding window. Therefore, 200-Sec SWMAC produces a smoother aggregate output compared to 2-Sec SWMAC. The drawback is the induced delay caused by the inherent delay of SWMAC algorithm which is equal to half the window length in time.

A simplified block diagram of this control method for the smoothing agent power adjustment is illustrated in Figure 3.41.

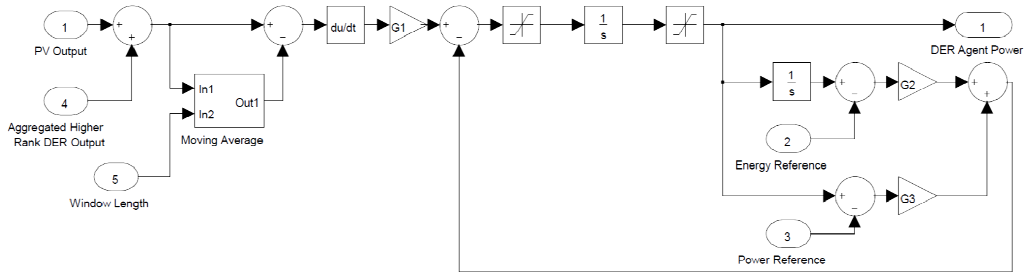


Figure 3.41: Control block diagram of the smoothing power reference calculation using SWMAC method.

The described controllers are designed and implemented in GridLAB-D as control modules. An instance of the appropriate controller adjusts each agent's power, and consequently energy level.

RRC Results

To illustrate how each agent can contribute to the smoothing process, the same PV power data is fed to both control systems. Frequency domain analysis is also performed on the results to clarify the effectiveness of the smoothing algorithms.

Figure 3.42, shows the contribution of NGPG and BES system to smoothing process with RRC controller. Different parameters setting will produce different effects. In Figure 3.43, the PV power and the total DER generation is shown. The smoothing algorithm worked appropriately for most of its operation cycle except at around 12pm to 1pm. During that period, due to the excessive intermittency in PV generation, the system was not able to smoothen the fluctuations completely. Sharp changes in the aggregate output are noticeable.

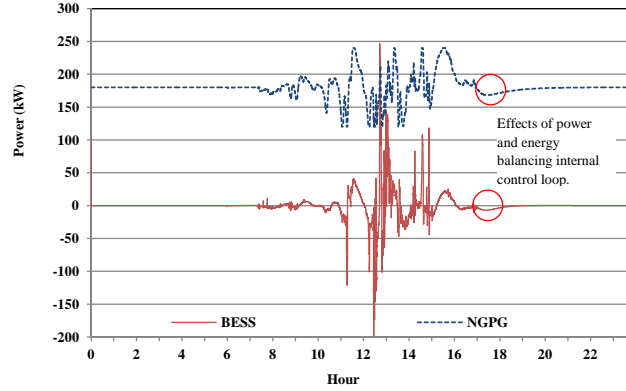


Figure 3.42: NGPG and BES system contribution to RRC smoothing. NGPG follows the PV fluctuations, but due to limited dynamic response and power capabilities, is not able to follow the fast varying portion of the PV. On the other hand, BES system ramps up and down keeping up with PV variations.

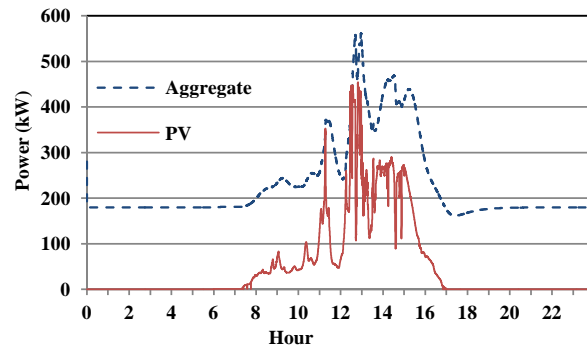


Figure 3.43: PV power and the aggregated output. Despite smoothing, there are still signs of fluctuation in the aggregated output.

The frequency spectrum of the original PV output and the aggregate power output of all available DER in the feeder are calculated and is shown in Figure 3.44. The Cumulative Density Functions (CDF) of both spectrum are also added to the picture. The smoothed signal characteristics show that a large portion of the energy delivered by the original signal which was spread over the frequency range of 1-Sec to DC, has moved toward lower

frequencies. The CDF also shows that a higher percentage of the smoother signal energy is concentrated close to lower frequency vicinity compared to the energy delivered by the original signal.

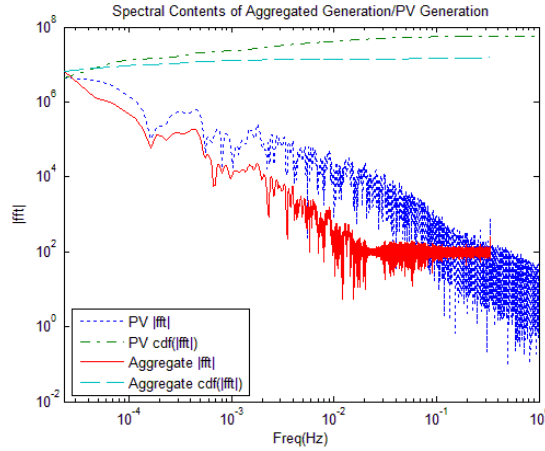


Figure 3.44: Frequency spectrum of the PV output and the smoothened aggregate power. Total energy concentration is shifted toward lower frequency ranges because of smoothing.

Total energy contribution is also another important factor in battery based storage systems. A major goal of this research is to find such solutions that reduce the stress on the batteries and their cycling depth. In Figure 3.45, the smoothing energy variation of both BES system and NGPG is shown. Clearly, the NGPG operation has reduced the amount of energy delivered by the batteries. Therefore, any available DER with lower overall costs can be used in order to reduce the need for more expensive battery support or to reduce the required size of the BES system.

SWMAC Results

A similar study is conducted to investigate the advantages and possible drawbacks of the SWMAC method. Figure 3.46 to 3.49 show similar graphs as figures 3.42 to 3.45 except

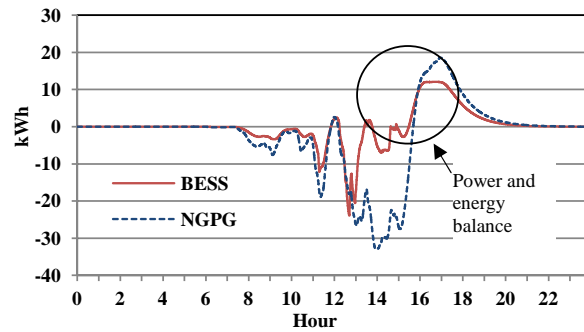


Figure 3.45: Energy exchange for smoothing between the BES system, the NGPG and the feeder.

for SWMAC method. Obviously, this method is superior for smoothing the PV output to a higher extent, by incorporating more energy from the storage system. The controller has energy and power balance internal loops which regulate total power and energy exchanged with the grid.

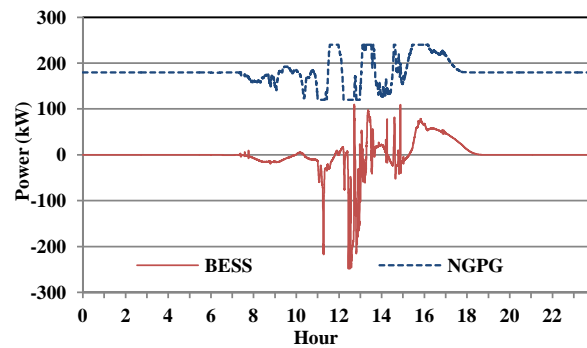


Figure 3.46: NGPG and BES system contribution to SWMAC smoothing.

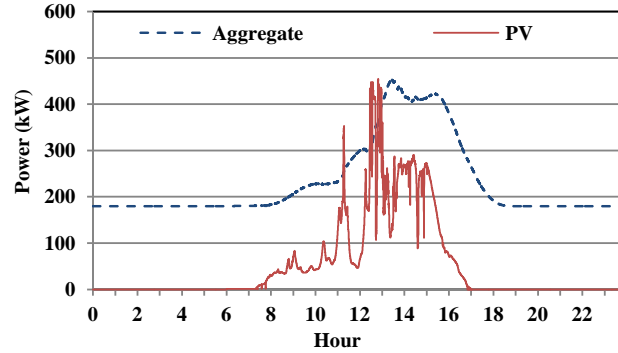


Figure 3.47: PV power and aggregated output. The aggregated output is smoother than the previous method at the expense of higher energy contribution by the battery.

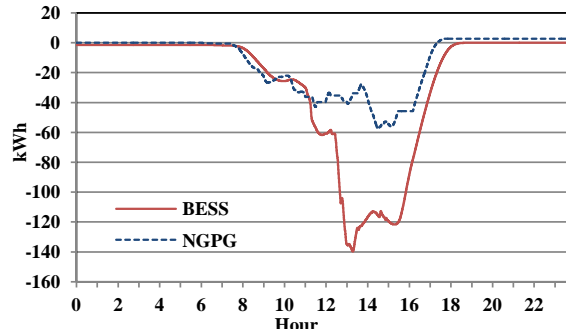


Figure 3.49: Smoothing energy, exchanged between BES system, NGPG and the grid. Apparently, the storage system is under more stress than RRC method. Compared to the previous case, the aggregated output is smoother at the expense of more BES contribution.

Similar analysis could be conducted for a collection of DERs, connected to the feeder. Associated with every DER, is a cost function which could be calculated independently based on operating cost, energy cost and other corresponding parameters. The calculated cost function can be used to define their rank, which is the basis for the algorithm to assign the appropriate output power control signal. However, access to reliable and accessible communication and processing power at low cost might be a drawback for the suggested

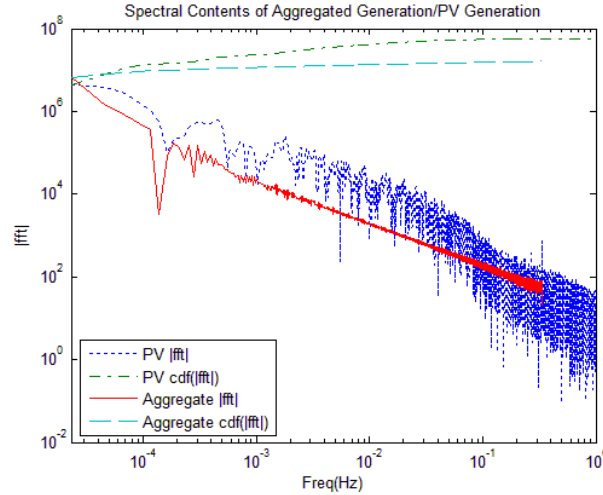


Figure 3.48: Frequency spectrum of the PV output and the smoothed aggregate power. High energy concentration in the lower frequency range is prevalent.

solution. A few suggestions are given later to address this problem by limiting required data transfer services.

Suggestions

Based on the presented analysis, a resource assignment strategy is suggested as below:

1. Cheaper resources with slower response, compensate the PV source or any other major renewable resource like wind turbine adopting the SWMAC method.
2. Fast response BES system - may be equipped with ultra batteries - compensate the aggregate generation with RRC method.
3. Slower responding BES systems which could constitute a collection of small community storage systems distributed along the feeder compensate the aggregated power using

SWMAC method. The aggregated power of the higher ranking resources would then carry lower frequency contents.

The described strategy helps avoid the need for costlier fast responding batteries while attaining the required level of smoothness of the aggregated local power generation. On the other hand, if the collection of the distributed resources are equipped with appropriate autonomous controllers with the required connectivity to a central controller, the feeder with all connected resources (DERs) could be a dispatchable resource if **properly** coordinated.

With both smoothing methods discussed, selection of the smoothing method boils down to the system operator policies – whether a microgrid operated independently or a distribution feeder run by a utility company. In other words, there could be no unique strategy defined for smoothing. Each case has to be studied individually and an appropriate (optimum) solution should be found case by case.

In this section, it was shown that multiple controllable resources, if available, could be coordinated to compensate for many undesired effects which otherwise would be inevitable in existence of uncontrollable DERs such as PV or wind generators. However, it was previously shown in section 3.2 that by incorporating a large number of distributed resources, an inherent smoothing effect takes place. Such smoothing effect caused by spatial diversity of those agents spread over the area eliminates the need for additional smoothing services.

3.4.2 Coordinated Demand Management

A community of residential premises is modeled as a part of the research to monitor various effects of having a high percentage of DERs in microgrids. Mesa del Sol as a developing PV-ready community is an appropriate benchmark for smart microgrids in near future. Mesa del Sol is physically located in the area served by the ST14 feeder which was modeled and studied before. Available load assets and the prospect of high penetration of PV generation

and PHEV utilization in that neighborhood are among the reasons it is selected for further studies.

The standard patterns for electricity consumption are established based on studies on US consumers behavior [119, 120]. To build a realistic model of the residential neighborhood, loads in a typical home in Southwest of the US are modeled using GridLAB-D. For the following electric loads, customized load shapes are defined according to the available load surveys:

- A/C

A/C system constitutes a significant part of the electrical load in a house. It has a cyclic on/off characteristic with a variable duty cycle which is mainly driven by the ambient temperature, inside temperature setting, number of occupants, square footage, degree of insulation.

- Water Heater

Water heater has also a repetitive characteristic but with much lower power than the A/C. It shows more frequent on cycles early in the morning and early in the evening when people take shower before leaving or after arriving home.

- Plug Loads

Fairly low powered compared to previous load types.

- Lights

It is fairly low in power level and normally peaks in the evening.

- Cloth Washer

The combined washer and dryer load is not a significant load compared to the rest of the loads in house. The expected duty cycle depends heavily on the number of residents and their life style. Run cycles frequency could vary from once every other week to a few times a week.

Chapter 3. Course of Study

- Dish Washer

Dish washer could have similar load pattern as a cloth washer, running from once a week to a few times a week.

- Refrigerator

Load power is small compared to major load in a house. However, it could have frequent on/off cycles especially when people get to their homes and start cooking.

For the A/C, water heater and refrigerator, the developed load models in GridLAB-D are considered. The GridLAB-D development team at PNNL have conducted extensive research on residential loads and have developed complex load models based on number of residents and thermal characteristics of the house such as square footage, ambient temperature, insulation efficiency and more. For the dish washer, cloth washer, plug loads and the lights, basic load shapes are used. Some loads such as washers have weekly cycles since those are not used on a daily basis. Other loads have daily profiles yet with different patterns for workdays and for weekends. The following graphs illustrate sample daily or weekly load profiles.

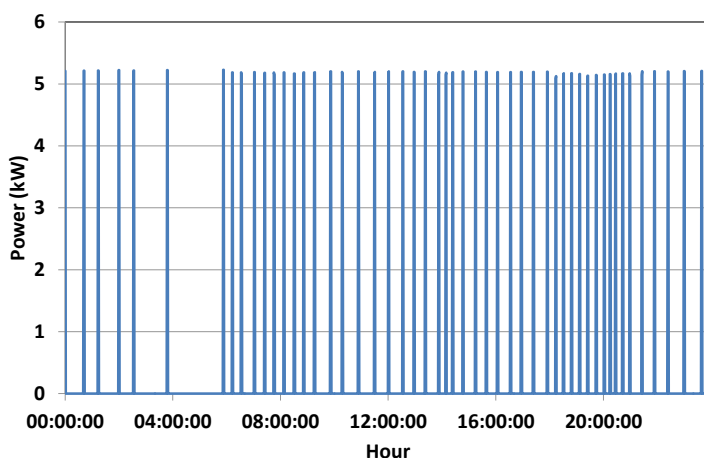


Figure 3.50: Typical profile of a residential A/C load.

A/C load varies according to ambient temperature and occupancy. Temperature rises during the day and declines over night. The graph correctly shows more frequent cycles

at the times of higher temperature or higher occupancy and less frequent operation at the times of lower temperature or less activity. After people leave home (for work), amount of the exchanged heat between outside and inside of the house due to convection decreases and consequently the A/C tends to operate less frequently (Figure 3.50).

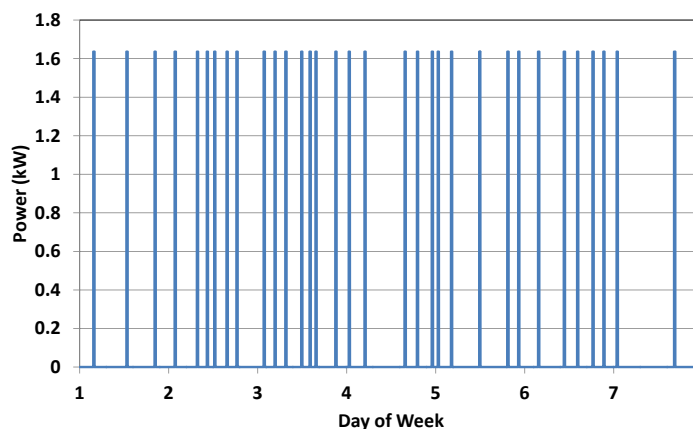


Figure 3.51: Typical residential water heater weekly load profile.

The water heater model takes some occupancy factors into account. Early mornings and evenings are the times when water heating load maximizes (shorter duty cycles) due to heavy shower usage (Figure 3.51).

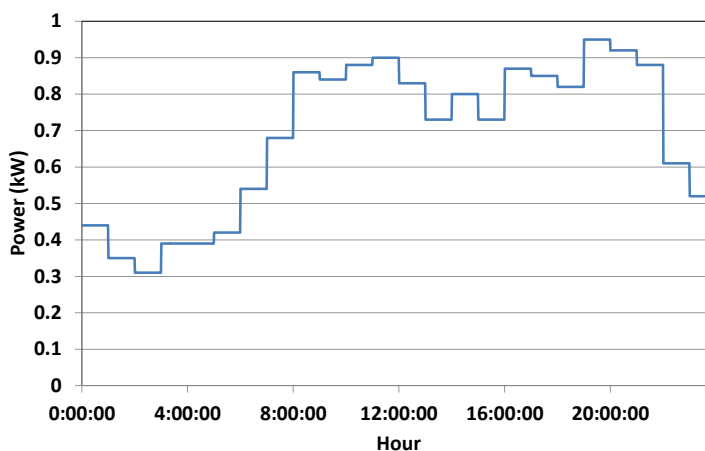


Figure 3.52: Typical daily load profile for plug loads.

Plug loads might have very different patterns, however since the cumulative power of the plug loads is generally insignificant compared to the major loads such as A/C and water heater, changing load pattern has limited effects on the total household load pattern (Figure 3.52).

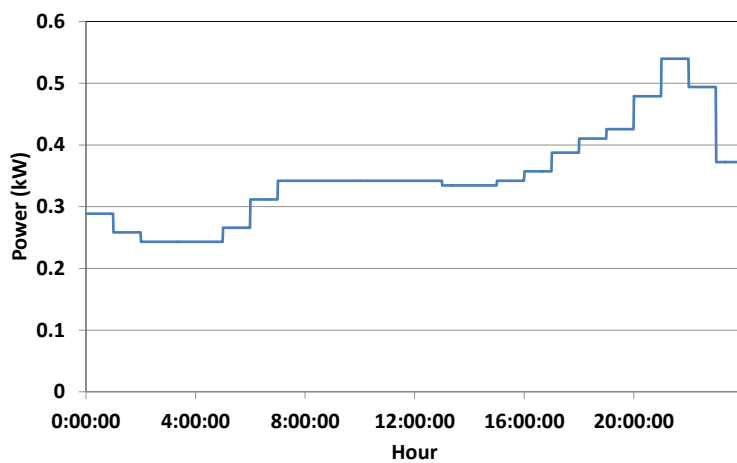


Figure 3.53: Typical daily lighting load profile.

Lighting load generally increases in the evening after dusk and people get back to their homes. By midnight lighting load is expected to return to its base level (Figure 3.53).

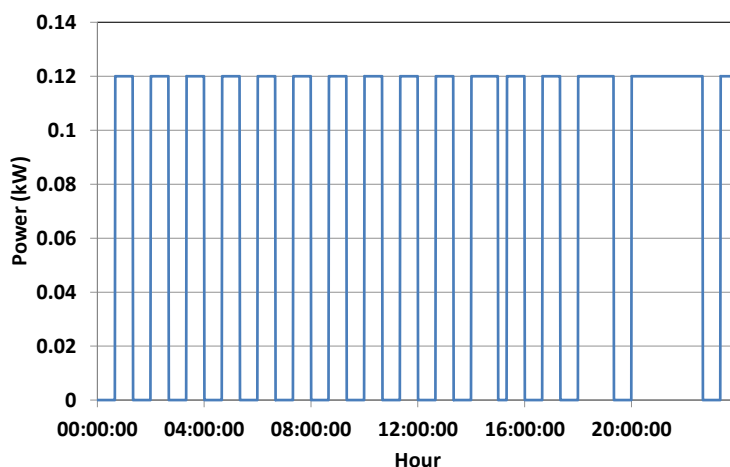


Figure 3.54: Typical refrigerator daily load profile.

Refrigerators normally follow a steady pattern of on and off cycles during minimum usage periods. As soon as people return from their daily businesses, refrigerator load begins to have longer on and shorter off times until occupants go to bed and fridge returns to its steady operation cycle (Figure 3.54).

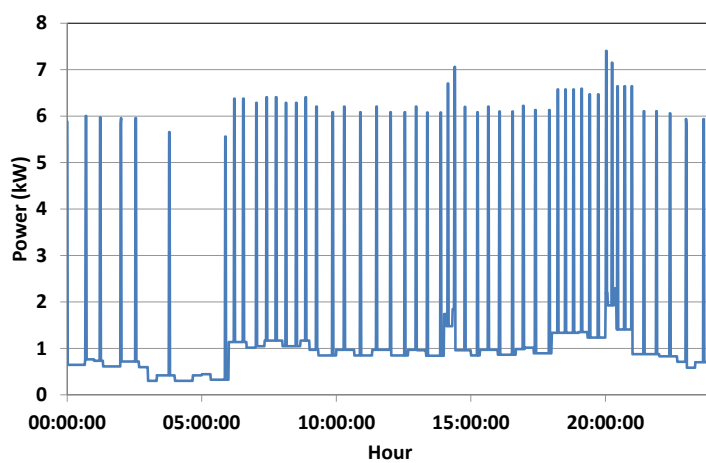


Figure 3.55: Typical house daily load profile on weekdays is shown. Significant and frequent load surges are related to the A/C on cycles. Because the A/C load constitutes the major portion of the total load, it is expected to be an ideal candidate for coordinated controlled operation for load management.

After combining all developed load shapes, a typical house load is established (Figure 3.55). As expected, A/C load is a major contributor to the total demand at residential level especially due to frequent high power spikes.

The load shapes developed during this research incorporate some stochastic parameters in order to establish diversified load models when several homes are to be modeled. Although a single home load model may not be an accurate representation of certain residences, as the model grows in size to include a larger number of homes, the aggregated load is, to a large extent, a valid model for a residential community in the area. Figure 3.56 illustrates a weekly load profile of a community of 7 homes. Considering all diversity factors and by reviewing typical applications at PNM, it is a reasonable assumption that a typical 50kVA distribution

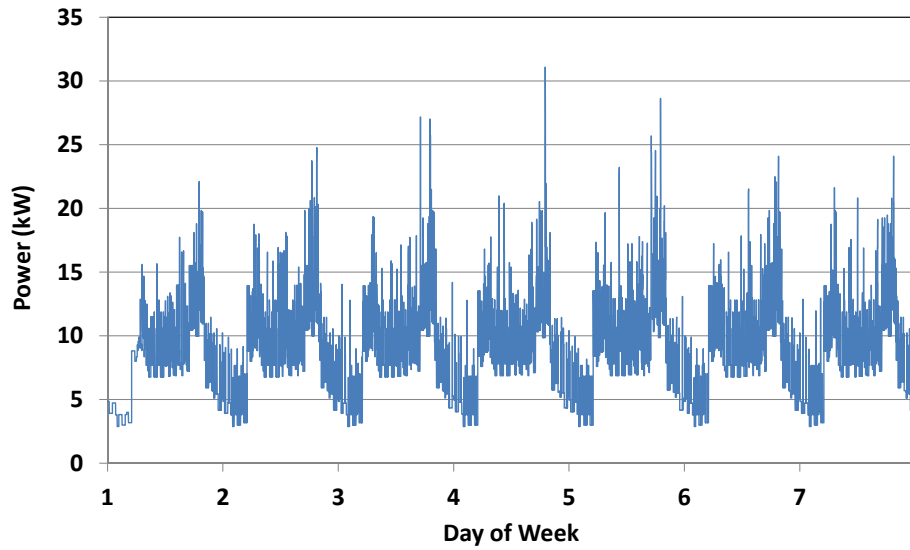


Figure 3.56: Typical weekly load profile of a community of 7 houses.

transformer is appropriate to feed 7 homes. The aggregated load profile demonstrates the credibility of such assumption.

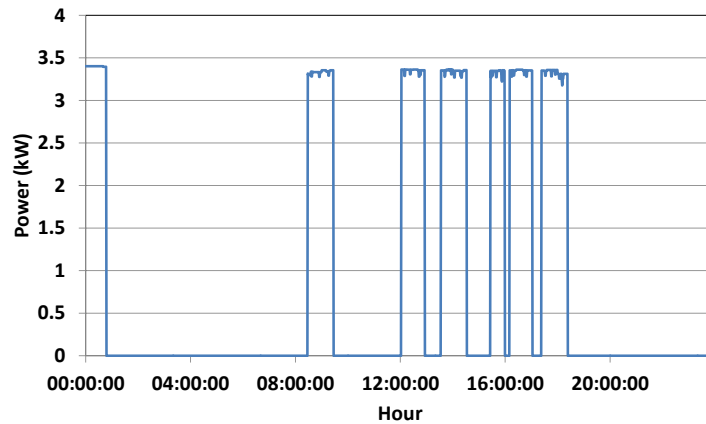


Figure 3.57: Typical EV charging profile over a weekend.

Plug-in Hybrid Electric Vehicles (PHEV) have gained popularity in recent years. According to a rather conservative estimation, it is expected that penetration level of all electric

vehicles and PHEVs to reach 11.9% by 2035 [121]. Other scenarios call for higher penetration levels due to recent advances in EV technology, higher energy contents in batteries, government subsidies and public awareness regarding environmental issues [122].

A simple PHEV model is incorporated in the simulation process based on energy capacity and power consumption of the plug-in Toyota Prius as a rather successful and popular model in the US. That model incorporates an initial State of Charge (SoC), charger power and availability of the charging device. It is assumed that 4 residents of the 7-home community own EVs. The very basic scenario is based on a non-controlled charge strategy which means the charging process is initiated regardless of the total load on the distribution transformer. The vehicle is plugged in every time parked in garage. Charge pattern change depending on the driving habits and whether it is a weekday or weekend. In a weekday the driver generally leaves home with a fully charged car and returns empty sometime after the end of working hours. Figure 3.57 shows a typical EV charge pattern on the weekend. Several trips are made from and to home maybe for different occasions such as shopping, dining and so on.

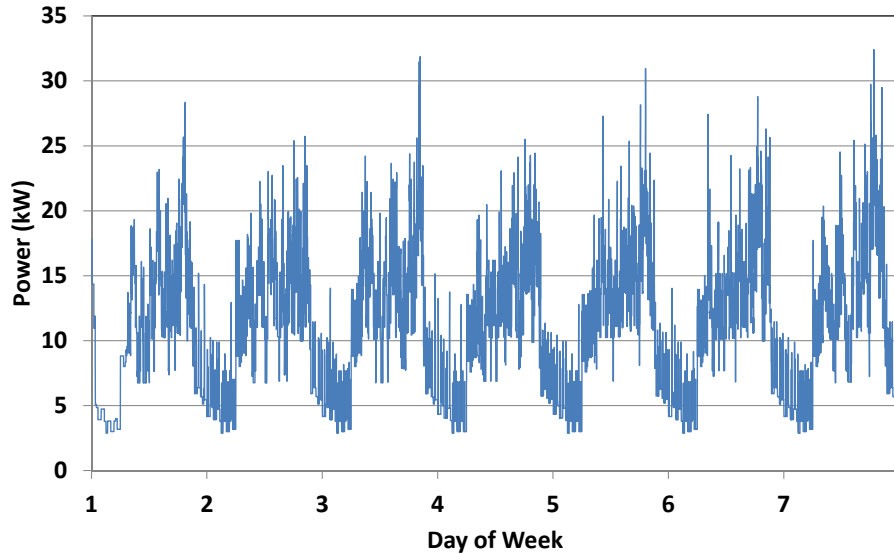


Figure 3.58: Weekly load profile of a community of 7 houses. 4 residents drive PHEVs) and plug their vehicles at their convenience and without any coordination with other PHEV users or with the grid operator. Frequent peaks exceeding 25kW and increase in demand is observed.

Chapter 3. Course of Study

Since inception, the commercially available PHEV has always been a point of great concern for the utilities or grid operators. The risks of an overwhelmed distribution system in the presence of simultaneous charging of multiple electric vehicles are not trivial.

Such risks include overload fault in protective devices due to higher than anticipated demand, reduced life expectancy of the distribution assets such as transformers and switches and potential demand for increasing the network capacity to fulfill reserve requirement.

To demonstrate that those concerns are real and there should be plans and strategies in place to address such possibilities, the community load is modeled by adding 4 electric vehicles to the existing model. A blind charging scenario with no correspondence and coordination between the grid operator and the charging devices is first examined. Figure 3.58 shows the weekly demand of the community including the EV charging loads. Thanks to the uncoordinated charging of the EVs, not only the average load is increased but also more frequent peaks occur which increase the risk of overload and tripping some power delivery equipment. If the community is powered by limited capacity resources, such as the case in an isolated microgrid, such peaks or faults may cause loss of power for the whole community.

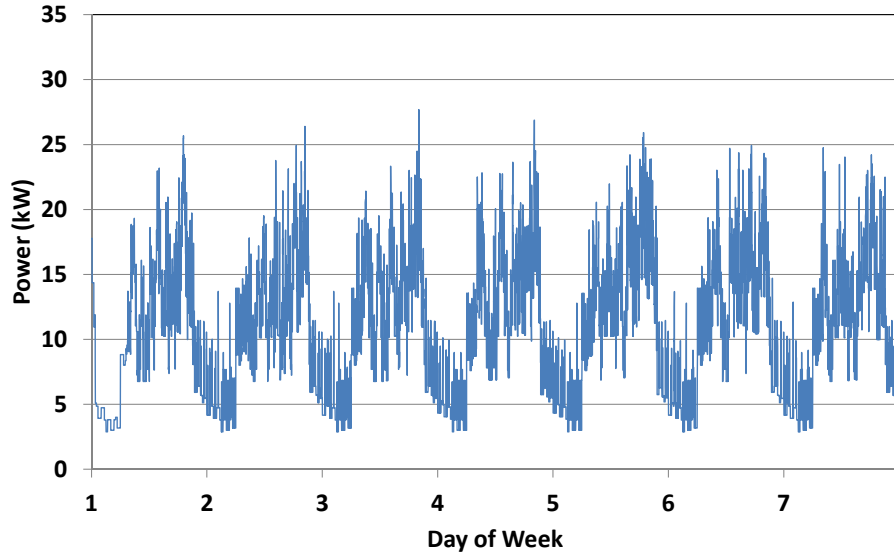


Figure 3.59: Weekly load profile of a community of 7 houses in presence of 4 PHEVs. The smart chargers consider peak load as a constraint and do not initiate a charging cycle if total community demand exceeds 25kW.

A fast and simple coordination scheme is devised to address the induced peaks due to uncorrelated EV charging start time. Total load at the transformer is monitored by a “Community Power Management” (CPM) device. The CPM broadcasts a demand percentage (D) signal calculated based on the ratio of the total load on the transformer and the transformer capacity. A higher than 100% is a sign for transformer overload. In this phase of study, the signal is assumed positive only since no energy resource is available downstream of the transformer that could inject power back into the grid.

Upon receiving the signal, EV charger either initiates, terminates, continues to charge or continues not to charge depending on a probability signal. State of charging for device i at step n is defined by :

$$CHG_{i,n} = \begin{cases} 1 & SoC_i < L_Thresh_i \text{ and } \alpha_i < D \\ 0 & SoC_i > H_Thresh_i \text{ or } \alpha_i > D \\ CHG_{i,n-1} & Otherwise \end{cases} \quad (3.10)$$

where α_i is a random variable with a uniform distribution between 0 and 1 and is generated independently by each charge controller agent, L_Thresh_i is the low threshold for agent i and H_Thresh_i is the high threshold for that agent.

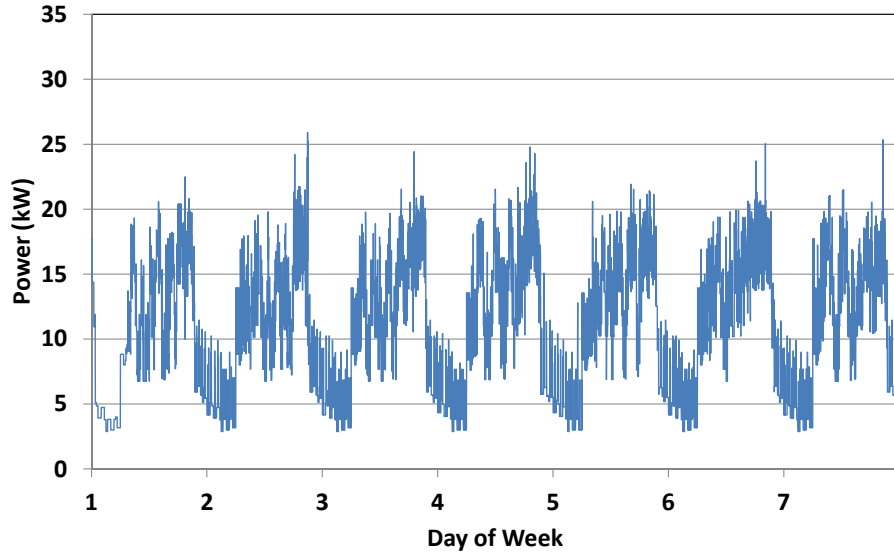


Figure 3.60: Weekly load profile of a community of 7 houses in presence of 4 PHEVs. Smart charge threshold is 20kW.

By adjusting or optimizing the agent's threshold levels (H_Thresh_i and L_Thresh_i) it is possible to achieve a community level load management strategy with the ability to fulfill a microgrid level objective, in our case peak demand shaving. Figure 3.60 illustrates a case in which the target demand level is set to 20kW.

It was mentioned at the beginning of this section that at Mesa del Sol, all newly developed homes are PV ready. The next step in this research is to consider a year 2025 level rooftop PV scenario. It is simulated assuming an aggregated PV generation equivalent to 15kW at peak is generated by the 7 rooftop PV systems in the community. In Figure 3.61, total PV power in a semi-cloudy day in the Fall is shown.

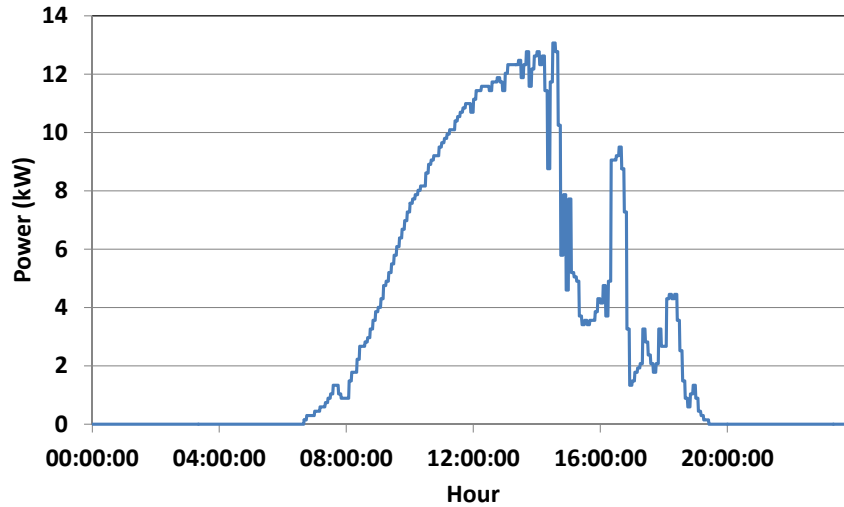


Figure 3.61: Typical cumulative rooftop PV generation profile for a 7-house community in a cloudy day.

In Figures 3.62 to 3.64 similar simulations are repeated except with inclusion of a consolidated rooftop PV generation. Effects of excessive PV generation during noon time (peak generation), when residential demand level is low, are illustrated with zero or negative demand. Since, in general, EV charging happens at the times when there is low or no PV generation, coordinated EV charging is not a practical solution to address the negative demand problem during weekdays. There is minimum or zero overlap between the times PV system generates power (day time) and when the EV could be plugged in (evening or night).

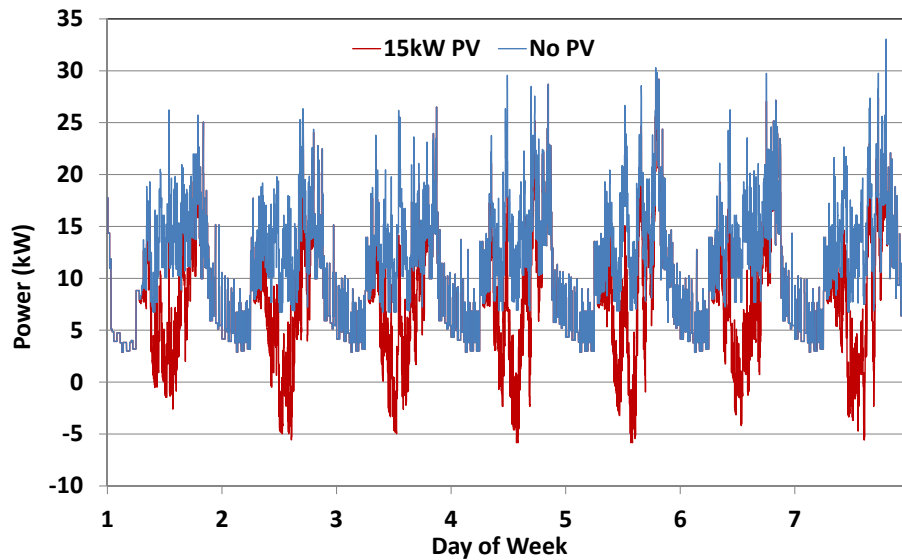


Figure 3.62: Weekly load profile of the community of 7 houses in presence of 4 PHEVs. Some houses have rooftop PVs. Negative demand and frequent peaking load are the potentially destructive outcomes of high penetration of PHEVs and PV generation in a microgrid.

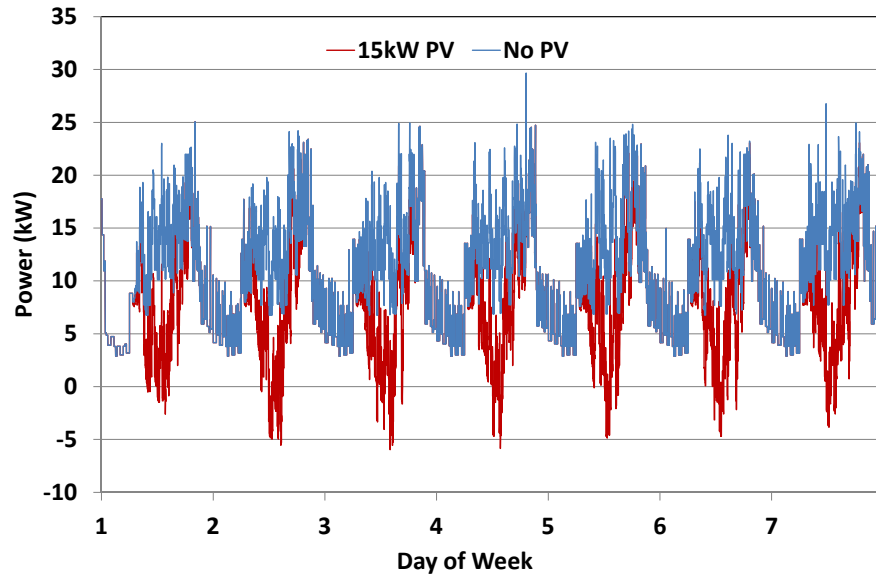


Figure 3.63: Weekly load profile of the community of 7 houses in presence of 4 PHEVs. Smart charge threshold is 25kW. Some houses have rooftop PVs. Coordinated operation of the EV chargers mitigates or minimizes the peak demand problem but negative demand is still inevitable.

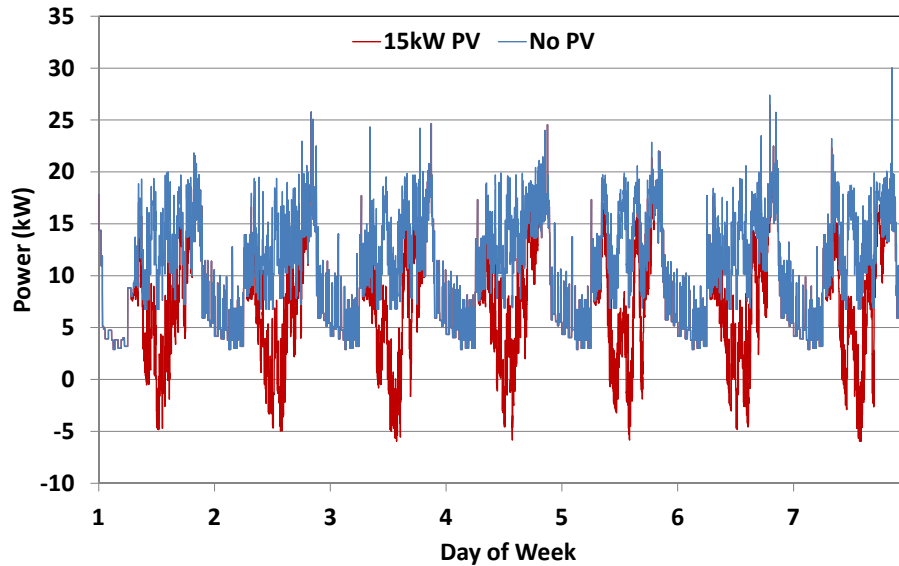


Figure 3.64: Weekly load profile of the community of 7 houses in presence of 4 PHEVs. Smart charge threshold is 20kW. Some houses have rooftop PVs. Coordinated operation of the EV chargers mitigates or minimizes the peak demand problem but negative demand is still inevitable. In a grid-tied system, occasional negative demand does not cause serious issues other than the need for readjusting some protective devices to allow reverse flow of energy. In an islanded system, that problem must be addressed by other means such as storage systems.

Negative demand level for a microgrid in islanded mode gives rise to over voltage or possible tripping of the protective devices and should be avoided. However, in grid-tied systems, negative demand is translated to making profit by selling the unconsumed energy back to the grid if allowed by the utility. If not, excessive generation must be curtailed or dumped. In an islanded microgrid, the issue of negative demand could be addressed by introducing a Community Energy Storage (CES) System to store and release (regulate) the available electric energy when necessary. CES operation could be optimized not only to maintain the demand level within the defined limits but to make some profit by storing the generated energy at the time of low demand (lower price) and selling it back to the grid operator or local consumers at the time of high demand (higher price) if some sort of real time pricing and open energy market becomes available. By establishing appropriate dynamic

Chapter 3. Course of Study

pricing methods and by enforcing the utility companies to accept an open market based on that concept, distributed energy exchange technology will be available at community or even at house level.

3.4.3 Coordinated Load Shifting

At Mesa del Sol, there are several filming studios with in-house ice-storage facilities which provide cooling and air conditioning services on demand. Assuming that the most scenes are captured during normal working hours, there would be some benefit in shifting the demand to the less expensive off-peak hours. The whole idea of incorporating an ice-storage system is to take advantage of the difference in cost of electricity between the on-peak and off-peak hours. This idea is behind the following studies conducted to understand whether there are benefits in incorporating ice-storage cooling systems in commercial buildings.

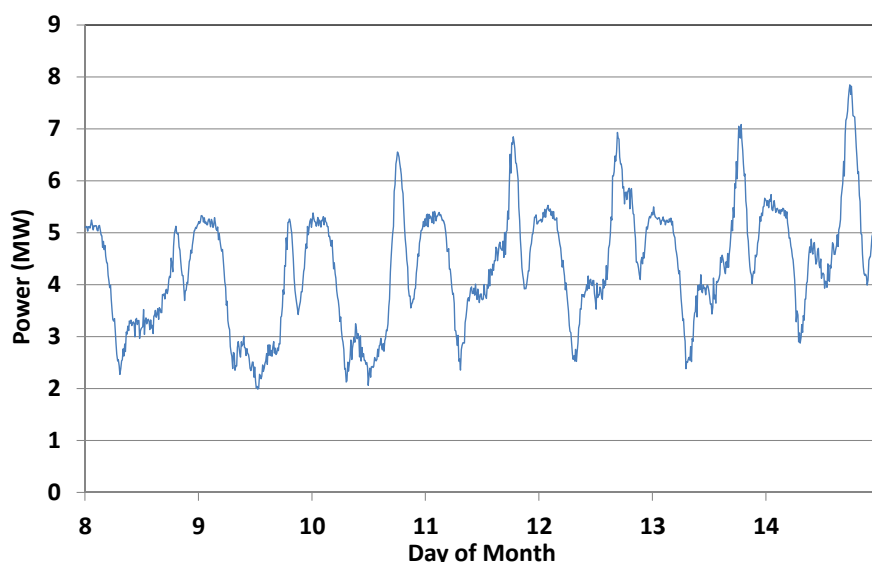


Figure 3.65: Expected demand of 10 commercial buildings estimated based on sample demand data from the Mechanical Engineering building.

To estimate the expected cooling load for commercial buildings, the mechanical engineering (ME) building at the university of New Mexico is chosen as a benchmark. Total electric load and cooling load are separately recorded by the Building Management System (BMS). Those data are used to synthesize cooling and non-cooling and total demand load shapes for a commercial complex which includes 10 buildings similarly sized as the ME building.

A commercial complex including ten buildings is fed by the distribution feeder. Each building is assigned a randomly shifted and scaled version of the base load shapes which are developed using the same method explained in section 3.1.5.

In Figure 3.65, the total expected demand of the commercial complex is shown. Peak load and base load are largely dependent on the season (ambient temperature) and usage (during summer time some departments may be lightly used), however the concepts introduced here apply regardless of the differences between buildings.

Figure 3.66 shows the cooling load expected at the feeder. Cooling constitutes a large portion of the total demand especially in hot summer days. Not only the utility companies incentivize large customers to shave their peak load at the time of heavy demand, there are benefits in shifting the loads to periods of light load usually after midnight in which electricity costs less if the customers opted for multi-tariff meters or other real-time pricing mechanisms become available.

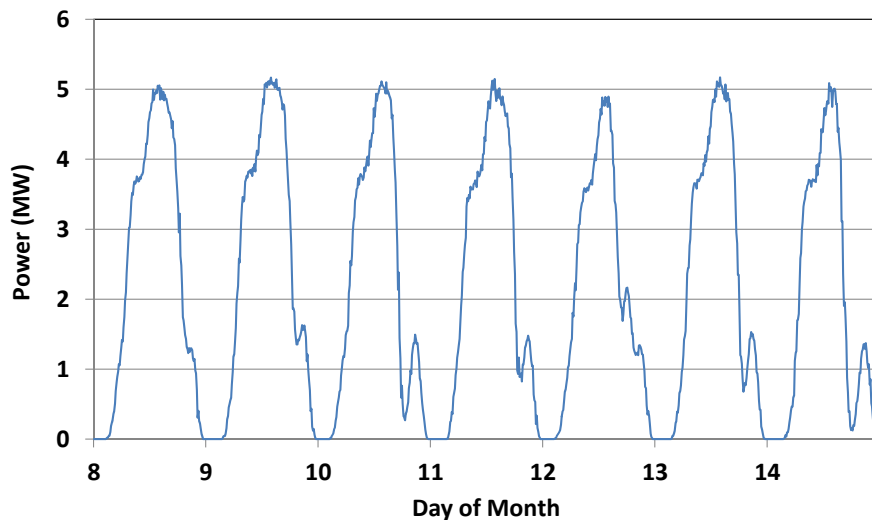


Figure 3.66: Expected cooling demand of the commercial complex estimated based on sample demand data from the Mechanical Engineering building.

Figure 3.67 illustrates the cooling load in a 24-hour period in a hot day in July. Almost half of the total energy is consumed during peak or shoulder hours, in which electricity costs more for the utilities, which have to run their peaking generation reserve, and consequently for the customers.

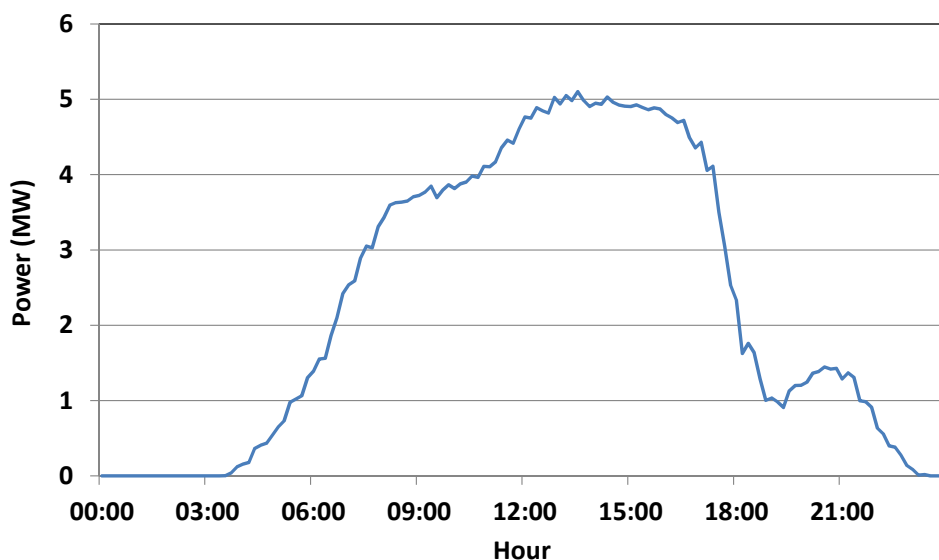


Figure 3.67: Sample 24-hour cooling demand for the commercial complex.

The necessary model for simulating cooling load in a commercial building was developed because no model for commercial buildings was available in GridLAB-D. Instead, GridLAB-D has a built-in house model which incorporates several factors such as surface area, ambient temperature and number of occupants. That model was used in section 3.4.2 to constitute the community load. Since the model provides excellent flexibility in defining various aspects of a building thermal characteristics, it was used as a building block for modeling larger facilities. A number of houses with equal square footage to the target building are aggregated to form an equivalent model of a commercial building. Figure 3.68 illustrates the simulated load which is synthesized by the commercial complex model including a collection of the developed commercial modules. The simulated load shape resembles the expected load shape which was developed based on the ME building cooling demand.

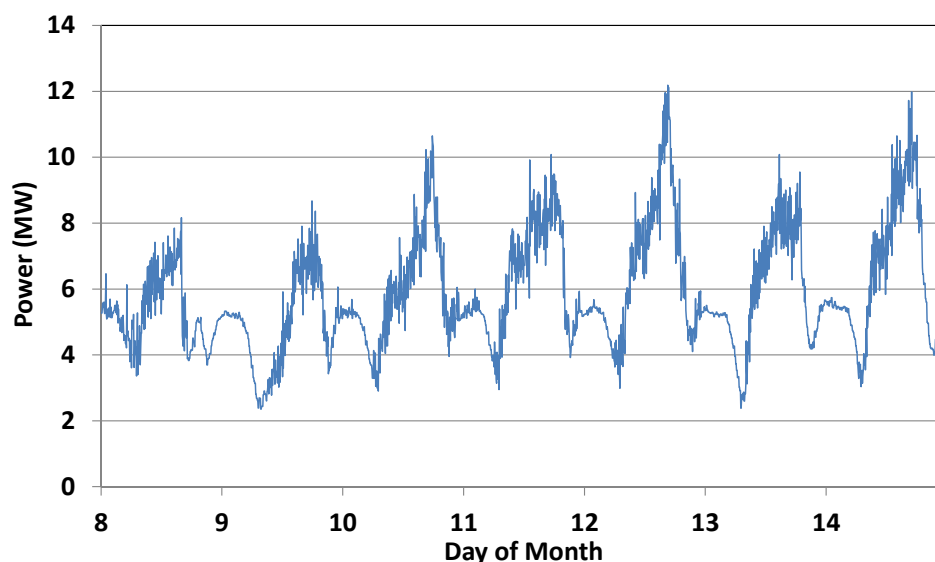


Figure 3.68: Simulated total load for the commercial complex.

To investigate possible advantages and potential disadvantages of using ice-storage systems for shifting the cooling demand from the times it costs more, to times when it is least costly, a reasonably sized ice-storage system facility is added to each building model. The simplest way to control the cooling system is just to deplete the ice reserve whenever cooling load is needed (a fixed schedule or based on the desired temperature inside each building) and to restore it based on a predetermined schedule.

The problem with this scenario is that it will most likely generate off-peak high demand excursions even exceeding the original peak values. That's because all or most storage systems will start to replenish their ice reserve at a certain time when the total load on the grid is expected to be at its lowest. In Figure 3.69, total cooling load at the feeder after ice-storage systems been added to each building is shown. Since there is no effective coordination in progress, very high load demand excursions are repeatedly seen.

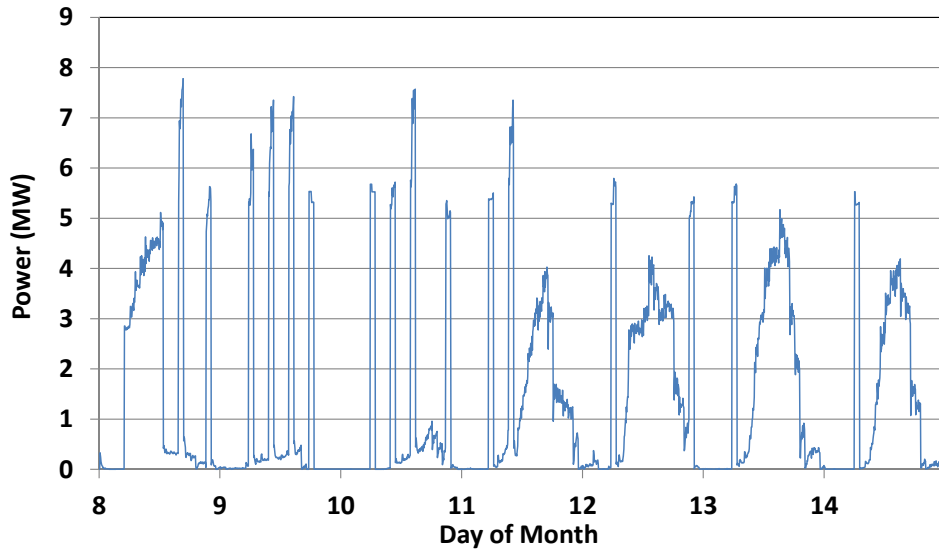


Figure 3.69: Total cooling load at the feeder after ice-storage system was added to each building. Shorter but significantly higher demand bursts are detected which are not desirable and must be avoided.

High peaks in total feeder load caused by simultaneous ice replenishing cycles are shown in Figure 3.70. Demand peaks are shifted to grid off-peak periods, however, from utility point of view that's not a desirable solution if it is intended to introduce ice-storage systems as a broader load management solution.

A fast and simple coordination scheme is devised to address the induced peaks due to uncorrelated ice replenish start time. Total load at the feeder source is monitored by the feeder operator (FO). The FO broadcasts a demand percentage (D) signal calculated based on the ratio of the total feeder load and the feeder capacity. A value higher than 1 is a sign of feeder overload. A negative value for D indicates reverse power flow from the feeder back to grid which is not allowed in this simulation but could be considered as a possible scenario happening in near future.

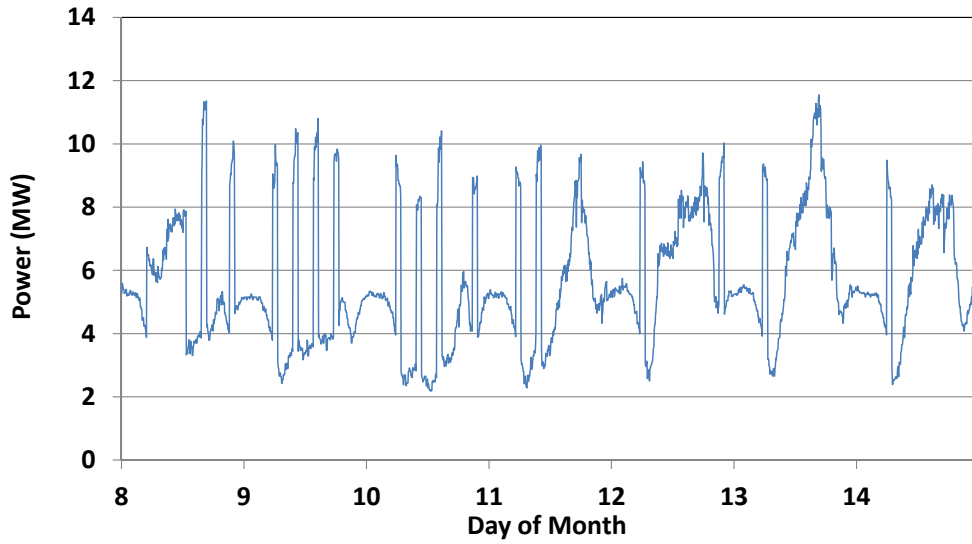


Figure 3.70: Total feeder load after ice-storage systems been added to each building. Shorter but higher peaks in feeder demand are not desirable.

Upon receiving the signal, ice-storage system either initiates, terminates, continues to operate or continues not to operate depending on a probability signal. Ice replenish command for device i at step n is defined by :

$$Rep_{i,n} = \begin{cases} 1 & Loi_i < L_Level_i \text{ and } \beta_i < D \\ 0 & Loi_i > H_Level_i \text{ or } \beta_i > D \\ Rep_{i,n-1} & Otherwise \end{cases} \quad (3.11)$$

where β_i is a random variable with a uniform distribution between 0 and 1 and is generated independently by each ice machine agent, L_Level_i is the low threshold for agent i and H_Level_i is the high threshold for that agent.

High and low threshold levels together with the level of remaining ice, the ambient temperature and the desired air condition output temperature determine how fast the ice contents are depleted, how frequent system starts to replenish the ice and how much total demand at the feeder source would vary.

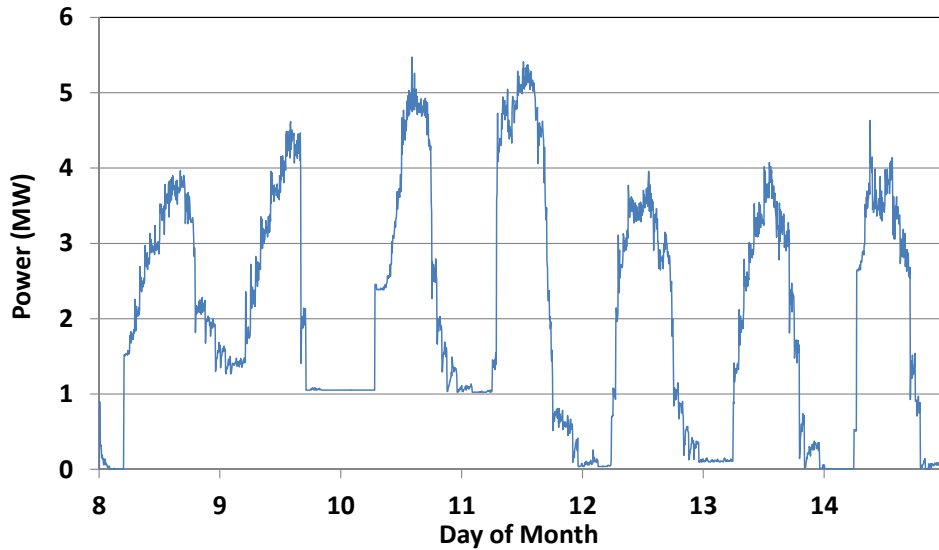


Figure 3.71: Total cooling load at the feeder after ice-storage systems been added to each building and coordination is implemented.

The following figures (3.71 and 3.72) illustrate cooling demand and total demand at the feeder source when the icing agents coordinate with FO to maintain the total demand within the specified targets (4-8MW) except for one incident.

It should be noted that the main target for this solution is to shape the demand not to preserve energy. Ice cooling system has a limited efficiency and due to inefficiencies in ice making and heat exchanging, the total energy consumed per tons of refrigeration might be higher than other commercial HVAC systems. However, the benefits of shifting the load to non-peak hours and flattening the load profile are expected to justify the usage of ice-storage cooling systems.

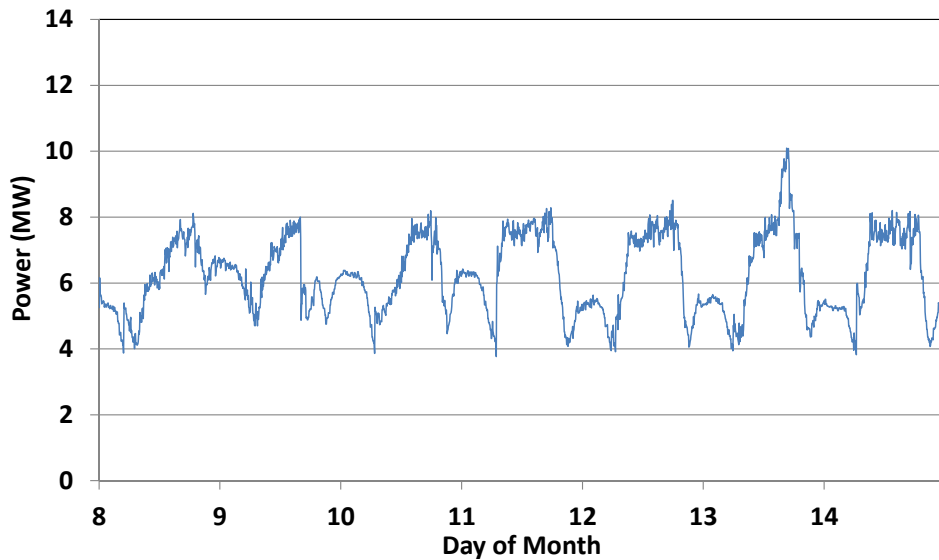


Figure 3.72: Total load at the feeder after ice-storage systems been added to each building and coordination is implemented. Total demand is well within the specified limits (4-8MW).

Figures 3.73 and 3.74 illustrate the concept of demand shaping and peak shaving introduced earlier. By trimming or optimizing the low and high thresholds, total demand at the source (or at a energy hub) could be reshaped to satisfy certain cost functions. To implement this scenario the FO would need to prioritize the agents in a way that larger and topologically closer loads will need to communicate faster and with higher bandwidth compared to other agents. This arrangement would provide adequate control over the total demand with reasonable communication cost and burden without overwhelming the whole data network and process load on the agents.

Technical and practical barriers to setup a real time demand broadcast system are not included in this research, however it will be elaborated in more details in the following sections to understand how much information should be transmitted, which agents have the priority to access to high definition and high speed data and how much the reach should be.

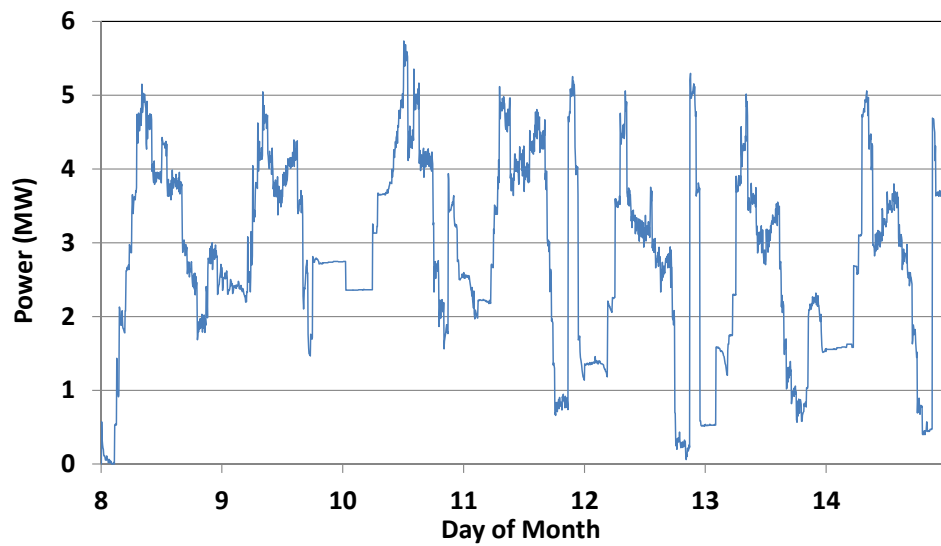


Figure 3.73: Total cooling load at the feeder in presence of ice-storage systems and different sets of limits (6-8MW).

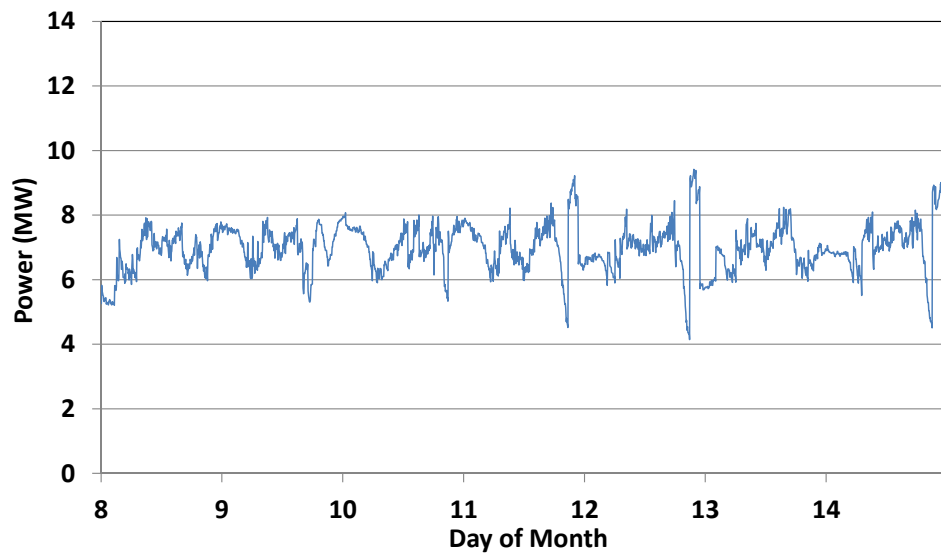


Figure 3.74: Total load at the feeder in presence of ice-storage systems and different sets of limits (6-8MW).

3.4.4 Categorization

It was demonstrated previously that DER systems do not necessarily have similar characteristics in terms of capacity, ramping capabilities, cost of operation, availability, controllability and so on. To define an effective coordination strategy to fulfill the target cost function, available DER systems must first be assigned a grade or rank which could be interpreted as a weight factor to be used later for contribution adjustments. Of possible ranking strategies, the following deemed to be more effective for that purpose.

Frequency Band

In section 1.2, it was first mentioned that recent work has demonstrated that a battery energy storage system (BES system) can effectively perform two important tasks: shifting renewable power delivery to times of peak demand, and smoothing intermittent PV generation before it is injected into the feeder. While this approach demonstrably works, batteries are still very expensive, and their lifetime is limited. One type of DER that is gaining increasing interest is the microgrid, in light of increased needs for both energy efficiency and high reliability. An islanded microgrid must have enough storage to compensate for any mismatch between load and generation while islanded. Use of thermal storage, as a second type of DER that is receiving renewed attention, was then extensively examined in section 3.4.2. Since, in the commercial and residential building sector, cooling loads account for much of the peak demand and cold storage devices allow the cooling load to be shifted to periods of lower demand. While cold storage devices are too small to affect the the overall system demand when acting individually, their aggregated action could be significant.

The DER demonstration project located at the ST14 distribution feeder, that was previously introduced, combines a microgrid – consisting of a 240kW natural gas powered generator (NGPG), an 80kW phosphoric acid fuel cell, a 50kW PV field, a lead acid battery storage system, a hot and cold thermal storage system – with a 500kW utility scale PV array and

an associated 1 MWh shifting and smoothing battery bank. Also on the same distribution feeder are several businesses (including movie studios with large ice storage devices) as well as a growing residential PV-ready community, which when fully built has the potential to reach a high penetration.

The intermittency characteristics of PV generation can be examined using power spectral density plots [123]. As an example, the spectral contents of a highly intermittent day in May are displayed in Figure 3.75, and were collected from the 500kW PV array irradiance sensors. By dividing the spectral contents into separate sub-sections, different techniques for managing those frequencies can be studied for each section.

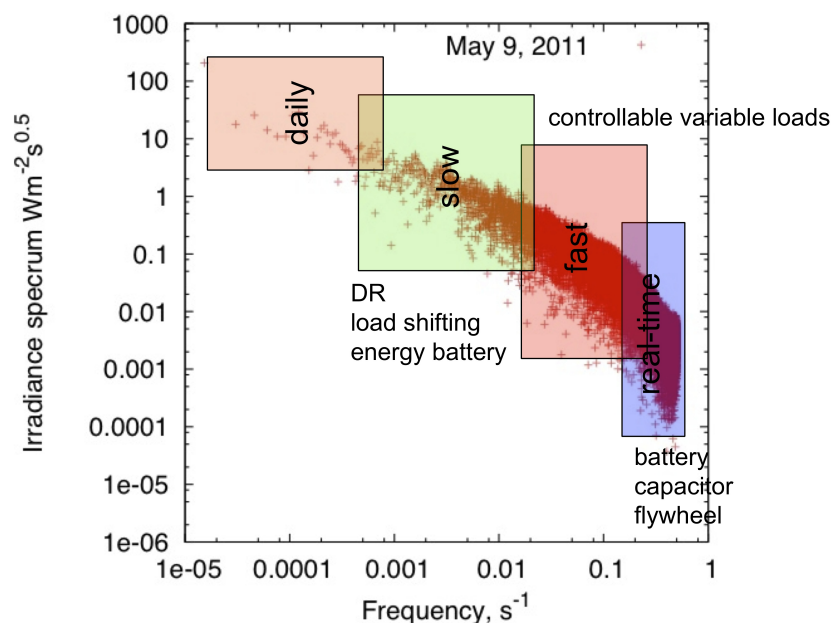


Figure 3.75: PV power spectral contents in a partly cloudy day. The spectrum is divided into frequency ranges based on the amount of energy contents (Data from PNM).

The power spectral density plot reveals that high-frequency fluctuations carry little power (and as a consequence little energy). Thus, these can be compensated with fast-responding devices (e.g. capacitors, flywheels, some high-performance batteries) with high power/ramp rate capacity and relatively small energy capacity. At the other end of the scale, daily

solar power generation cycles can, at least partially, be compensated with thermal storage devices, off-peak (baseload) grid generation, and night-time grid-scale wind generation when available.

Electrical Distance

In section 2.4.1 it was shown that the power networks equations can be formed in the bus frame of reference in which the performance is described by n linear independent equations for $n+1$ number of nodes. In the admittance forms, the performance equation can be described by Kirchoff's Laws as

$$\bar{I}_B = \bar{Y}_B \cdot \bar{V}_B \quad (3.12)$$

where

$$Y_{kl}^{bus} = \begin{cases} G_{kl} + jB_{kl} & k \neq l \\ -\sum_{k \neq l} (G_{kl} + jB_{kl}) & k = l \end{cases} \quad (3.13)$$

Such definition of the Y_{bus} matrix captures both the real and reactive portions of the line admittances. In this analysis the inverse of the Y_{bus} matrix or Z_{bus} is used which is a non-sparse (dense) matrix. The equivalent electrical distance between nodes k and l is thus given by the magnitude of the relevant entry of the Z_{bus} matrix. Smaller $|Z_{kl}^{bus}|$ corresponds to shorter electrical distances. In other words, if a scale-free or random network has properties similar to Kirchoff's Laws, it will be very difficult to contain the propagation of information to an area much smaller than a random or scale free network.

That being said, depending on the electrical distance between the target DER systems and the point where the optimization criteria is being processed and applied, effectiveness (weighting factors) of the DERs could be calculated. A DER located at a nodes with high electrical distance is expected to have lower capability than similar agent located at a closer

(less electrical distance) node to contribute to voltage correction or energy compensation. That phenomenon is called “effectiveness.”

Topological Centrality and Betweenness

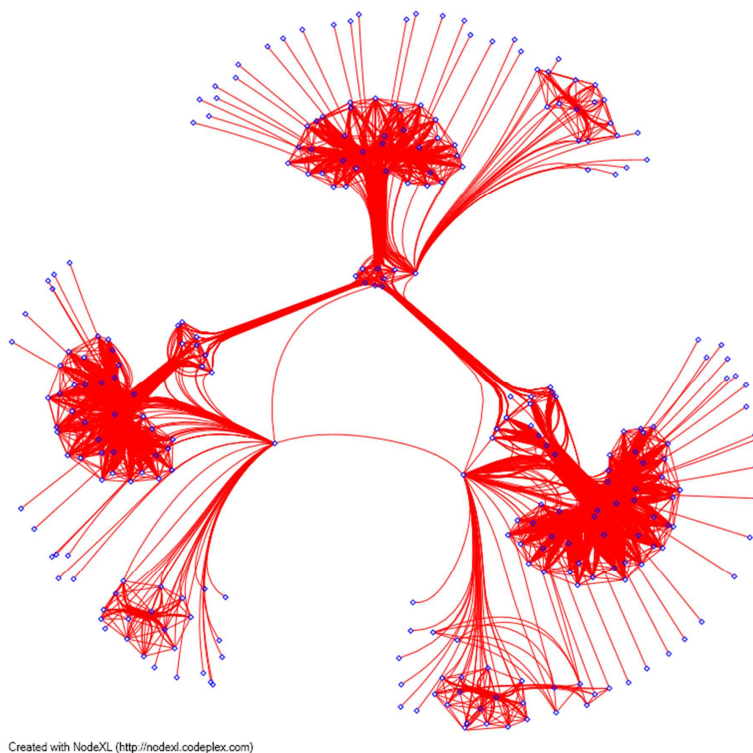


Figure 3.76: Topological representation of ST14 impedance graph. The electrical hubs carry a considerably large portion of the energy exchange by being central nodes. (Data from PNM, Graph generated in NodeXL)

It was elaborated in section 3.3.2 that from a topological point of view, the feeder networks look neither like a random network nor like a scale-free network. However, from an electrical perspective, which captures the behavior of the network (not simply the physical structure), both networks look to have distinct groups of nodes that are “electrical hubs”. Electrical hubs are the nodes with the highest electrical connectivity to the rest of the network. Gov-

erned by Kirchoff's Law, power, flowing through the electrical network, most likely pass through one or more of those hubs. In the language of social networks, the electrical hubs would correspond to nodes with high betweenness or information centrality. Figure 3.76 illustrated the topological representation of the ST14 feeder. The electrical hubs could be easily distinguished by finding the highest concentration of the edges. Bulk of energy delivered through the ST14 feeder most likely pass through those hubs. It is highly possible that, a solution involving multi-agent coordination for energy flow management include at least one of those so called "energy hubs". Therefore, if a ranking mechanism is to be devised based on centrality, nodes with higher electrical centrality should be assigned a higher rank compared to others.

Voltage Sensitivity

In section 3.2, it was discovered that some nodes along the feeder could be susceptible to voltage problems due to increased penetration of the DERs. On the other hand, some nodes, mostly close to the stronger body of the feeder, are more robust and stable in similar situations.

From the utility point of view, those robust nodes could be the best candidates for being DER "hubs". That said, those nodes can tolerate large amount of power injection during high productivity and low consumption periods. To find the most suitable nodes to install large size DERs, like utility scale PV farms, such electrical hubs should be detected. To locate the so called "electrical hubs" similar feeder simulations described earlier must be performed.

Chapter 4

Conclusions

The problem of devising a comprehensive method for coordination between DERs in order to achieve a collective goal was the main target of the studies extensively described in previous chapters.

In the first chapter, an introduction to the ever increasing idea of utilizing distributed energy resources was presented. Over the course of the recent years, it has become more clear that a nontrivial but viable solution to the problems of the aging electrical infrastructure, inefficiencies in transmission and distribution of electricity, crucial effects of blackouts and brownouts on economy and people's lives could be a smart grid which utilizes and coordinates all available resources toward a collective target which is beneficial to both customers and grid operators. Some of the related researches and reports was then reviewed and studied to understand where other researchers stand and which areas are overlooked.

Among others, the followings were of the most encouraging reasons this research was started and continued:

- PNM PV and BES system demonstration project was started which was planned to provide basis for the future smart grid projects,

Chapter 4. Conclusions

- Constructive collaboration between the local utility company (PNM) and the university,
- Access to HPC machines,
- Invaluable support by GridLAB-D and Open-DSS teams,
- Study on smart building energy management systems was already started in the mechanical engineering department. That provided a supportive road map for the study.
- Roof top PV systems were installed and were to be installed in various locations on campus,
- Constructive collaboration with the research team based in Sandia National Laboratories,
- Available test bed at Mesa del Sol for the scenarios and prospective solutions,

Chapter 2 included a broad review of the researches performed by others on the areas to be covered in this research. Although the concept of smart grid is a rather new topic in the field of power distribution systems, due to the sensitivity and popularity of the ideas involved in it, valuable reports, articles and papers are available for review. Those resources were used firstly to find out what had been done and secondly to develop a research plan encompassing a road map for this research and probably a good reference for future.

In chapter 3, the studies and simulations were presented step by step. The target was to build a simulative and theoretic basis and to demonstrate a comprehensive method for coordinating DERs in order to achieve the collective goal of making the most profit for the customers or grid operators.

The very first step was to develop a rather accurate model for the distribution system, appropriate for modeling distributed agents and capable of performing time series analysis. By incorporating GridLAB-D and Open-DSS, both open source software tools designed for

Chapter 4. Conclusions

similar applications, models were developed and tested against recorded data. In section 3.1, this process was described.

Later on, in section 3.2, the robust nodes suitable for accommodating large capacities of renewable DER power injection were detected. By running similar simulations on any distribution feeder, it could be shown that some nodes demonstrate robustness and insensitivity to higher penetration levels of renewable DERs. Those robust nodes would be the ideal choice for the utility company to connect large capacities of DER if needed.

In section 3.3, the developed topological model for electrical grids which adopted the graph theory and transformed it with regards to the physics of electricity (Kirchhoff's law) was implemented on ST14 and TR11 feeders. It was then demonstrated that some nodes in a distribution feeder have a very high connectivity and the electricity flowing through the feeder is most likely passing through one or more of those nodes (electrical hubs). Those hubs are the most critical nodes in case of cyber attacks or faults. Loss of power at the so called hubs will most likely cause loss blackout or brownout downstream. On the other hand, to connect large scale DERs to the distribution feeder, the power company would require to find such electricity hubs. By detecting the electrical hubs, it would be understood which nodes have to access to broadband communication with the aggregator.

Coordinated operation of the distributed agents was the essence of this dissertation and was further elaborated in chapter 3.4. There is a large selection of DERs commercially available in the market and more advanced or affordable technologies are yet to be developed. Therefore, it is almost impossible to find a unique or standard way of selecting and arranging those resources. Utility companies or microgrid operators have limited control over the type, location and capacity of the DERs to be adopted by the customers. That being said, there would be multiple methods to coordinate or to balance available resources in such complex and diverse distribution system. Out of various possible implications, it was decided to concentrate on the following:

Chapter 4. Conclusions

- Coordinated smoothing using multiple resources
- Coordinated demand management by selective load enabling
- Coordinated load shifting using storage
- Categorization of the available resources

The first three methods described possible low cost solutions to coordinate available resources to attain a collective solution at feeder or community (microgrid) level. The last part described a road map to establish simple but effective ranking methods which translate effectiveness of the available resources into numbers (ranks). Ranks could be calculated based on the applicable criteria. As an example, for smoothing purposes, the resources with higher dynamic response and closer electrical distance would have higher ranking. Consequently, those would provide higher level of contribution to smoothing compared to other lower rank resources. It is by the way understood that depending on the ranking criteria, the resulted rank number might drastically change. A fast high power/low capacity battery storage system could highly contribute to smoothing services while it's share for providing load shift service would be limited.

End.

May 2015

Shahin Abdollahy

University of New Mexico

Albuquerque, NM USA

Publications and Presentations

This research is presented or submitted in parts to the following conferences, journals or technical reports:

- “Coordinated Collaboration Between Heterogeneous Distributed Energy Resources,”
Published in “Journal of Solar Energy.”
- “Integrating heterogeneous distributed energy resources to manage intermittent power at low cost,”
Presented and Published in “1st IEEE Conference on Technologies for Sustainability (SusTech),” 2013.
- “Distributed compensation of a large intermittent energy resource in a distribution feeder,”
Presented and published in “Innovative Smart Grid Technologies (ISGT),” 2013 IEEE PES.
- “PNM smart grid demonstration project from modeling to demonstration,”
Presented and published in “Innovative smart grid Technologies (ISGT),” 2012 IEEE PES.
- “Case Study on the Demonstration of Storage for Simultaneous Voltage Smoothing and Peak Shifting,”

Publications and Presentations

Electric Power Research Institute, October 2012.

- “Analysis of battery storage utilization for load shifting and peak smoothing on a distribution feeder in New Mexico,”

Presented and published in “Innovative smart grid Technologies (ISGT),” 2012 IEEE PES.

- “Modeling of PV plus storage for Public Service Co. of New Mexico’s Prosperity energy storage project,”

Presented and published in “Electrical Energy Storage Applications and Technologies Annual meeting,” San Diego, CA, October 2011.

- “Analysis of a High Penetration of DER and Electric Vehicles on Residential Distribution Networks,”

Presented in “4th International Conference on Integration of Renewable and Distributed Energy Resources”, December 6-10, 2010, Albuquerque, New Mexico.

Appendix A

Classic Network Modeling Metrics

According to Newman [67], the following terms are usually used in common language of complex networks:

- Vertex: The fundamental unit of a network, also called a site (physics), a node (computer science), or an actor (sociology).
- Edge: The line connecting two vertices. Also called a bond (physics), a link (computer science), or a tie (sociology).
- Directed/undirected: An edge is directed if it runs in only one direction (such as a one-way road between two points), and undirected if it runs in both directions. Directed edges, which are sometimes called arcs, can be thought of as sporting arrows indicating their orientation. A graph is directed if all of its edges are directed.
- Component: The component to which a vertex belongs is that set of vertices that can be reached from it by paths running along edges of the graph.

The adjacency matrix A uniquely represents the configuration of the graph, such that $a_{ij} = 1$ if and only if there is an edge between nodes i and j . For a simple undirected graph,

Appendix A. Classic Network Modeling Metrics

A is symmetric, with zeros on the diagonal, representing the absence of self loops.

Network researchers have introduced a large number of centrality indices according to one criterion or another [134]. Those indices provide great value in the analysis and understanding of the social networks, citation networks, computer networks, and biological networks. Perhaps the simplest centrality measure is node degree, which is the number of edges incident on a vertex in a network. A more sophisticated centrality measure is closeness, which is the mean geodesic distance between a vertex and all other vertices connected directly to it. Closeness can be interpreted as a measure of the delay for information to spread from a given vertex to other nodes in the network [134].

Another important class of centrality measures is betweenness. Betweenness is a measure of the extent to which a vertex lies on the paths between other nodes [134].

In many networks, information does not flow only along geodesic paths. News, a rumors or a message does not know the ideal route to take to get from one place to another. Even in the famous small-world experiment of Milgram [70], there is no evidence that people got a message to a target by the most direct route possible. Therefore, in most cases a realistic betweenness measure should include non-geodesic paths in addition to geodesic ones [134].

Some of the metrics evaluated here require the use of a graph distance matrix (D). D has the same dimensions as the adjacency matrix. d_{ij} indicates the minimum number of edges that one crosses to traverse from node i to node j . D is also known as the geodesic distance matrix [135]. When there are no paths between i and j , $d_{ij} = 0$. The diameter of a network is defined to be the length of the longest geodesic path between any two vertices. The metrics used here are introduced in the following sections.

A.1 Degree Distribution

The degree of a node indicates the number of nodes adjacent to that node. One can also define the degree of node i in terms of the adjacency matrix as the sum of the elements of the corresponding row (or column since A is symmetric):

$$k_i = \sum_{j=1}^N a_{ij} \quad (\text{A.1})$$

The degree distribution is a useful way to represent the global connectivity of a network. However, in cases which the degree varies over several orders of magnitude, it is useful to visualize the parameters of the probability mass function for areas of interest, such as in the tail. For instance, two networks can have similar average degree, but dramatically different dynamical behavior, resulting from the presence of high degree nodes (hubs) [68, 135].

A.2 Clustering Coefficient

The clustering coefficient, C , is a common metric that provides information about the transitivity of a network; i.e., if two pairs of nodes, $\{x, y\}$ and $\{x, z\}$, are clustered then there also exists an edge between nodes x and z . In social networks, the clustering coefficient indicates whether two individuals with a common friend may also know each other. In that case they would form a cluster. C is defined as follows in terms of the coefficient c_i or the individual clustering coefficient for each node [136].

$$C = \frac{1}{N} \sum_{i=1}^N c_i, \quad (\text{A.2})$$

Appendix A. Classic Network Modeling Metrics

where the individual clustering coefficient, c_i , is defined as

$$c_i = \frac{e_i}{k_i(k_i-1)/2} \quad (\text{A.3})$$

and e_i is the number of edges within the cluster of nodes including node i and its immediate neighbors N_i :

$$e_i = \sum_{\forall j,k \in \{N_i \cup i\}} a_{jk}/2. \quad (\text{A.4})$$

A.3 Average Shortest Path and Diameter

The average shortest path (or characteristic path length), L , is a measure to recognize if the network has the properties of small-world networks or not. Regardless of the size of the network, it demonstrates whether a short path between any given pair of nodes exists or not [71]. This property has been studied for many real networks. For example, Kochen *et al.* [137] found that on average, two random people in the US could communicate with each other by establishing a path of just six degrees of separation. L is defined from the distance matrix as the average value of all the possible geodesic entries for every combination of nodes, given that the geodesic entry d_{ij} is the number of edges along the shortest path from i to j .

$$L = \frac{1}{n(n-1)} \sum_{\forall i,j \ i \neq j} d_{ij}. \quad (\text{A.5})$$

Often some d_{ij} are infinite because there are unconnected components. In this case it is useful to consider only the distances among the nodes within the largest connected component (or the “giant component”). The diameter of a network is the maximum value among all the

Appendix A. Classic Network Modeling Metrics

average shortest path lengths.

$$d_{max} = \max_{ij} (d_{ij}) . \quad (\text{A.6})$$

A.4 Assortativity

In complex networks, the assortativity coefficient, r , describes the extent to which nodes tend to attach to nodes with similar degree. Although assortativity can be used to measure other similarities in networks, it is most commonly measured with respect to the node degree. The assortativity of the network directly influences the size of the giant component [138] and therefore the assortativity coefficient helps to understand macro behaviors such as contagion phenomena or network resilience. In this study, to compare different networks, the normalized form for r , which is equivalent to the Pearson correlation coefficient for the degree of node pairs, is used [67]:

$$r = \frac{m^{-1} \sum_i j_i k_i - [m^{-1} \sum_i (j_i + k_i)/2]^2}{m^{-1} \sum_i (j_i^2 + k_i^2) - [m^{-1} \sum_i (j_i + k_i)/2]^2} , \quad (\text{A.7})$$

where m is the number of links in the network and j_i/k_i are the degrees of the endpoints of link i . Accordingly, a network with assortativity coefficient of 1 would be completely assortative, in which, hubs only connect to hubs. On the other hand, an assortativity coefficient of -1 comes from a completely disassortative network. r is zero for a network with no assortative mixing [139].

A.5 Betweenness

Another metric, more popular in the analysis of social networks than physical or technological networks, is betweenness [140, 141], defined in [134] as the fraction of shortest paths between pairs of nodes that happen to pass through a given node. The betweenness of a vertex i is defined to be the fraction of shortest paths between pairs of vertices in a network that pass through i . If there is more than one shortest path between a given pair of vertices, then each such path is given equal weight such that the weights sum to unity. To be precise, suppose that g_i^{st} is the number of geodesic paths from vertex s to vertex t that pass through i , and suppose that n_{st} is the total number of geodesic paths from s to t . Then the betweenness of vertex i is:

$$b_i = \frac{\sum_{s < t} g_i^{st} / n_{st}}{\frac{1}{2}n(n-1)}, \quad (\text{A.8})$$

where n is the total number of vertices in the network.

In a network in which flow is entirely or at least mostly along geodesic paths, the betweenness of a vertex measures how much flow will pass through that particular vertex.

Betweenness suffers from the same modeling issue as the degree distribution does. It considers the topological structure of the network, but not the pattern of network flow propagation. To address that, social network analysts have introduced a measure known as information centrality to describe how information is passed through a network of associates [142, 143]. The information centrality associated with a given node describes how much of the network flow travels along each path beginning or ending with that node.

References

- [1] R. Billinton and R. N. Allan, *Reliability Evaluation of Power Systems*. Pitman Books, 1984, new York and London.
- [2] S. Jonnavithula and R. Billinton, “Minimum cost analysis of feeder routing in distribution system planning,” *IEEE Transactions on Power Delivery*, vol. 11, no. 4, October 1996.
- [3] S. Bums and G. Gross, “Value of service reliability,” *IEEE Transactions On Power Systems*, vol. 5, no. 3, August 1990.
- [4] T. Gonen, *Electric power distribution system engineering*. McGraw-Hill, 1986, new York and London.
- [5] U.S. Energy Information Administration, “Annual energy outlook 2013,” [http://www.eia.gov/forecasts/aeo/pdf/0383\(2013\).pdf](http://www.eia.gov/forecasts/aeo/pdf/0383(2013).pdf), 2013, assumptions to the Annual Energy Outlook 2013.
- [6] [Online]. Available: http://www.eia.gov/forecasts/aeo/MT_electric.cfm
- [7] [Online]. Available: <http://www.eia.gov/oiaf/aeo/tablebrowser/#release=AEO2012&subject=0-AEO2012&table=2-AEO2012®ion=1-0&cases=ref2012-d020112c>
- [8] [Online]. Available: [http://www.xcelenergy.com/staticfiles/xcel/Corporate/ Corporate PDFs/HiawathaAppendixD3a.pdf](http://www.xcelenergy.com/staticfiles/xcel/Corporate/Corporate%20PDFs/HiawathaAppendixD3a.pdf)
- [9] [Online]. Available: [http://www.pnl.gov/main/publications/external/technical_ reports /PNNL-17826.pdf](http://www.pnl.gov/main/publications/external/technical_reports/PNNL-17826.pdf), Climate Change Impacts on Residential and Commercial Loads in the Western U.S. Grid
- [10] [Online]. Available: [http://www.pnl.gov/main/publications/external/technical_ reports /PNNL-17826.pdf](http://www.pnl.gov/main/publications/external/technical_reports/PNNL-17826.pdf), Climate Change Impacts on Residential and Commercial Loads in the Western U.S. Grid

References

- [11] [Online]. Available: http://www.pnl.gov/main/publications/external/technical_reports/PNNL-17826.pdf, Climate Change Impacts on Residential and Commercial Loads in the Western U.S. Grid
- [12] [Online]. Available: <http://www.solareworld.com/solar-learning-center/myths-and-facts-of-solar-panel-systems>
- [13] [Online]. Available: <http://www.solareworld.com/solar-learning-center/myths-and-facts-of-solar-panel-systems>
- [14] [Online]. Available: <http://www.solareworld.com/solar-learning-center/myths-and-facts-of-solar-panel-systems>
- [15] J. Smith, “Impact of high-penetration pv on distribution system performance: Example cases and analysis approach,” EPRI, Palo Alto, CA, Tech. Rep. 1021982, 2011.
- [16] —, “Impact of high-penetration pv on distribution system performance: Example cases and analysis approach,” EPRI, Palo Alto, CA, Tech. Rep. 1021982, 2011.
- [17] B. M. Buchholz and Z. Styczynski, “Integration of renewable and dispersed resources: lessons learnt from german projects,” in *Power Engineering Society General Meeting*. IEEE, 2006.
- [18] S. Abdollahy, O. Lavrova, and A. Mammoli, “PNM smart grid demonstration project from modeling to demonstration,” in *Innovative Smart Grid Technologies(ISGT '12)*. IEEE PES, 2012.
- [19] [Online]. Available: <http://der.lbl.gov/News/grand-opening-nedo-aperture-center-micro-grid>
- [20] R. Lasseter, A. Akhil, C. Marnay, J. Stephens, J. Dagle, R. Guttromson, A. Meliopoulos, R. Yinger, and J. Eto, “The certs microgrid concept,” *White paper for Transmission Reliability Program, Office of Power Technologies, US Department of Energy*, 2002.
- [21] J. Kumagai, “Swiss warehouse helps buffer the grid,” *IEEE Spectrum*, no. 6, pp. 17–18, 2013.
- [22] Itron, Inc. Consulting and Analysis Services, “Public service new mexico electric energy efficiency potential study,” www.nmenv.state.nm.us/cc/documents/Sahu_Exhibit3part1.pdf, 2006, chapter 3. Data Development and Economic Inputs.
- [23] A. Mammoli, C. Birk Jones, H. Barsun, D. Dreisigmeyer, G. Goddard, and O. Lavrova, “Distributed control strategies for high-penetration commercial-building-scale thermal storage,” in *Transmission and Distribution Conference and Exposition*. IEEE PES (T&D), 2012, pp. 1–7.

References

- [24] [Online]. Available: <http://www.afdc.energy.gov/vehicles/electric.html>
- [25] [Online]. Available: <http://online.barrons.com/article/SB50001424053111904628504577591633105550046.html>
- [26] J. Lopes, F. Soares, and P. Almeida, "Integration of electric vehicles in the electric power system," *Proceedings of the IEEE*, vol. 99, no. 1, pp. 168–183, 2011.
- [27] M. Galus and G. Andersson, "Demand management of grid connected plug-in hybrid electric vehicles," in *IEEE Energy 2030 Conference*, 2008.
- [28] K. Dyke, N. Schofield, and M. Barnes, "The impact of transport electrification on electrical networks," *IEEE Transactions on Industrial Electronics*, vol. 57, no. 12, December 2010.
- [29] [Online]. Available: <http://www.cfr.org/united-states/nuclear-power-expansion-challenges/p16886#p2>
- [30] J. P. Lopes, C. Moreira, and A. Madureira, "Defining control strategies for analyzing micro-grids islanded operation," in *IEEE Power Tech*, Russia, 2005.
- [31] [Online]. Available: <http://certs.lbl.gov/pdf/50829.pdf>
- [32] P. Piagi and R. Lasseter, "Autonomous control of microgrids," in *IEEE PES Meeting*, Montreal, June 2006.
- [33] S. Lu, M. A. Elizondo, N. Samaan, K. Kalsi, E. Mayhorn, R. Diao, C. Jin, and Y. Zhang, "Control strategies for distributed energy resources to maximize the use of wind power in rural micro-grids," in *IEEE PES General Meeting*, 2011.
- [34] [Online]. Available: http://www.smartgrid.gov/project/amber_kinetics_inc_fly-wheel.energy_storage_demonstration
- [35] [Online]. Available: http://www.smartgrid.gov/project/city_painesville_ohio_vanadium_redox_battery_demonstration_program
- [36] [Online]. Available: <http://certs.lbl.gov/pdf/micro-grid-battery-storage.pdf>
- [37] [Online]. Available: http://energy.gov/sites/prod/files/2014/09/f18/Grid_Energy_Storage_December_2013.pdf
- [38] M. Thomson and D. Infield, "Impact of widespread photovoltaics generation on distribution systems," *IET Renewable Power Generation*, vol. 1, no. 1, pp. 33–40, 2007.
- [39] —, "Impact of widespread photovoltaics generation on distribution systems," *IET Renewable Power Generation*, vol. 1, no. 1, pp. 33–40, 2007.

References

- [40] J. Smith, “Modeling high-penetration pv for distribution analysis: Solar pv systems and relevant grid-related responses,” EPRI, Palo Alto, CA, Tech. Rep. 1021980, 2011.
- [41] X. Feng and T. Wei, “Study on voltage quality of distribution network with high penetration of dg,” in *International Conference on Power System Technology*, 2010.
- [42] T. Kato, T. Inoue, and Y. Suzuoki, “Estimation of total power output fluctuation of high penetration photovoltaic power generation system,” in *IEEE Power and Energy Society General Meeting*, 2011.
- [43] J. A. Carr, J. C. Balda, and H. A. Mantooth, “A survey of systems to integrate distributed energy resources and energy storage on the utility grid,” in *Energy 2030 Conference*. IEEE, 2008.
- [44] W. Wu, J. Liu, Y. Liu, and Y. Tang, “Revolution brought by der to intelligent marketing,” in *International Conference on Electricity Distribution (CICED)*, China, 2010.
- [45] D. Pudjiant, C. K. Gan, V. Stanojevic, M. Aunedi, P. Djapic, and G. Strbac, “Value of integrating distributed energy resources in the uk electricity system,” in *IEEE Power and Energy Society General Meeting*, 2010.
- [46] Y. Zhu and K. Tomsovic, “Analysis and control of distributed energy resources,” in *IEEE Power and Energy Society General Meeting*, 2011.
- [47] J. Duval and B. Meyer, “Frequency behavior of grid with high penetration rate of wind generation,” in *IEEE PowerTech*, Bucharest, 2009.
- [48] F. A. Rahimi, “Challenges and opportunities associated with high penetration of distributed and renewable energy resources,” in *Innovative Smart Grid Technologies (ISGT)*. IEEE, 2010.
- [49] Y. Zong, D. Kullmann, A. Thavlov, O. Gehrke, and H. Bindner, “Model predictive control strategy for a load management research facility in the distributed power system with high wind penetration -towards a danish power system with 50% wind penetration,” in *Power and Energy Engineering Conference (APPEEC)*, Asia-Pacific, 2011.
- [50] E. I. Vrettos and S. A. Papathanassiou, “Operating policy and optimal sizing of a high penetration res-bess system for small isolated grids,” *IEEE Transactions on Energy Conversion*, vol. 26, no. 3, pp. 744 – 756, 2011.
- [51] H.E.Farag, E. El-Saadany, and L. E. Chaar, “A multilayer control framework for distribution systems with high dg penetration,” in *2011 International Conference on Innovations in Information Technology (IIT)*, April 2011.

References

- [52] J. Smith, R. Dugan, and W. Sunderman, "Distribution modeling and analysis of high penetration pv," in *Power and Energy Society General Meeting*. IEEE, July 2011.
- [53] Z. Zhao, K.-H. Wu, J.-S. Lai, and W. Yu, "Utility grid impact with high penetration pv micro-inverters operating under burst mode using simplified simulation model," in *Energy Conversion Congress and Exposition (ECCE)*. IEEE, September 2011.
- [54] S. Lin, M. Han, R. Fan, and X. Hu, "Configuration of energy storage system for distribution network with high penetration of pv," in *IET Conference on Renewable Power Generation*. IET, 2011.
- [55] X. Liu, A. Aichhorn, L. Liu, and H. Li, "Coordinated control of distributed energy storage system with tap changer transformers for voltage rise mitigation under high photovoltaic penetration," *IEEE Transactions on Smart Grid*, vol. 3, no. 2, pp. 897 – 906, 2012.
- [56] A. I. Estanqueiro, J. M. F. D. Jesus, J. Ricardo, A. dos Santos, and J. A. P. Lopes, "Barriers (and solutions...) to very high wind penetration in power systems," in *Power Engineering Society General Meeting*. IEEE, 2007.
- [57] K. Schneider, J. Fuller, and D. Chassin, "Multi-state load models for distribution system analysis," *IEEE Transactions on Power Systems*, November 2011.
- [58] S. Acha and H. A. Carlos, "Integrated modeling of gas and electricity distribution networks with a high penetration of embedded generation," in *SmartGrids for Distribution*. IET-CIRED, 2008.
- [59] L. Mihalache, S. Suresh, Y. Xue, and M. Manjrekar, "Modeling of a small distribution grid with intermittent energy resources using matlab/simulink," in *IEEE Power and Energy Society General Meeting*, July 2011, pp. 24–29.
- [60] A. Eajal and M. El-Hawary, "Optimal capacitor placement and sizing in distorted radial distribution systems part i: System modeling and harmonic power flow studies," in *14th International Conference on Harmonics and Quality of Power (ICHQP)*, 2010.
- [61] [Online]. Available: <http://etap.com/distribution-systems/distribution-systems-software.htm>
- [62] J. Y. Wen, L. Jiang, Q. H. Wu, and S. Cheng, "Power system load modeling by learning based on system measurements," *IEEE Transactions on Power Delivery*, vol. 18, no. 2, pp. 364 – 371, 2003.
- [63] J. Wan and K. N. Miu, "Weighted least squares methods for load estimation in distribution networks," *IEEE Transactions on Power Systems*, vol. 18, no. 4, pp. 1338 – 1345, 2003.

References

- [64] P. Palensky, F. Kupzog, A. A. Zaidi, and K. Zhou, “Modeling domestic housing loads for demand response,” in *34th Annual Conference of Industrial Electronics (IECON)*. IEEE, 2008.
- [65] K. Qian, C. Zhou, M. Allan, and Y. Yuan, “Modeling of load demand due to ev battery charging in distribution systems,” *IEEE Transactions on Power Systems*, vol. 26, no. 2, pp. 802 – 810, 2011.
- [66] J. E. C. Sanchez, “A complex network approach to analyzing the structure and dynamics of power grids,” diploma thesis, The Graduate College of The University of Vermont, October 2009.
- [67] M. Newman, “The structure and function of complex networks,” *SIAM Review*, vol. 45, no. 2, pp. 167–256, 2003.
- [68] R. Albert and A. Barabasi, “Statistical mechanics of complex networks,” *Reviews of Modern Physics*, vol. 74, pp. 47–97, 2002.
- [69] P. Erdos and A. Renyi, “On random graphs,” *Publ. Math. Debrecen*, vol. 6, pp. 290 – 297, 1959.
- [70] S. Milgram, “The small world problem,” *Psychology Today*, vol. 2, pp. 60–67, 1967.
- [71] D. Watts and H. Strogatz, “Collective dynamics of ‘small-world’ networks,” *Nature*, vol. 393, pp. 440 – 442, 1998.
- [72] A. Barabasi and R. Albert, “Emergence of scaling in random networks,” *Science*, vol. 286, pp. 509 – 512, 1999.
- [73] P. Hines, S. Blumsack, E. C. Sanchez, and C. Barrows, “The topological and electrical structure of power grids,” in *Proceedings of the 43rd Hawaii International Conference on System Sciences*, 2010.
- [74] L. Amaral, A. Scala, M. Barthelemy, and H. Stanley, “Classes of small-world networks,” *Proceedings of the National Academy of Sciences*, vol. 97, no. 21, pp. 11 149 – 11 152, 2000.
- [75] R. Albert, I. Albert, and G. Nakarado, “Structural vulnerability of the north american power grid,” *Physical Review*, vol. 69, no. 2, February 2004.
- [76] P. Crucitti, V. Latora, and M. Marchiori, “Topological analysis of the italian electric power grid,” *Physica A*, vol. 338, pp. 92–97, 2004.
- [77] D. Chassin and C. Posse, “Evaluating north american electric grid reliability using the barabási-albert network model,” *Physica A*, vol. 355, pp. 667 – 677, 2005.

References

- [78] G. Chen, Z. Dong, D. Hill, and G. Zhang, “An improved model for structural vulnerability analysis of power networks,” *Physica A*, vol. 388, pp. 4259–4266, 2009.
- [79] [Online]. Available: http://en.wikipedia.org/wiki/List_of_power_outages
- [80] K. Wang, B. Zhang, Z. Zhang, X. Yin, and B. Wang, “An electrical betweenness approach for vulnerability assessment of power grids considering the capacity of generators and load,” *Physica A*, vol. 390, no. 23–24, pp. 4692–4701, 2011.
- [81] P. Hines and S. Blumsack, “A centrality measure for electrical networks,” in *Proceedings of the 41st Hawaii International Conference on System Sciences*, 2008.
- [82] U. Brandes and D. Fleischer, “Centrality measures based on current flow,” in *Proceedings of the 22nd Symposium on Theoretical Aspects of Computer Science*, 2005, pp. 533–544.
- [83] E. Bompard, D. Wu, and F. Xue, “The concept of betweenness in the analysis of power grid vulnerability,” in *Proceedings of 2010 Complexity in Engineering*, 2010, p. 5254, rome.
- [84] J. Das, *Power System Analysis*. Marcel Dekker Inc., 2002.
- [85] T. Dang, “The energy web: Concept and challenges to overcome to make large scale renewable and distributed energy resources a true reality,” in *7th IEEE International Conference on Industrial Informatics, (INDIN)*. IEEE, 2009.
- [86] R. D. Robinett and D. G. Wilson, “Transient stability and control of renewable generators based on hamiltonian surface shaping and power flow control: Part i-theory,” in *International Conference on Control Applications (CCA)*. IEEE, 2010.
- [87] A. Vaccaro, G. Velotto, and A. F. Zobaa, “A decentralized and cooperative architecture for optimal voltage regulation in smart grids,” *IEEE Transactions on Industrial Electronics*, vol. 58, no. 10, pp. 4593 – 4602, 2011.
- [88] H. Pu, J. Kalagnanamand, R. Natarajan, M. Sharma, R. Ambrosio, D. Hammerstrom, and R. Melton, “Analytics and transactive control design for the pacific northwest smart grid demonstration project,” in *First IEEE International Conference on Smart Grid Communications (SmartGridComm)*. IEEE, 2010.
- [89] J. Shah, B. F. Wollenberg, and N. Mohan, “Decentralized power flow control for a smart micro-grid,” in *Power and Energy Society General Meeting*. IEEE, 2011.
- [90] Z. Jiang, “Agent-based control framework for distributed energy resources microgrids,” in *International Conference on Intelligent Agent Technology (IAT ’06)*. IEEE/WIC/ACM, 2006.

References

- [91] M. A. Pedrasa, E. D. Spooner, and I. MacGill, “Robust scheduling of residential distributed energy resources using a novel energy service decision-support tool,” in *Innovative Smart Grid Technologies (ISGT)*. IEEE PES, 2011.
- [92] J. Slootweg, E. Veldman, and J. Morren, “Sensing and control challenges for smart grids,” in *International Conference on Networking, Sensing and Control (ICNSC)*. IEEE, 2011.
- [93] A. N. Venkat, I. A. Hiskens, J. B. Rawlings, and S. J. Wright, “Distributed mpc strategies with application to power system automatic generation control,” *IEEE Transactions on Control Systems Technology*, vol. 16, no. 6, pp. 1192 – 1206, 2008.
- [94] E. Franco, L. Magni, T. Parisini, M. M. Polycarpou, , and D. M. Raimondo, “Cooperative constrained control of distributed agents with nonlinear dynamics and delayed information exchange: A stabilizing receding-horizon approach,” *IEEE Transactions on Automatic Control*, vol. 53, no. 1, pp. 324 – 338, 2008.
- [95] M. B. Delghavi and A. Yazdani, “Islanded-mode control of electronically coupled distributed-resource units under unbalanced and nonlinear load conditions,” *IEEE Transactions on Power Delivery*, vol. 26, no. 2, pp. 661 – 673, 2011.
- [96] H. Nian and R. Zeng, “Improved control strategy for stand-alone distributed generation system under unbalanced and non-linear loads,” *IET Renewable Power Generation*, vol. 5, no. 5, pp. 323 – 331, 2011.
- [97] Y. Zong, D. Kullmann, A. Thavlov, O. Gehrke, and H. W. Bindner, “Application of model predictive control for active load management in a distributed power system with high wind penetration,” *IEEE Transactions on Smart Grid*, vol. 3, no. 2, pp. 1055 – 1062, 2012.
- [98] P. Piagi and R. Lasseter, “Autonomous control of microgrids,” in *IEEE PES Meeting*, Montreal, June 2006.
- [99] S. Lu, M. A. Elizondo, N. Samaan, K. Kalsi, E. Mayhorn, R. Diao, C. Jin, and Y. Zhang, “Control strategies for distributed energy resources to maximize the use of wind power in rural micro-grids,” in *IEEE PES General Meeting*, 2011.
- [100] H. F. Wang, “Multi-agent co-ordination for the secondary voltage control in power-system contingencies,” *IEE Proceedings on Generation, Transmission and Distribution*, vol. 148, no. 1, pp. 61 – 66, 2001.
- [101] M. Pedrasa, T. Spooner, and I. MacGill, “Coordinated scheduling of residential distributed energy resources to optimize smart home energy services,” *IEEE Transactions on Smart Grid*, pp. 134 – 143, September 2019.

References

- [102] T. Logenthiran, D. Srinivasan, and D. Wong, “Multi-agent coordination for der in microgrid,” in *IEEE International Conference on Sustainable Energy Technologies (ICSET 2008)*, 2008.
- [103] P. Nguyen, W. Kling, and P. Ribeiro, “Smart power router: A flexible agent-based converter interface in active distribution networks,” *IEEE Transactions on Smart Grid*, vol. 2, no. 3, pp. 487 – 495, September 2011.
- [104] M. Hommelberg, B. van der Velde, C. Warmer, I. Kamphuis, and J. Kok, “A novel architecture for real-time operation of multi-agent based coordination of demand and supply,” in *Power and Energy Society General Meeting, Conversion and Delivery of Electrical Energy in the 21st Century*. IEEE, 2008.
- [105] A. Dominguez-Garcia and C. Hadjicostis, “Distributed algorithms for control of demand response and distributed energy resources,” in *50th IEEE Conference on Decision and Control and European Control Conference (CDC-ECC)*, 2011.
- [106] T. L. Vandoorn, B. Zwaenepoel, J. D. M. D. Kooning, B. Meersman, and L. Vandevelde, “Smart microgrids and virtual power plants in a hierarchical control structure,” in *2nd IEEE PES International Conference and Exhibition on Innovative Smart Grid Technologies (ISGT Europe)*. IEEE, 2011.
- [107] A. D. Dominguez-Garcia, C. N. Hadjicostis, and N. H. Vaidya, “Resilient networked control of distributed energy resources,” *IEEE Journal on Selected Areas in Communications*, vol. 30, no. 6, pp. 1137–1148, July 2012.
- [108] G. Mokhtari, F. Zare, G. Nourbakhsh, and A. Ghosh, “A new der coordination in lv network based on the concept of distributed control,” in *3rd International Symposium on Power Electronics for Distributed Generation Systems (PEDG)*. IEEE, 2012.
- [109] [Online]. Available: http://sourceforge.net/apps/mediawiki/electricdss/index.php?title=Main_Page
- [110] [Online]. Available: http://sourceforge.net/apps/mediawiki/gridlab-d/index.php?title=Main_Page
- [111] [Online]. Available: <http://www.linuxpromagazine.com/Online/News/Top-500-85-Percent-of-all-Super-Computers-Runs-on-Linux/%28kategorie%29/0>
- [112] [Online]. Available: <http://www.hpc.unm.edu/systems-table/?searchterm=pequena>
- [113] K. Qian, C. Zhou, M. Allan, and Y. Yuan, “Load modeling in distributed generation planning,” in *International Conference on Sustainable Power Generation and Supply. SUPERGEN '09*, April 2009.

References

- [114] M. Baran and T. E. McDermot, “State estimation for real time monitoring of distribution feeders,” in *Power & Energy Society General Meeting*. IEEE PES ’09, 2009.
- [115] A. K. Ghosh, D. L. Lubkeman, and R. H. Jones, “Load modeling for distribution circuit state estimation,” *IEEE Transactions on Power Delivery*, vol. 12, no. 2, pp. 999 – 1005, April 1997.
- [116] J. Smith, “Impact of high-penetration pv on distribution system performance: Example cases and analysis approach,” EPRI, Palo Alto, CA, Tech. Rep. 1021982, 2011.
- [117] F. Cheng, S. Willard, J. Hawkins, B. Arellano, O. Lavrova, and A. Mammoli, “Applying battery energy storage to enhance the benefits of photovoltaics,” in *Energytech*. IEEE, 2012, pp. 1–5.
- [118] [Online]. Available: <http://nodexl.codeplex.com>
- [119] [Online]. Available: https://www.smartgrid.gov/recovery_act/consumer_behavior_studies
- [120] [Online]. Available: <http://www.eia.gov/consumption/residential/>
- [121] P. J. Balducci, “Plug-in hybrid electric vehicle market penetration scenarios,” PACIFIC NORTHWEST NATIONAL LABORATORY, P.O. Box 62, Oak Ridge, TN 37831-0062, Tech. Rep. PNNL-17441, September 2008.
- [122] T. Trigg and P. Telleen, “Global ev outlook,” International Energy Agency, Tech. Rep., April 2013.
- [123] A. E. Curtright and J. Apt, “The character of power output from utility-scale photovoltaic systems,” *Progress in Photovoltaics: Research and Applications*, vol. 16, no. 3, pp. 241–247, 2007.
- [124] O. Lavrova, F. Cheng, S. Abdollahy, H. Barsun, A. Mammoli, D. Dreisigmayer, S. Willard, B. Arellano, and C. van Zeyl, “Analysis of battery storage utilization for load shifting and peak smoothing on a distribution feeder in new mexico,” in *IEEE PES Innovative Smart Grid Technologies (ISGT)*. IEEE, 2012.
- [125] S. Willard, B. Arellano, J. Hawkins, J. Simmins, K. George, A. Ellis, A. Mammoli, O. Lavrova, D. Dreisigmayer, W. Greenwood, F. Cheng, S. Abdollahy, D. Schoenwald, S. Boland, and B. Mckeon, “Case study on the demonstration of storage for simultaneous voltage smoothing and peak shifting,” EPRI, Technical Update, October 2012.

References

- [126] S. Abdollahy, O. Lavrova, A. Mammoli, M. Sanchez, J. Hawkins, S. Willard, and B. Arellano, "Analysis of a high penetration of der and electric vehicles on residential distribution networks," in *4th International Conference on Integration of Renewable and Distributed Energy Resources*, Albuquerque, New Mexico, USA, December 2010.
- [127] S. Abdollahy, N. Heine, S. Poroseva, O. Lavrova, and A. Mammoli, "Integrating heterogeneous distributed energy resources to manage intermittent power at low cost," in *1st IEEE Conference on Technologies for Sustainability (SusTech)*. IEEE, 2013.
- [128] D. Li, S. K. Jayaweera, O. Lavrova, and R. Jordan, "Load management for price-based demand response scheduling-a block scheduling model," in *International Conference on Renewable Energies and Power Quality (ICREPQ'11)*, Las Palmas de Gran Canaria, Spain, April 2011.
- [129] O. Lavrova, F. Cheng, S. Abdollahy, A. Mammoli, S. Willard, B. Arellano, and C. van Zeyl, "Modeling of pv plus storage for public service company of new mexico's prosperity energy storage project," in *Electrical Energy Storage Applications and Technologies Conference (EESAT)*, San Diego, CA, October 2011.
- [130] B. Kim and O. Lavrova, "Optimal power flow and energy-sharing among multi-agent smart buildings in the smart grid," in *Energytech*. IEEE, May 2013.
- [131] O. Lavrova, H. Barsun, R. Burnett, and A. Mammoli, "Renewable energy and smart grid principles integration into campuswide energy strategy at the university of new mexico," *International Journal of Technology, Policy and Management*, vol. 12, no. 2, pp. 212–232, 2012.
- [132] B. Kim and O. Lavrova, "Two hierarchy (home and local) smart grid optimization by using demand response scheduling," in *IEEE PES Conference On Innovative Smart Grid Technologies Latin America (ISGT LA)*. IEEE, April 2013.
- [133] S. Abdollahy, O. Lavrova, and A. Mammoli, "Coordinated collaboration between heterogeneous distributed energy resources," *Journal of Solar Energy*, vol. 2014, December 2014.
- [134] M. E. J. Newman, "A measure of betweenness centrality based on random walks," *Social Networks*, vol. 27, pp. 39 – 54, 2005.
- [135] S. Boccaletti, V. Latora, Y. Morenod, M. Chavez, and D. U. Hwang, "Complex networks: Structure and dynamics," *Physics Reports*, vol. 424, pp. 175 – 308, 2006.
- [136] [Online]. Available: <http://www.electricdrive.org/index.php?ht=d/sp/i/20952/pid/20952>

References

- [137] I. de Sola Pool, M. Kochen, S. Milgram, and T. Newcomb, *The Small world*. Ablex Pub., 1989.
- [138] M. E. J. Newman, “Spread of epidemic disease on networks,” *Physical Review E*, 2002.
- [139] J. E. C. Sanchez, “A complex network approach to analyzing the structure and dynamics of power grids,” Thesis for the Degree of Master of Science Specializing in Electrical Engineering, The University of Vermont, October 2009.
- [140] L. C. Freeman, “A set of measures of centrality based upon betweenness,” *Sociometry*, vol. 40, pp. 35 – 41, 1977.
- [141] —, “Centrality in social networks: Conceptual clarification,” *Social Networks*, vol. 1, pp. 215 – 239, 1979.
- [142] K. Stephenson and M. Zelen, “Rethinking centrality: Methods and applications,” *Social Networks*, vol. 11, pp. 1 – 37, 1989.
- [143] S. Wasserman and K. Faust, *Social Network Analysis: Methods and Applications*. Cambridge University Press, 1994.